The Diurnal Cycle of Clouds and Precipitation: An Evaluation of multiple Data Sources

kumulative Dissertation
zur Erlangung des Doktorgrades
der Naturwissenschaften

vorgelegt beim Fachbereich Geowissenschaften
der Johann Wolfgang Goethe -Universität
in Frankfurt am Main

von
Uwe Anton Pfeifroth
aus Karlstadt am Main

Frankfurt 2016

vom Fachbereich Geowissenschaften

der Johann Wolfgang Goethe - Universität als Dissertation angenommen.

Dekan:
Prof. Dr. Ulrich Achatz

Gutachter:
Prof. Dr. Bodo Ahrens
Prof. Dr. Andreas Fink

Datum der Disputation:
27.06.2016

Contents

Deutsche Zusammenfassung

Wolken und Niederschlag sind meteorologische Parameter, die eine wichtige Rolle im Klimasystem der Erde spielen. Wolken beeinflussen maßgeblich die Energiebilanz der Erde in dem sie mit kurzwelliger solarer Strahlung und mit langwelliger terrestrischer Strahlung interagieren. Wolken reflektieren einerseits solare Strahlung in Richtung Weltraum zurück – ein kühlender Effekt, und Wolken absorbieren und emittieren andererseits terrestrische Wärmestrahlung – ein wärmender Effekt. In der Summe haben Wolken im Mittel einen negativen Strahlungseffekt von ca. $20-30 W/m^2$ (Stuhlmann, 1995). Niederschlag beeinflusst nicht nur das Leben auf der Erde, sondern hat auch Einfluss auf den Energie- und Wasserkreislauf der Erde. Niederschlag führt zu einer Abkühlung der Erdoberfläche, da Wärme für dessen Verdunstung aufgebracht werden muss. Die dabei entstehende latente Wärme in Form von Wasserdampf, wird bei der Wolkenbildung durch die Kondensation von Wasserdampf wieder freigesetzt. Der Einfluss von Wolken und Niederschlag auf das Klima der Erde betrifft verschiedene räumliche und zeitliche Skalen. Um Wolken und Niederschlag auf verschiedenen räumlichen und zeitlichen Skalen analysieren und verstehen zu können ist deren systematische, globale, räumlich und zeitlich hoch-aufgelöste Beobachtung notwendig.

Die Beobachtung von Wolken und Niederschlag ist mittels verschiedener Messsysteme möglich, welche jeweils individuelle Stärken und Schwächen haben. In dieser Arbeit werden Daten von Wolken und Niederschlag jeweils basierend auf klassischer synoptischer Beobachtung/ Messung, auf Satellitenbeobachtung, und auf Basis von numerischer Wetter- und Klimamodelle analysiert. Die klassische Beobachtung von Wolken an synoptischen Wetterstationen basiert auf Augenbeobachtungen, welche geometriebedingte Unsicherheiten haben. Zudem ist die Schätzung von Wolken in der Nacht schwierig. Hinzu kommt dass der weitaus größte Teil der Erde auf diese Weise nicht beobachtet werden kann. Satelliten beobachten Wolken aus großer Höhe und nutzen dafür meist abbildende Sensoren im sichtbaren und infraroten Wellenlängenbereich. Aufgrund der flächendeckenden Beobachtung erfassen Satelliten Wolken global und, im Falle von geostationären Satelliten (z.b. der METEOSAT-Satelliten), auch in hoher zeitlicher und räumlicher Auflösung. Einschränkungen bei der Wolkendetektion gibt es über hellen Oberflächen, und

nachts entfällt die Nutzung der sichtbaren Spektral-Kanäle des Satelliten. Satelliten ermöglichen auch die Ableitung der Wolkenhöhe durch die Detektion von Wolkenoberkantentemperaturen.

Die synoptische Messung von Niederschlag erfolgt klassisch durch Regenmesser – meist automatisierte Messtöpfe. Diese Art der Regenmessung ist weit verbreitet und bietet eine gute Messqualität. Für eine globale Abschätzung von Niederschlag ist die räumliche Verteilung von Regentöpfen jedoch nicht ausreichend, da weite Teile der Erd- und besonders der Ozeanoberfläche nicht abgedeckt sind. Satellitenbeobachtungen können diese Lücken im klassischen Regenmessnetz füllen – wenn auch im Allgemeinen mit geringerer Beobachtungsqualität (Tian and Peters-Lidard, 2010). Aufgrund der großen räumlich und zeitlichen Variabilität von Niederschlag ist die Schätzung von Niederschlag basierend auf Satellitendaten jedoch meist unsicherer als die satelliten-basierte Wolkenbeobachtung. Zudem ist die satellitenbasierte Ableitung von Niederschlag am Boden indirekter als jene von Wolken.

Wolken und Niederschlag sind meteorologische Parameter die in der Modellierung von Wetter und Klima eine große Rolle spielen. Die Prozesse die zur Entstehung von Wolken und Niederschlag führen, können von diesen Modellen jedoch meist nicht aufgelöst werden. Dies gilt auch für Wolken und Niederschlag selbst. Diese kleinskaligen Prozesse und Phänomene müssen dann in den Modellen parametrisiert werden. Parametrisierungen stellen immer eine standardisierte und stark vereinfachte numerische Beschreibung der Wirklichkeit dar und sind somit eine Quelle für Unsicherheiten und Fehler im Modell (e.g. Dirmeyer et al., 2012).

Von Relevanz ist auch der Tagesgang von Wolken und Niederschlag, der maßgeblich Energieflüsse in der Atmosphäre beeinflusst und eine wichtige klimatische Eigenschaft darstellt. Auf globaler Skala ist eine Analyse der Tagesgänge von Wolken und Niederschlag nur mit Hilfe von Satellitenbeobachtungen möglich. Satellitendaten fanden in der letzten Jahren verstärkt Anwendung im Bereich der Klimaanalyse und Klimavariabilität (Schulz et al., 2009). Satellitendaten werden außerdem genutzt um regionale und globale Wetter- und Klimamodelle auf verschiedenen raumzeitlichen Skalen zu validieren. Aus Mangel an geeigneten Referenzdaten ist die Validierung der Satellitendaten selbst oft nur regional und zeitlich begrenzt möglich, aber dennoch von großer Wichtigkeit um Stärken und Schwächen von Satellitendaten zu erkennen und letztlich um Fehlinterpretationen zu vermeiden. Oft gibt es eine Vielzahl von Satellitendatensätzen, die jedoch nicht alle für sämtliche Anwendungen geeignet sind. Referenzdaten für Niederschlag am Boden, in hinreichender zeitlicher Auflösung um den Tagesgang von Niederschlag analysieren zu können sind daher von großer Wichtigkeit. Diese Niederschlagsdaten können zur Validierung von Modell- und Satellitendaten und deren Tagesgang genutzt werden.

Besonders in den Tropen, wo große Tagesgänge im Niederschlag existieren (cf. 4.2), sind Regenmessdaten rar. Von großem Wert ist daher die Datenbank des *African Monsoon Multidisciplinary Analysis—Couplage de l'Atmosphere Tropical et du Cycle Hydrologique* (AMMA-CATCH)- Projektes, welche hochauflösende Niederschlagsdaten für die Wissenschaft zur Verfügung stellt (Lebel et al., 2010). Jene AMMA-CATCH Daten werden in dieser Arbeit genutzt um verschiedene satelliten-basierte Niederschlagsdatensätze im tropischen bis subtropischen Klima Afrikas zu validieren. Es zeigte sich hierbei, dass die Satellitendaten die am Boden gemessenen Tagesgänge des Niederschlags insgesamt gut reproduzieren können. An den innertropischen Stationen in der Westafrikanischen Region um Ouémé zeigt sich einerseits die gute Qualität der Satellitenprodukte, andererseits jedoch auch die klare Tendenz vieler Satellitendatensätze den Zeitpunkt des maximalen Niederschlags im Tagesgang um 1 bis 2 Stunden verspätetet zu "beobachten". Dies trifft besonders auf den *Precipitation Estimation from Remotely Sensed Information using Artificial Neural Networks* (PERSIANN) - Datensatz zu, der als einziger der analysierten Datensätze ausschließlich auf Satellitenbeobachtungen im infraroten (IR) Spektralbereich basiert. Es wird daher als sehr wahrscheinlich betrachtet, dass der typische Tagesgang, bzw. der Zyklus eines lokalen (tropischen) Schauers von IR-Satellitensensoren, die den Niederschlag ausschließlich auf Basis von Wolkenoberkantentemperaturen schätzen, systematisch fehlinterpretiert wird. Dies wird von der Beobachtung gestützt, dass der Tagesgang der Wolkenoberkantentemperaturen mit dem Tagesgang des vom Satelliten geschätzten Niederschlags übereinstimmt. Auch Satellitendatensätze deren Algorithmen IR-Sensoren zusammen mit anderen Sensoren (meist Mikrowellen-Sensoren) für die Ableitung von Niederschlag verwenden, sind vom verspäteten Niederschlagsmaximum im Tagesgang teilweise betroffen.

Es wurden zusätzlich die *Modern-Era Retrospective Analysis for Research and Application* (MERRA) und die Simulation des *Consortium for Small Scale Modelling - Climate Local Model* (CCLM) in West Afrika analysiert und mit den Beobachtungsdaten verglichen. Es zeigte sich in MERRA und CCLM dass der Niederschlagstagesgang, der vor allem durch lokal entstehende Regenschauer am Abend entsteht, nicht korrekt simuliert wird. Die simulierten Tagesgänge weisen an den innertropischen Stationen nur ein Maximum im Tagesgang am Mittag auf, während in der Realität im Mittel zwei Peaks (am Morgen und am Abend) während der Monsoon-Saison in West Afrika vorherrschen. Beide modellbasierte Produkte simulieren das Niederschlagsmaximum am Abend mehrere Stunden zu früh. Diese zeitliche Verschiebung im Tagesgang des Niederschlags ist ein bekanntes Problem, welches auf die Verwendung von Parametrisierungen für Konvektion und Niederschlag zurückgeführt wird (Hohenegger et al., 2008), dennoch steckt in der Verwendung von Parametrisierungen noch Potential für Verbesserungen (e.g. Bechtold

et al., 2014). Die Analyse der CCLM Simulationen in West Afrika zeigt auch, dass eine verbesserte Behandlung der Energieflüsse zwischen Boden und Grenzschicht den Tagesgang des Niederschlags beeinflusst.

Im Allgemeinen zeigen Satellitenbeobachtungen das bekannte Verhalten des Tagesgangs von Niederschlag mit Unterschieden zwischen Ozean und Kontinent. Über Land zeigt der Tagesgang ein Minimum am Morgen und ein Maximum am Nachmittag. Über Ozean ist das Verhalten umgekehrt. In den Küstenbereichen der Ozeane oder im gebirgigem Terrain gibt es größere Abweichungen vom allgemeinen Muster. Insgesamt ist der Tagesgang von Niederschlag über Land deutlich ausgeprägter als über Ozean.

Der klimatologische Tagesgang der Wolkenbedeckung ähnelt dem Tagesgang von Niederschlag. Große systematische Tagesgänge der Wolkenbedeckung gibt es in den subtropischen Ozeanbereichen östlich von Amerika und Afrika – den Bereichen der Passatinversion. Diese Tagesgänge können durch Satellitendaten gut erfasst werden und auch das regionale Klimamodell CCLM und globale modellbasierte Reanalysen können die Tagesgänge in diesen subtropischen Stratocumulus-Bereichen gut simulieren können – auch wenn Abweichungen im mittleren Bedeckungsgrad existieren. Die Abweichungen sind auch auf die unterschiedlichen Definitionen von Wolke in Modellen und Satellitendaten zurückzuführen und omnipresent – auch zwischen verschiedenen Satellitendatensätzen.

Auch in Europa wurde der Tagesgang der Wolkenbedeckung analysiert. Dort stimmten die Tagesgänge zwischen den Satellitenprodukten des *International Cloud Climatology Project* (ISCCP) und der *EUMETSAT Climate Monitoring Satellite Application Facility* (CM SAF) gut überein. Als unabhängige Referenz wurde ein gegitterter Datensatz basierend auf synoptischen Beobachtungen des Wolkenbedeckungsgrades erstellt. Der Vergleich mit den Satellitendaten zeigt eine gute Übereinstimmung der Tagesgänge im Sommer, wenn der Tagesgang am größten sind. Im Winter treten nur kleine Tagesgänge der Wolkenbedeckung auf, wobei die Satellitendaten größere Tagesgänge detektieren. Ein Grund für diese Unterschiede ist die zusätzliche Nutzung von sichtbaren Spektralkanälen der Satellitensensoren solange Tageslicht vorhanden ist. Dieser zusätzliche Spektralbereich verbessert einerseits die Wolkendetektion der Satelliten, führt aber andererseits zu einem kleinen künstlichen Tagesgang mit einem Maximum während der Mittagszeit. Die klaren Tagesgänge der Wolkenbedeckung im Sommer Europas mit maximaler Wolkenbedeckung am Nachmittag konnten von der analysierten CCLM Klimasimulation nicht wiedergegeben werden. Dieser Fehler hat direkten Einfluss auf die Strahlungsrechnungen im Modell. Eine wahrscheinliche Folge dessen ist die beobachtete Unterschätzung der täglichen Temperaturamplitude im Modell im Vergleich zu Stationsdaten in Zentral- und Osteuropa.

Über den Ozeanen gibt es kaum bodengebundene Niederschlagsmessungen über

einen längeren Zeitraum. Eine Ausnahme stellen Niederschlagsmessungen auf Atollen im Pazifischen Ozean dar, welche in der *Comprehensive Pacific Rainfall Database* (PACRAIN) enthalten sind. Atolle sind sehr kleine und flache Inseln, deren Niederschlagscharakteristik als sehr ähnlich zum offenen Ozean angesehen werden (Sobel et al., 2011). Diese Niederschlagsdaten sind aber nicht in ausreichend hoher zeitlicher Auflösung verfügbar um die Analyse des Tagesganges zu erlauben. Trotzdem ermöglichen es diese Atoll-Daten ozeanischen Niederschlag zu analysieren und Satellitendaten sowie Modelldaten über dem Ozean zu validieren. In dieser Arbeit wird der monatliche Niederschlag zweier Satelliten- und zweier Reanalysen mit den Daten der Atoll-Stationen validiert. Die Validation zeigt mittlere monatliche Abweichungen der Satellitenprodukte des *Global Precipitation Climatology Project* (GPCP) und *Hamburg Ocean and Atmosphere Parameters from Satellites* (HOAPS) von der Referenz am Boden von etwa 20 bis 30 %. Die Abweichungen der *European Center for Medium-range Weather Forecast Interim Reanalysis* (ERA-Interim) und der MERRA Reanalyse zu den Atoll-Regenmessern sind ähnlich groß. Die Korrelationskoeffizienten der monatlichen Absolutwerte zwischen den Satellitenprodukten bzw. der Reanalysen und der PACRAIN Atolldaten liegen im Bereich von 0.6 bis 0.8. Die besten Validierungsergebnisse zeigte der GPCP Niederschlagsdatensatz, obwohl er die schlechteste räumliche Auflösung bietet. Der Niederschlag aus dem HOAPS Datensatz und die Reanalyse-Daten von ERA-Interim und MERRA lieferten insgesamt ähnliche Validierungsergebnisse bezüglich der mittleren Fehler und Korrelationen, bei Verwendung der Daten in Original-Auflösung. Bei der Analyse auf einem gemeinsamen, gröberen Gitter von $2.5° \times 2.5°$ zeigten sich reduzierte Abweichungen und erhöhte Korrelationen – besonders beim HOAPS Datensatz. Der HOAPS Datensatz basiert nur auf einer Art Satelliten-Sensor einer polarumlaufenden Satellitenserie, was in Bezug auf die räumlich-zeitliche Abdeckung erhöhte Unsicherheiten in den Anfangsjahren des HOAPS Datensatzes zur Folge hat. Dies zeigte die separate Validierung für die Zeiträume wenn ein, zwei und drei Satelliten zur Erstellung des HOAPS Datensatzes zur Verfügung standen: die Abweichungen zur Referenz reduzierten sich signifikant. Können drei Satelliten gleichzeitig verwendet werden, übersteigt die Datenqualität die der Reanalysen und nähert sich der Qualität der GPCP Daten an.

Es zeigte sich auch dass die Daten des GPCP den Niederschlag insgesamt unterschätzen. Auch bei der globalen Analyse der Energiebilanz der Erde wird meist der GPCP verwendet. Der latente Wärmefluss, der durch Niederschlag (von GPCP) kompensiert wird, wird teilweise kontrovers diskutiert. Einige Analysen deuten auch hier auf eine Unterschätzung des Niederschlags von GPCP im globalen Mittel hin, welches maßgeblich durch den tropischen Niederschlag geprägt ist (Trenberth et al., 2009; Stephens et al., 2012; Wild et al., 2015).

Zusammenfassend zeigt diese Arbeit dass die Erfassung des Tagesganges von Wolken und Niederschlag mit Hilfe von Satelliteninformationen mit guter Qualität möglich ist. Die Validierungen der Satellitendaten mit unabhängigen Referenzdaten im tropischen Afrika und in Europa zeigten aber auch situationsbedingte Schwächen bei der Ableitung von Niederschlag und Wolken basierend auf Satellitendaten.

Bei der Erfassung der Wolkenbedeckung zeigten sich Probleme bei Sonnenauf- und Sonnenuntergang und über sehr hellen Oberflächen, wie Wüsten, die zu künstlichen Wolkentagesgängen in Satellitendaten führen können. Bei letzteren ist die Verwendung mehrerer Spektralkanäle von Vorteil, wie dies bei den verwendeten Wolkendaten des CM SAF der Fall ist. Über den Ozeanen, die einen homogenen Hintergrund für die Beobachtung durch Satelliten darstellen, ist die Wolkendetektion tendenziell sensitiver als über Land und auch Tagesgänge können gut erfasst werden. Vor der vergleichenden Analyse absoluter Werte der Wolkenbedeckung ist dagegen eher abzuraten, da keine datensatz- bzw. datenquellenübergreifende Definition von Wolkenbedeckung bzw. Wolke existiert und mittlere Abweichungen daher allein definitionsbedingt existieren.

Satelliten-basierte Datensätze des Niederschlags sind nicht nur in der Lage die globale klimatologische Verteilung von Niederschlag sondern auch deren Tagesgänge zu erfassen. Intensive Niederschläge aus hochreichender Bewölkung können mit Hilfe von Satellitenbeobachtungen gut abgeleitet werden (Ebert et al., 2007). Andererseits bringt die hohe raumzeitliche Variabilität von Niederschlag Unsicherheiten mit sich, da die Abdeckung der Satelliten zu keiner Zeit global vollständig ist, denn Satelliten beobachten die Atmosphäre immer nur zu einzelnen Zeitpunkten. Die Nutzung einer Vielzahl verschiedener Satelliten verbessert somit die raumzeitliche Abdeckung und letztlich die Ableitung von Niederschlag, was beispielsweise die separate Analyse des HOAPS Datensatzes zeigt.

Das Verfahren zu Ableitung von Niederschlag ist zwar vom verwendeten Satellitensensor abhängig, aber meist unabhängig vom Niederschlagsregime. Die Analyse der Niederschlagstagesgänge im tropischen Afrika zeigt, dass die Ableitung des Niederschlags bei lokal entstehenden konvektiven Niederschlägen teils zeitlich versetzt zur Bodenmessung erfolgt. Der maximale Niederschlag im Tagesgang am Abend, wird, höchstwahrscheinlich durch Satellitendaten im infraroten Spektralbereich, zeitlich systematisch bis zu zwei Stunden zu spät abgeleitet. Ein Grund dafür ist dass der maximale Niederschlag im Lebenszyklus einer tropischen Gewitterwolke zu einem relativ frühen Zeitpunkt auftritt, noch bevor die Wolke ihre maximale Höhe und Ausdehnung erreicht hat (Futyan and Del Genio, 2007).

Die beobachteten tropischen Niederschlagstagesgänge können weder von den analysierten Klimasimulationen des CCLM noch von der MERRA Reanalyse korrekt wiedergegeben werden. Der größten Verbesserungen bzgl. Konvektion und

folglich des Tagesgangs von Wolken und Niederschlag zeigen sehr hoch aufgelöste, sogenannte konvektions-erlaubende Simulationen (e.g. Ban et al., 2014; Fosser et al., 2015; Brisson et al., 2016) – allerdings ist deren globale Anwendung auf langen Zeitskalen derzeit (Stand 2016) noch zu aufwendig.

List of contributing Peer-reviewed Publications

Pfeifroth, U., Hollmann, R. and Ahrens B. (2012): Cloud Cover Diurnal Cycles in Satellite Data and Regional Climate Model Simulations. *Meteorologische Zeitschrift*, 21(6):551-560.

Pfeifroth, U., Mueller, R. and Ahrens B. (2013): Evaluation of Satellite-based and Reanalysis Precipitation Data in the Tropical Pacific. *Journal of Applied Meteorology and Climatology*, 52(3):634-644.

Pfeifroth, U., Trentmann, J., Fink, A. H. and Ahrens B. (2016): Evaluating satellite-based diurnal cycles of precipitation in the African tropics. *Journal of Applied Meteorology and Climatology*, 55(1):23-39.

List of Figures

List of Tables

Chapter 1

Introduction

Knowledge of the energy- and water cycle of the Earth-atmosphere system is essential for understanding the current and predicting the future climate. The energy cycle is controlled by the radiative energy coming from the sun, which reaches the troposphere mainly in the visible spectral range from 0.6 to about 4 μm. This incoming solar radiation is then subject to extinction by the troposphere until it reaches the Earth's surface. There, it is partly reflected and primarily absorbed, resulting in an increase of surface temperatures. The Earth itself emits long wave, terrestrial radiation in the spectral range of 8 to 14 μm back into space, approximately following Planck's law of black body radiation, modified through atmospheric extinction. The atmosphere and especially the troposphere is strongly affecting the energy fluxes that control the Earths climate. A global averaged overview of the relevant energy fluxes is shown in Figure 1.1 (Wild et al., 2015).

A climate variable, which is directly influencing the Earths energy fluxes, is cloudiness. Overall clouds have a cooling effect on surface temperatures (e.g. Raschke et al., 2005; Loeb et al., 2009). Assuming a constant amount of uniform clouds throughout the day, the cloud radiative effect would be relatively easy to determine by radiative transfer calculations, if cloud properties are given. In reality, clouds are micro- and macro-physically variable in space and time. Hence, it has to be of major concern where and when during the day a cloud develops or clears away, as this is directly affecting local meteorological conditions. It is important to know about diurnal variations of clouds around the globe (Cairns, 1995; Schulz et al., 2009). Precipitation is not only essential for life on Earth, but also leads to significant heat fluxes between the surface and the troposphere and has a surface cooling effect. Precipitation leads to a moistening of the surface and to a subsequent cooling through evaporation at the surface owing to the amount of energy necessary to evaporate water. As a consequence the atmosphere is moistened. This in turn favors the development of clouds again, which release latent heat during the condensation of water vapor. Overall, this evaporation-condensation cycle

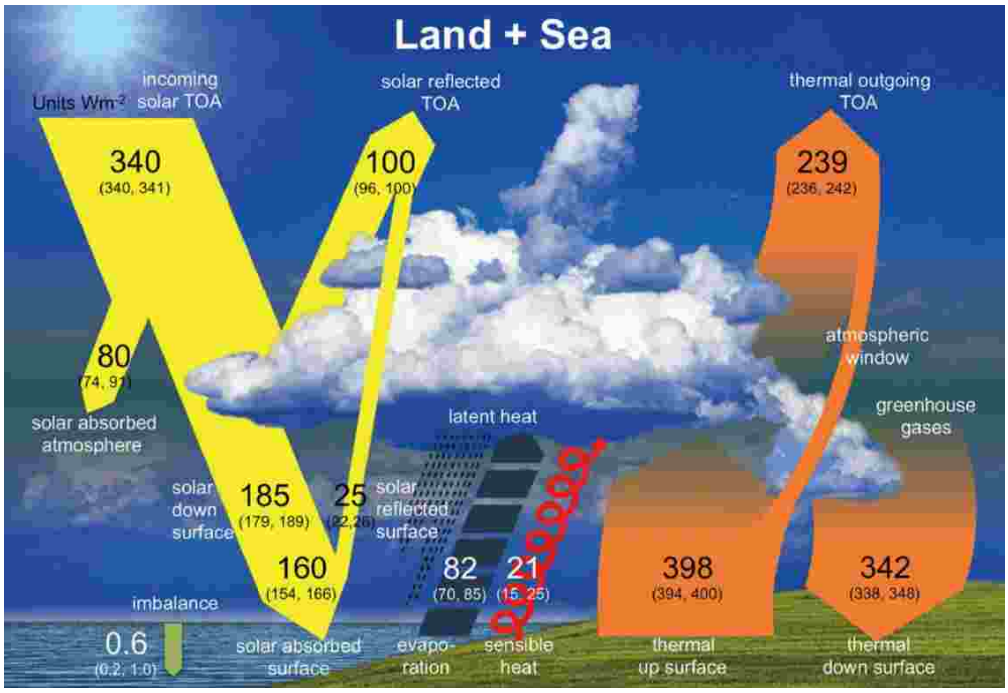

Figure 1.1: Globally averaged energy flows;
Source: Wild et al. (2015)

transports heat from the surface and from the lower troposphere to the middle and upper troposphere.

Clouds and cloud types are still observed through eye-observations, usually four to eight times per day at synoptic stations. Unfortunately these observations are globally irregularly distributed and their quality is reduced during nighttime, and additionally may depend on the individual observer. Furthermore, there is a tendency towards the automation of meteorological observations. This increases the importance of alternative cloud observations, like the ones possible by satellites. But different types of cloud observations may have different properties, which is a simple consequence of the different definitions of clouds. This in turn requires the evaluation of the different cloud observations. Nowadays satellite observations are an indispensable data source (Cairns, 1995). Satellites enable the global observation of clouds including its spatial and temporal variability (c.f. Figure 1.2).

Hence, satellite observations are a unique tool to validate weather and climate models from the global to regional scale. But satellite-based observations of clouds are also subject to uncertainties owing to different observational sensitivities under certain conditions. This thesis will give some advice on the usage of such data.

Measuring surface precipitation can be simple. It has been done since the early days of meteorological observations by using rain buckets or rain gauges. Rain is

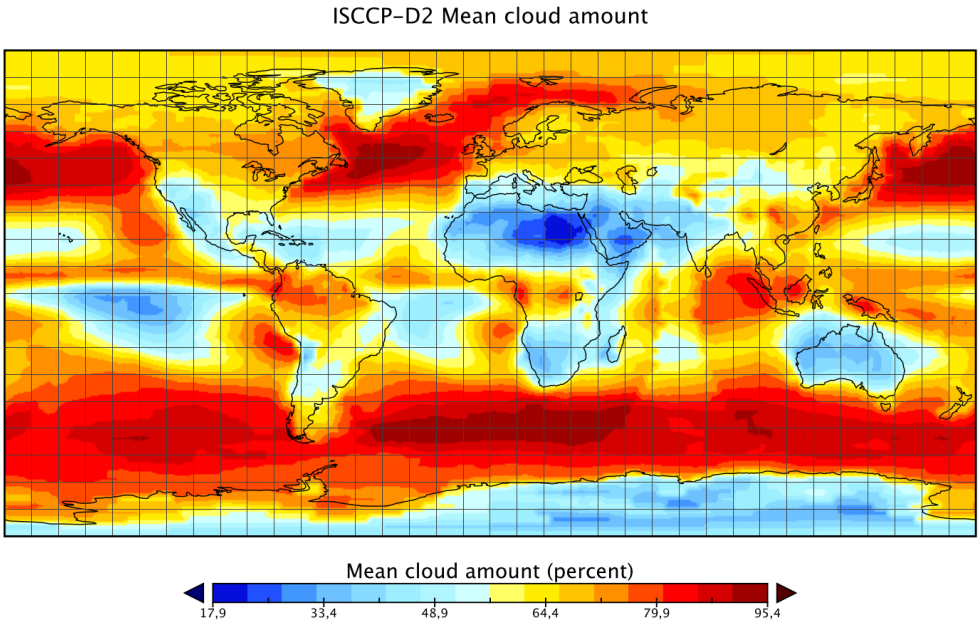

Figure 1.2: Long-term mean cloud amount (percent), based on ISCCP-D2 data

collected in the bucket and its amount can then be calculated using simple mathematics. But measuring precipitation consistent on the globe is still a big challenge (Michaelides et al., 2009). Regionally, the density of rain gauges is very sparse (Schneider et al., 2013) and observations over oceans are almost absent. Owing to the high spatiotemporal variability of precipitation, the interpolation of rain gauge data is inherent to uncertainties, especially on short time scales. Although the global surface-based precipitation measurement network is incomplete, the Global Precipitation Climatology Center (GPCC) (Schneider et al., 2013) and the Climate Research Unit (Harris et al., 2014) have successfully collected rain gauge data and provide gridded rainfall information, at least over land areas. Precipitation can also be observed by ground-based radar measurements, but such radar data is absent in most parts of the Earth. Satellite data is the only observational data source of precipitation in many parts of the world.

Since the 1990s, precipitation is estimated by means of satellite remote sensing to fill the gaps in rain gauge networks (Kucera et al., 2013). Satellite-based precipitation data requires the solution of an under-determined inverse problem which can only be done by using several assumptions that induce uncertainties to the precipitation estimates. Established datasets, like the Global Precipitation Climatology Project (GPCP) (Huffman et al., 2009), have enhanced our knowledge on the global distribution of precipitation (c.f. Figure 1.3). In the meantime a number of satellite-based datasets have been developed (Kidd and Levizzani,

2011) and some of them offer quasi-global data coverage in high spatial and temporal resolution. Theses datasets allow also for the analysis of precipitation on the sub-daily temporal scale (e.g. Janowiak et al., 2005).

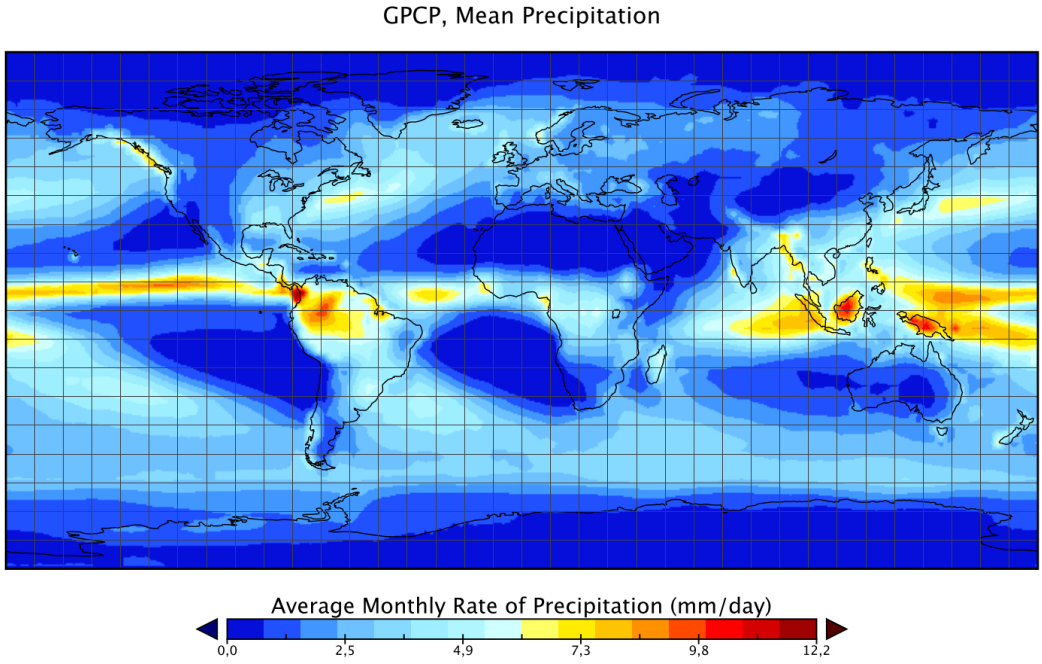

Figure 1.3: Long-term mean precipitation (mm/d), based on GPCP data

The systematic diurnal variability, referred to as diurnal cycle, is an important climate feature that is influencing larger scales and vice versa. Nevertheless, the sub-daily scale is often disregarded in the climatological analysis, and the main focus is usually on the daily and lower resolution temporal scales. This is partly a consequence of the missing of observations in high-frequency and high-quality.

The diurnal cycle is often driven by local small-scale processes, like convection. These processes are often not well represented in numerical models, e.g. climate and weather prediction models. This model weakness in representing diurnal cycles is problematic as the micro- and macro-scale processes can influence the meso-scale up to even larger scales. Models usually have difficulties to get the small scales correctly, because small-scale processes cannot be resolved explicitly. Parametrization are used instead (Dai, 2006). To overcome model deficiencies on small scales, models are usually tuned to get the larger scales as best as possible, but the large scale may then be right for the wrong reasons. Hence it is not a straightforward exercise to improve models on the sub-daily scale. It has been shown that spatially highly resolved atmospheric models perform better in reproducing the sub-daily variability of parameters like clouds and precipitation (Hohenegger et al., 2008),

but their computational costs are immense. As a consequence its long-term application on a global scale is not possible at the moment.

In a changing climate, it is likely that there might also be changes in small scale processes, which then may influence the diurnal variability systematically. The scientific community is still not having profound knowledge on the coupling of smaller and larger scales neither in the current nor in a future climate. However, it is a necessity to analyze the current status of the diurnal cycles of climatological relevant parameters, like clouds and precipitation, e.g. by using appropriate observational data.

In this thesis, different satellite-based and numerical model-based data, including reanalysis data, are used to analyze their ability to reproduce the correct variability of clouds and precipitation, focusing on climatological diurnal cycles. Within this scope, the determination of the quality of a certain dataset is assessed, and possible weaknesses are revealed, by evaluating different satellite- and numerical-model-based data with reference measurements if available, or integrated within the meteorological background. The reference data used for precipitation and cloud cover are rain gauge data and Synop observations of clouds by meteorologists, respectively.

The main goals of this thesis are

- the assessment of the current status of the global climatological distribution of cloud cover, precipitation, and its diurnal cycles as given by observational datasets

- the evaluation of satellite-based and numerical-based data of clouds and precipitation by comparison to reference observations, with focus on its diurnal cycles, in order to

  ⇒ support current and future users of cloud and precipitation data to choose appropriate data for their application and let the user be aware of certain data limitations that exist for each of the data sources analyzed

  ⇒ support the generators of the satellite- and model-based data to further develop and improve their datasets

This thesis is structured as shown in the flowchart of Figure 1.4. In chapter 2 the meteorological background of clouds and precipitation and its importance for the climate system are described. The theoretical basics of estimating clouds and precipitation by means of satellite remote sensing are given, together with an introduction to the treatment of clouds and precipitation in numeric models. In chapter 3, the used datasets based on satellites, ground-based observations, and

numerical models are described. The main results of the thesis are shown and discussed in chapter 4.

The global distribution of clouds and precipitation and its diurnal cycles diurnal are presented for land and ocean areas in sections 4.2 and 4.1.

In Europe, cloud cover diurnal cycles of the satellite products of the International Cloud Climatology Project (ISCCP) and of the Satellite Application Facility on Climate Monitoring (CM SAF) are compared and evaluated with gridded Synop observations of clouds. Further, long-term simulations of the Consortium for Small Scale Modelling - Climate Local Model (COSMO-CLM) are validated with the ISCCP data in Europe (see Section 4.2.1).

In the West African tropics, precipitation data from several satellite-based datasets, including Tropical Rainfall Measuring Mission (TRMM) Satellite datasets, Climate Prediction Center Morphing technique (CMORPH) datasets, and Precipitation Estimation from Remotely Sensed Information using Artificial Neural Networks (PERSIANN) data are evaluated for climatological diurnal cycles and its variability using high-resolution rain gauge data from the African Monsoon Multidisciplinary Analysis - Couplage de l'Atmosphère et du Cycle Hydrologique (AMMA-CATCH) database (see Section 4.2.2). Also COSMO-CLM simulations are evaluated in the same region.

In the tropical Pacific, monthly rain gauge data from atolls, provided by the Comprehensive Pacific Rainfall Database (PACRAIN), are used to evaluate the satellite-based data of the Hamburg Ocean Atmosphere Parameters from Satellite Data (HOAPS), and the Global Precipitation Climatology Project data (GPCP), and the reanalysis datasets of European Center for Medium-range Weather Forecast Interim Reanalysis (ERA-Interim) and Modern-Era Retrospective Analysis for Research and Application (MERRA), in open ocean-like conditions (see section 4.1.2).

Conclusions are drawn in chapter 5, while the three peer-reviewed publications that form the basis of this doctoral thesis can be found in the appendix, together with two more relevant studies.

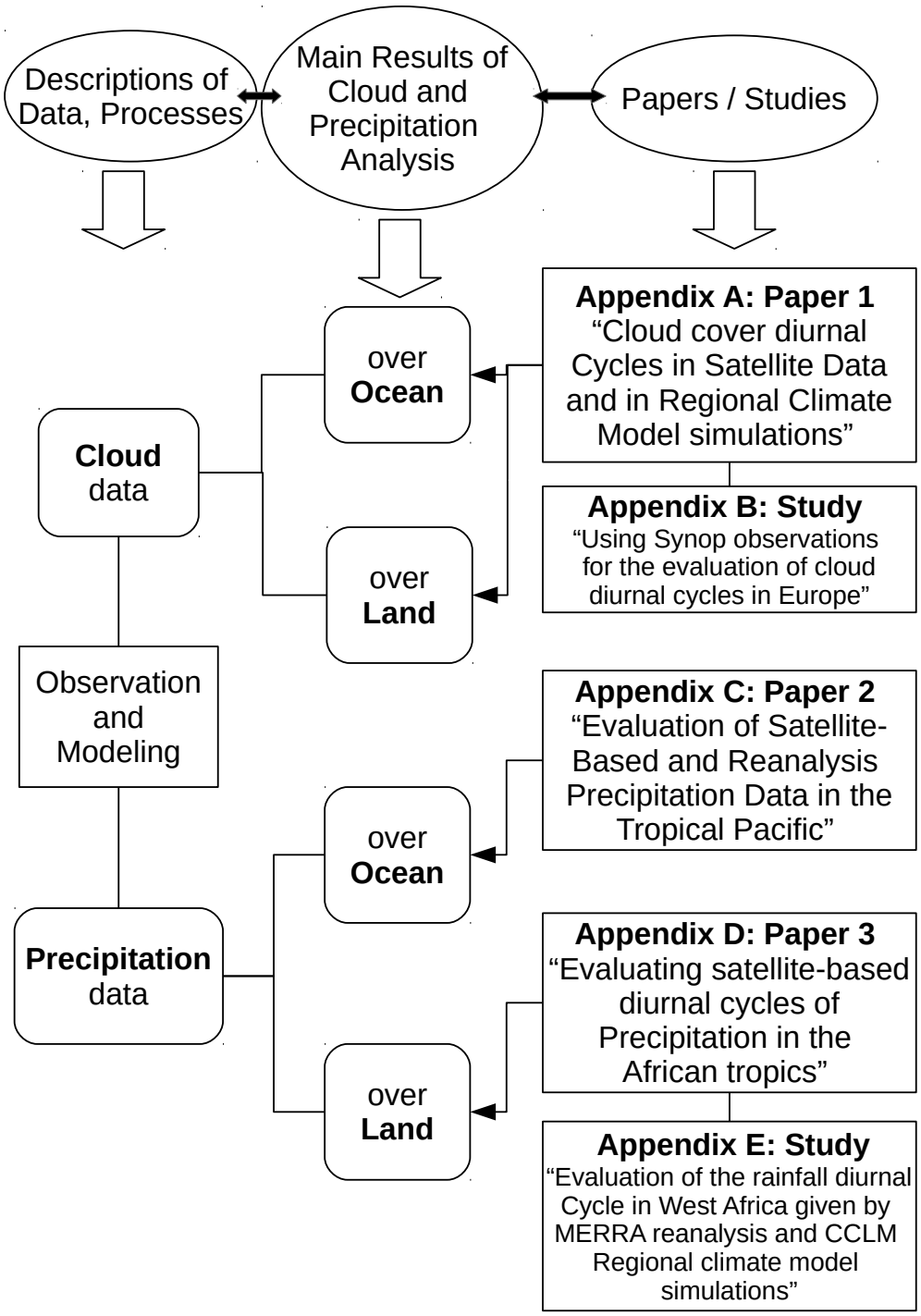

Figure 1.4: Flowchart of the structure of the thesis.

Chapter 2

Meteorological and Theoretical Background

2.1 Clouds and Precipitation

A cloud is defined as a visible aggregate of water droplets and/or ice particles in the atmosphere (see `http://glossary.ametsoc.org`). In general, tropospheric air contains a certain amount of water vapor. When air is cooled, e.g. because of upward motion or radiative cooling, the relative humidity is increased. When the relative humidity exceeds 100 % the water vapor condensates on aerosol particles, which act as cloud condensation nuclei. When the air is cooled down further, the cloud droplets grow by condensation and coagulation processes. At temperatures below about −30 °Celsius ice crystals begin to form, depending on the availability of ice nuclei. At temperatures below about −40 °Celsius no liquid water is present in clouds. Precipitation is usually formed through the ice phase of clouds.

Clouds occur at different levels in the troposphere - from fog at the bottom to cirrus clouds in the upper troposphere. Moreover, clouds can have different vertical extensions; Cumulonimbus clouds may reach a maximum vertical extend from cloud base to cloud top of more than 10 km, while thin cirrus clouds are often only about 100 m thick. Clouds have a certain temperature which is air mass dependent and in particular dependent on the vertical position of the cloud in the troposphere. The temperature of a cloud, which is usually lower than the surface background, plays a major role for its remote sensing by satellites. More information on the detection of clouds by means of satellite remote sensing are given in section 2.3.1

Clouds are mainly formed through large-scale lifting, radiative cooling or convective processes. Large-scale lifting occurs at the frontal zones of different air masses. Radiative cooling occurs in case of low solar insolation, and is often the

process responsible for the development of fog. Convection is the process leading to a lifting of air mass in the troposphere that is described in more detail in section 2.2.

Clouds are of highest importance for the Earths climate. Clouds interact with the solar shortwave and terrestrial longwave radiation. Incoming solar radiation is reflected by clouds—a surface cooling effect. On the other hand, clouds absorb and emit radiation—a surface warming effect. Globally averaged, clouds have a negative radiative forcing of about -15 to $-20\,\mathrm{W/m^2}$, i.e. the presence of clouds has a net cooling effect at the surface (e.g. Stuhlmann, 1995; Raschke et al., 2005).

On smaller temporal and spatial scales clouds can have a much larger impact on the local radiation budget and hence on the state of the troposphere. The mean radiative cloud effect is dependent of the mean spatial and temporal distribution of clouds. Cloud diurnal cycles can have substantial impacts on the local and global climate (Arkin, 1991). In the context of global warming, changes in clouds and in its spatial and temporal distributions are likely. This poses a major challenge for the assessment of impacts and cloud feedbacks in a changing climate (Bony et al., 2015).

Precipitation is formed when cloud droplets and/or ice crystals reach a certain size and weight so that they overcome the buoyancy and fall toward the ground. Surface precipitation is highly variable in space and time. Long-lasting precipitation events can occur at stationary fronts while precipitation formed through convective processes is usually more short-lived and spatially more small-scale. But convection can also be organized, e.g. in so-called Mesoscale Convective Systems (MCSs) (Mathon et al., 2002; Houze Jr., 2004).

The climatological amount of precipitation (cf. Figure 1.3) is of major importance for the society, economy and for human life in general. Moreover not only the mean precipitation but also its temporal variability is of high relevance. The mean diurnal cycle of rainfall controls not only river discharge, but is also relevant for the local evapotranspiration, which leads to reduced surface temperatures and to a moistening of the troposphere. The diurnal cycle of precipitation is an important regional but also global climate feature that affect the state of the troposphere.

2.2 Tropospheric Convection

Tropospheric convection is the main driver for diurnal cycles of clouds and precipitation. Convection describes the process of the vertical motion of air due to buoyancy forces. Buoyancy forces in the troposphere occur, for example, when air parcels are heated, resulting in a reduced density and upwards buoyancy. A continued lifting of air due to buoyancy occurs if tropospheric conditions are favorable for convection, i.e. if the stratification of the troposphere is unstable. If the vertical

temperature gradient is stronger than the adiabatic laps rate of 0.65 K/100 m for moist air and 1 K/100 m for dry air, a lifted air parcel will continue to be warmer than its surrounding air, and will therefore be further lifted. The lifting air mass will be cooled as it reaches higher altitudes and might form cloud droplets and ice crystals and finally rain droplets, if tropospheric conditions are favorable and sufficient moisture is available.

Convection is frequent in the tropics and occurs in different forms—from shallow to deep convection—and even deep convection can be of different kind (Houze Jr. et al., 2015). As convection is mostly triggered by the heating of air close to the surface by solar insolation over land masses, convection most often occurs in the tropics and on the respective summer hemisphere of the Earth, assuming the availability of sufficient water vapor. Convection can also be triggered due to a forced lifting of air while overflowing some rough topographic terrain. Over the oceans, the process of convection is mostly induced by the temperature gradient between the ocean water and a relatively cooler lower troposphere, owing to the different heat capacities of land and water. On average, convection is more intense over land. The time of day when the maximum vertical temperature gradients occurs, and hence the troposphere is layered most unstable, often coincides with the time when convection occurs most likely. The time during day that is most favorable for convection significantly differs between land and ocean. Timing differences between land and oceans have already been found by Dai et al. (1999) for diurnal cycles of surface wind convergence. Over the oceans, the vertical temperature gradient between the surface and the free lower troposphere is usually maximal during the early morning. At that time the air has cooled down during nighttime, while the ocean water remains relatively warm because of its larger heat capacity. Over land, the maximum temperature gradient usually exists in the afternoon, when the land mass is heated up by solar radiation. These differences result in different diurnal cycles of clouds and precipitation over land and ocean areas.

West Africa West Africa is a region with frequent convective activity during the monsoon season (May–September). The monsoonal circulation in that region transports moist and moderate tempered air in the lowermost troposphere (up to 1-2 km height) from the Atlantic Ocean towards the West African continent. Over land, this moist airmass is heated by the strong solar insolation during daytime. At the same time, colder and dryer air is advancing in south-western direction towards West Africa in the mid-tropospheric levels, the so-called Northeasterly Trades (Lafore et al., 2011). When these two air masses meet, strong vertical temperature gradients occur, which are accompanied by a large convective available potential energy (CAPE). If the warm and moist boundary layer airmass gets lifted and

enters into the colder and dryer air above, the warm and moist air gets further lifted. This lifting process may come along with the development of vertically extended deep convective clouds, thunderstorms and heavy rainfall. The typical life cycle of a deep convective system in the African tropics is described in Futyan and Del Genio (2007). A further interesting aspect revealed by this study is that the greatest convective rainfall amounts occur in a relatively early stage of the thunderstorm development. Beside locally initiated convection, also organized convection in Mesoscale Convective Systems (MCSs) occur in West Africa. MSCc are larger than local thunderstorms, have a much longer life time, and often travel with the prevailing upper-air winds (Fink et al., 2006; Cetrone and Houze, 2009).

2.3 Satellite Remote Sensing

2.3.1 Remote Sensing of Clouds

Since the early days of meteorological satellites clouds have been observed and analyzed by satellite imagery (e.g. Reed and Jaffe, 1981). The remote sensing of clouds is a relative direct measure by using visible (VIS) and infrared (IR) sensors (Feijt, 2000; Roebeling et al., 2014). Clouds are usually brighter in the visible spectrum, and colder in the infrared spectrum, than the earths surface; hence it is, theoretically, rather easy to distinguish between clouds and the earths surface. In practice, the quantification of clouds is done by using a cloud fraction or cloud percentage value, which is the area fraction of a certain grid box covered by clouds. The derived cloud fraction is dependent on the thresholds used and determine the cloud detection sensitivity. Further, the fact that visible sensors can only be used during daytime might induce inconsistencies if both spectral ranges are used when available. The possibilities to detect clouds during daytime are therefore better than during the night. VIS and IR sensors are available onboard geostationary (GEO) satellites that observe large areas of the globe with a high temporal sampling rate of below one hour, which allows to derive reliable diurnal cycle information. The spatial resolution of these sensors is typically high with only a few kilometers, despite the large distance between the earth and the GEO satellite.

Beside the observation of cloud fractions, also information on cloud top temperatures can be estimated with IR sensors. Cloud top heights can be derived by using auxiliary data of the vertical temperature profile in the troposphere. Cloud top information information can be very useful for analyzing convective clouds that often reach high tropospheric levels and low cloud top temperatures.

2.3.2 Remote Sensing of Precipitation

A comprehensive review about precipitation modelling and observation, including the possibility to derive precipitation from satellite observations that became more popular in recent decades, is provided by Michaelides et al. (2009). Further, Kidd and Levizzani (2011) review the status of current satellite remote sensing of precipitation. In fact, the remote sensing of precipitation using satellites is more indirect and hence more uncertain than the remote sensing of clouds. It is a challenge to estimate from satellite the amount of precipitation that reaches the ground, since surface precipitation cannot be directly observed from satellite. In addition the limited spatiotemporal sampling is problematic in case of a parameter as variable as precipitation.

By using the VIS and IR spectral range, as used for the observation of clouds, only information from the cloud top can be gathered. Even though surface precipitation is related to a brighter and cooler cloud, the quantification of precipitation using VIS and IR information remains very uncertain.

A more direct approach to estimate precipitation from satellites is to make use of the microwave spectral range. The wavelength of microwave radiation is in the order of millimeters and interacts with precipitation sized particles, which usually have a diameter in the range of millimeters. The estimation of surface precipitation using microwave sensors is therefore more directly linked to the actual precipitation. Therefore, passive microwave (PMW) imager data is commonly used to estimate precipitation.

The physical process used to estimate precipitation based on PMW sensors is the microwave emission and scattering of precipitation. The emission signal of precipitation-sized particles is often small compared to the emitted radiation from the Earths surface. A clear identification of the signal from the precipitation requires low microwave emissions from the surface, which is true for the oceans. The scattering signal, which weakens the observed microwave signal coming from the Earths surface, is mainly due to ice particles. This implies that the scattering signal is best usable for ice clouds over land areas. Convective precipitation, that is mostly formed through the ice phase of the cloud particles, can be reasonably estimated by using the microwave scattering signal.

PMW instruments are usually flying onboard low earth orbiting (LEO) satellites, as the microwave radiative signal given by the Earth and its atmosphere is relatively weak, and hence the sensor needs to be closer to the troposphere to get a processable signal. However, the spatial resolution of PMW imagers is relatively low with about 50 km, plus some additional navigation uncertainties. Further, owing to the low-earth orbit and the limited instrument swath, one LEO satellite can observe a certain point on earth only once to twice per day. The sampling increases if multiple satellites can be used. Still, the spatiotemporal coverage of

PMW-only datasets remains limited, which poses a problem when trying to analyze precipitation at the sub-daily scale.

A way to improve the spatiotemporal coverage is to use both LEO and GEO satellites to generate combined products. Some of the datasets used in this thesis are of such kind. These so-called multi-satellite datasets thereby combine the relatively direct measure using PMW data with the high spatiotemporal sampling offered by GEO data. Those multi-satellite precipitation datasets are expected to be superior to single sensor datasets (Huffman and Bolvin, 2007) because of using synergy effects.

Satellite remote sensing of precipitation remains challenging. Additional issues exist and should be briefly mentioned and kept in mind when discussing uncertainties. There is for example the problem of beam filling, which means that due to the large footprint of the PMW radiometers, the actual rain area is often not filling a satellite pixel completely. This induces uncertainties in precipitation estimation, since the algorithm assumes the pixels to be uniformly filled by precipitation. Further the measured signal usually originates from the mid- (emission signal) or high-levels (scattering signal) of a cloud. Therefore, horizontally drifting rain and rain that is evaporated below the cloud-base can not be observed correctly. However, the individual quantification of these inherent uncertainties is difficult.

The ability to estimate precipitation is mainly dependent on the satellite sensor and the algorithms used, but also depends on the prevailing precipitation regime. Overall, tropical precipitation, which is often of convective form and hence more intense, can be better detected by satellites than precipitation in higher latitudes, that is on average less intense (Ebert et al., 2007). On the other hand, convective rainfall is often more short-lived than large-scale stratiform precipitation. This may hinder the estimation of rainfall owing to the limited temporal sampling of satellite measurements.

2.4 Modeling of Clouds and Precipitation

The interpretation of clouds and precipitation is a major factor of uncertainties in atmospheric modeling because of its dependency on small-scale processes. These processes can not be explicitly resolved by the numerical weather and climate models, owing to the models limited spatial and temporal resolutions. Hence, those processes have to be parameterized (e.g. Randall et al., 2003; Dirmeyer et al., 2012; Crétat et al., 2014). Clouds are an important input parameter into the radiation schemes of the models, which affect many important model variables and determine the model simulations. Recently, attempts have been made to better resolve cloud and convection processes with the help of simulations in very high spatial resolutions of only a few kilometres or less, so-called 'cloud-resolving' or

'convective-permitting' simulations with promising results for the representation on the diurnal cycle of clouds and precipitation (e.g. Shin et al., 2007; Hohenegger et al., 2008; Ban et al., 2014; Fosser et al., 2015; Brisson et al., 2016). But those convective-permitting simulations are computationally very expensive and are therefore not applicable for long-term climate simulations in large domains. Precipitation is usually parameterized connected to the cloud and convection parameterizations schemes. Convection is also parameterized by the models used in this thesis, which use spatial resolutions of about 50 to 100 km grid spacing.

In atmospheric models with a grid spacing of more than 10 km, like in the COSMO-CLM simulations, it is usually distinguished between grid scale, sub-grid scale, and convective cloud processes. The grid-scale cloudiness is described as a function of the relative humidity in the respective model layer. Precipitation is generated depending on the availability of cloud water and cloud ice. The respective fluxes between each vertical layer are integrated from top to bottom, which finally can lead to precipitation at the surface. The parameterizations of convection used by the analyzed model systems (see section 3.3) are based on the widely used schemes developed by Tiedke (1989) and Arakawa and Schubert (1974). Both schemes are mass-flux schemes that include various processes leading to the formation or breakup of convective clouds and rainfall. The initiation of convection is dependent on the vertical layering of the troposphere and on the Convective Available Potential Energy (CAPE). As the model grid-size is expected to be much larger than the individual convective plumes, the convection schemes use an ensemble of idealized convective cells. The convection schemes represent entrainment into the convective cloud, as well as detrainments out of the convective cloud. Vertical fluxes of mass, moisture, momentum, and water are considered, and even feedback from the convective processes to the large-scale is partly included in the model systems. Autoconversion from cloud to precipitation particles, and sub-cloud layer evaporation of precipitation are also accounted for. A recently developed convective scheme, which also accounts for non-equilibrium convection in large scale models, has been introduced by Bechtold et al. (2014) that also makes use of CAPE.

Still there are a number of assumption and limitations in the representation of clouds and precipitation in numerical models (e.g. Birch et al., 2014). An uncertainty factor is, for example, the fact that each grid-cell is considered isolated concerning convection, and hence large-scale convective systems, like MCSs, can not be correctly simulated. Further, assumptions on precipitation fall velocities have to be made, and often rain is assumed to be falling out instantaneously in the same model time step. A transition of rain from one grid box to a neighbouring box is not possible owing to the limitation of the process to the vertical dimension. Partial cloudiness is possible in grid boxes but variations within one vertical layer

are not accounted for. Another difficulty is to simulate the total cloud cover in a grid box. The procedures of using maximum overlap in case of clouds in neighbouring vertical layers, and random overlap for clouds separated by at least one cloud-free layer, as done in the used COSMO-CLM simulations, may introduce biases. This may result in overestimations of cloud cover in the case of grid-scale clouds and underestimations of cloud cover for convective clouds. Often only a limited area fraction can be covered by convective rain in a grid box. This may result in underestimations of extreme values.

In the model system clouds are input to the radiation schemes. Owing to extensive costs, the full radiation schemes are often executed only each 1 to 3 h, and also only at a limited number of grid boxes. In between interpolations are necessary in space and time. Therefore the possible feedback frequency between cloud and radiation processes is reduced. Because of the described assumptions and limitations, it is a big challenge for mesoscale models to reasonably simulate clouds and precipitation—from the monthly to the sub-daily scale.

Chapter 3

Data

In the following chapter the data sets used in this thesis are presented. The data can be divided into three main categories: ground-based data, satellite-based data and numerical-model-based data. The data section in this theses is divided accordingly, while some main aspects of each category are given respectively.

The main parameters analyzed are surface precipitation and clouds, mainly cloud cover but also cloud top information. There is a clear relation between clouds and precipitation in nature. Nevertheless, the process of observing or estimating clouds and precipitation is quite different and each measurement technique is afflicted with uncertainties. This chapter describes general properties of the individual data sets used and also provides further aspects on individual data uncertainties and limitation, if they are relevant for the interpretations of results.

3.1 Ground-based Data

Ground-based data, meaning in-situ data, is the backbone of long-term meteorological measurements. Ground-based means data measured by instruments located on the ground, mainly at meteorological synoptical stations (Synop data). The quality of Synop data is usually high and the data is considered as the observational reference for most climate variables. For the observations of clouds this is debatable because ground-based cloud observations are mainly done by human eye observations. The measurement of precipitation is usually conducted by rain gauges. Therefore the ground-based observations of clouds and precipitation are quite different. Even though both cloud and precipitation observations are subject to uncertainties, they are considered and used as the measurement reference. Difficulties typically occur when rain-gauge point measurement are extrapolated into larger areas, or at the observation of clouds during nighttime. More details on the ground-based observations of clouds and precipitation and on the specific

data used in this thesis are given in the following subsections.

3.1.1 Ground-based Cloud Observations

Synop observations of cloud cover are still done by human-made eye observations. The observer estimates the cloud cover in octa, and sometimes in tenth, which means that the resolution is relatively low with 10 to 12.5 %. An issue is the observation during nighttime when the observer is not able to see the sky very well. Further uncertainty is also induced by the varying viewing geometry and in case of vertical extended clouds. In case of fog, no cloud cover estimation is possible. In addition to these difficulties, the observation might be dependent on the individual observer itself, even though observation guidelines from the World Meteorological Organization exist. The ground based cloud cover observations used in this study are 3-hourly Synop observations. For analyzing the diurnal cycle of cloud cover, the individual stations were gridded to a dataset of 3-hourly cloud cover observations. For the validation of satellite and model-based datasets, a European cloud cover dataset was generated, offering a spatial resolution of 0.25° lat-lon. Over oceans only ship-based observations are available. Owing to its weak density and changing location, it is not feasible to do a gridding of ship measurements. Hence ground-based observations of clouds over oceans are not used in this thesis.

3.1.2 In-situ Precipitation Measurements

In contrast to clouds, surface precipitation can be measured relatively accurate by rain gauges on the ground. There are several ten thousand of rain gauges installed around the globe, which can be used as data reference. Nevertheless, there are also some issues concerning the ground based measurement of precipitation. First, there is the issue of precipitation undercatch when measuring with rain gauges in windy conditions (Schneider et al., 2013; Kidd and Levizzani, 2011). This results in an underestimation of the true precipitation amount by rain gauges, on average. Second, rain gauges are very inhomogeneously distributed. This impacts the quality of gridded data, which are usually used for climate analysis or validation studies. A higher station density usually leads to a higher data quality. Large areas on earth are only sparsely covered by rain gauges, which is especially true for the tropics. In these regions precipitation can only be estimated by using extrapolation of rain gauge data on great distances, which can be very uncertain owing to the high spatial and temporal variability of precipitation. Third, over oceans continuous observations are almost absent. Still some buoys, ships or rain gauges on very small islands, like atolls, exist. Furthermore when focusing on sub-daily precipitation, its analysis is often hampered owing to the limited temporal

resolution of the data. Rain gauge data is often only available as daily sums.

African Monsoon Multidisciplinary Analysis Data

The African Monsoon Multidisciplinary Analysis (AMMA) project and the related AMMA-Couplage de l'Atmosphère Tropicale et du Cycle Hydrologique (AMMA-CATCH) project deal with the intra-seasonal and inter-annual variability of the West-African monsoon (Lebel et al., 2010). Within the course of the projects, meteorological data are collected and, amongst others, precipitation measuring sites were set up. A highly appreciated outcome of the AMMA-CATCH project is a database containing various meteorological data, including data gathered within the project, which is now available to the research community (see `http://www.amma-catch.org`). For this thesis, the AMMA-CATCH rain gauge data is of highest importance because the network provides long timeseries of precipitation data with a subdaily temporal resolution (e.g. 1-hourly sums). The AMMA-CATCH data enables the analysis of tropical diurnal cycles as measured at the surface for the inner-tropical Ouémé mesosite in Benin and for the outer-tropical Niamey mesosite in Niger.

Comprehensive Pacific Rainfall Database

The Comprehensive Pacific Rainfall Database (PACRAIN) is a collection of rain gauge station data in the tropical Pacific. PACRAIN is a National Oceanic and Atmospheric Administration (NOAA) initiative and includes rain gauge data from different sources including data from Pacific atolls (Greene et al., 2008). Atolls are very small and flat islands. Rainfall conditions on atolls can be considered as relatively similar to open ocean conditions, as analyzed by Sobel et al. (2011). As alternative long-term ground-based precipitation data over oceans do not exist, data from atolls, as provided by PACRAIN, are a unique data source. The PACRAIN atoll data are used as reference for analyzing monthly rainfall over the Pacific ocean in this thesis. For having the most robust measure of rainfall on the ground, the individual atoll rain gauges have partly been gridded before using them for the validation of satellite and reanalysis datasets. The PACRAIN data is available via `http://pacrain.ou.edu`, and has already been successfully used for validation purposes in other studies (e.g. Chen et al., 2013).

3.2 Satellite data

Satellite data, i.e. meteorological data derived from radiance measurements through sensors onboard satellites, became an important data source in recent decades for various fields of meteorology. However, using satellite data for climate analysis

and climate model validations is a relatively young field in climatology. Efforts have been made in recent years to develop and apply algorithms on historical satellite data to derive several meteorological parameters. This includes radiation, clouds, but also precipitation (Schulz et al., 2009). While the estimation of clouds is a relative direct measure by using VIS and IR satellite sensors, the estimation of precipitation is much more indirect and therefore more uncertain (see Section 2.3.2). Both, the estimation of clouds and precipitation by using satellite data is of high importance for understanding the climate system as a whole, but also for understanding various smaller scale processes, like local systematic variability. The validation of satellite-derived parameters is essential for a resilient analysis. Though each satellite-based product cannot be used for any purpose. The validation of various satellite products is one of the goals of this doctoral theses.

3.2.1 Satellite-based Cloud Observations

Cloud cover observations by using satellite imagery usually makes use of VIS and IR sensors. As these sensors are operated on geostationary meteorological satellites, like on the GOES or METEOSAT satellites, large parts of the globe can be observed with a high resolution of about 3 to 5 km in space and 1 to 3 hours in time. This clearly enables the data to be used for a wide range of applications, including the analysis of the diurnal cycle of clouds. An inevitable fact is the missing of VIS information during the night, hence only IR information can be used. This reduces the abilities of cloud detection during nighttime, a similar problem as for the classical eye observations of clouds (cf. section 3.1.1).

Beside the estimation of cloud cover, also information on cloud top temperatures and cloud top heights can be derived by using IR sensors. In this thesis, information on cloud cover and cloud top temperatures are used for evaluating the diurnal cycle of precipitation from convective clouds. In the following, the satellite-based cloud datasets used are briefly described.

International Cloud Climatology Project

The International Cloud Climatology Project (ISCCP) was one of the first initiatives that generated a long-term cloud cover dataset using different GEO and LEO satellites (Rossow and Garder, 1993; Rossow and Schiffer, 1999). Meanwhile the ISCCP cloud cover dataset covers more than 30 years. ISCCP derives the cloud cover based on temperature difference thresholds between the clear-sky case and the actual scene using mainly the IR-channels of the satellite sensors. The clear-sky or background temperature is derived by different spatial and temporal variability tests of brightness temperatures for being able to distinguish between

clouds and the surface background in the individual satellite pixels. The ISCCP-D2 dataset is a result of the averaging of the individual instantaneous satellite-based cloud cover estimates in space and time. ISCCP-D2 data is available globally at 3-hourly temporal and $2.5° \times 2.5°$ spatial resolution.

EUMETSAT Climate Monitoring Satellite Application Facility

The EUMETSAT Climate Monitoring Satellite Application Facility (CM SAF) is one of several SAFs initiated by the European Organisation for the Exploitation of Meteorological Satellites (Schulz et al., 2009). The CM SAF is dealing with the generation and provision of high-quality long-term satellite based datasets usable for climate purposes. The CM SAF was founded in 1999 and provides a suite of climate variables covering the main parameters of the energy- and water-cycle of the Earth like radiation, clouds, water vapor and precipitation.

In this thesis, the cloud fraction data from the operational CM SAF cloud products and the cloud top information data from the CMSAF cloud property dataset using SEVIRI (CLAAS) (Stengel et al., 2014) are used. Both products are based on the SEVIRI instrument aboard the geostationary METEOSAT 2nd generation satellites located in 36.000 km height at 0° longitude / latitude. The METEOSAT field-of-view covers Africa, Europe and the surrounding oceans, and parts of South America. For the cloud detection, the CM SAF makes use of several channels from the VIS to the IR spectral range, and applies scene dependent threshold tests.

3.2.2 Satellite-based Precipitation Observations

It has been shown that satellite based precipitation data are a useful tool to study various aspects of precipitation, from the global to the regional scale (e.g. Xie and Arkin, 1997; Zipser et al., 2006). In opposite to the observation of cloud cover, the estimation of precipitation is less accurate, as it is a more indirect measure (see Section 2.3.2). Most datasets use IR or PMW sensors, or combinations of both to estimate precipitation. The combination of multiple satellites and sensors is usually superior to single satellite or single sensor based products, as former studies have shown (e.g. Huffman and Bolvin, 2007; Kidd and Levizzani, 2011). But not every dataset is suitable for any purpose. An important property determining data quality is the spatiotemporal coverage of the product, which is strongly dependent on the individual sensors used to generate the dataset. Further, rain gauge data is incorporated into some datasets to reduce biases. Most of the satellite-based precipitation datasets used in this thesis are chosen to in principle allow for the analysis of the diurnal cycle of precipitation.

Global Precipitation Climatology Project Data

The Global Precipitation Climatology Project (GPCP) dataset (Adler et al., 2003; Huffman et al., 2009) is a well established global precipitation dataset, which incorporates various satellites and satellite sensors, but also gridded rain gauge data on the monthly scale, provided by the Global Precipitation Climatology Center (GPCC) (Schneider et al., 2013). The GPCP data is provided on a relatively coarse grid of $2.5° \times 2.5°$, but with a long time record starting in 1979. As the GPCP data is provided only on a monthly time scale, it cannot be used for analyzing diurnal cycles, but it is used to evaluate how satellite-based precipitation datasets can estimate the precipitation climatology over ocean, which has been rarely analyzed so far.

Hamburg Ocean and Atmosphere Parameters from Satellites Data

The Hamburg Ocean and Atmosphere Parameters from Satellites (HOAPS) dataset consists of several parameters and fluxes of the energy- and water cycle over ice-free oceans (Andersson et al., 2011), including precipitation. The HOAPS data is solely based on the Special Sensor Microwave/ Imager sensor (SSMI) onboard the Defense Meteorological Satellite Program (DMSP) satellite series. The number of satellites used varies over time, which may result in a time-varying quality of the dataset. Up to three SSM/I microwave sensors have been used to generate the HOAPS dataset during the years after 1998. The HOAPS version-3 data offers a spatial resolution of $0.5° \times 0.5°$ on a monthly time scale. Therefore the HOAPS dataset cannot be used for the analysis of diurnal cycles but it is used in the validation together with GPCP data and reanalysis data to evaluate the ability of the datasets to reasonably estimate precipitation over the ocean (see Appendix C).

Tropical Rainfall Measuring Mission Datasets

There are several datasets that are based on the Tropical Rainfall Measuring Mission (TRMM) satellite data. The TRMM satellite mission was launched in late 1997 with the dedicated goal to measure tropical precipitation by using several instruments (Kummerow et al., 1998). The TRMM satellite ended providing data in April, 2015. The TRMM data gave new insights on the distribution and variability of rainfall in the tropics and is widely used. The TRMM satellite orbit was chosen to be non-sun-synchronous, which enables to observe the same location at different times during the day. This allows to analyze the diurnal cycle of precipitation in the tropics (Yang and Slingo, 2001). Different TRMM based precipitation dataset, which are briefly described below, are used in this thesis with the focus on the evaluation of its ability to capture the diurnal cycle of precipitation.

TRMM Multi-Satellite Precipitation Analysis (TMPA) The TMPA dataset, also referred to as TRMM-3B42, is one of the most widely used satellite-based precipitation datasets, in case high spatiotemporal resolution is required. The TMPA product incorporates various satellites into a final merged product; the calibration reference is the TRMM precipitation radar (TRMM-PR)—an active radar that offers high-quality precipitation information. Beside the TRMM-PR, the TMPA product includes PMW and IR sensor data. The TMPA dataset offers a spatial resolution of $0.25° \times 0.25°$ and a temporal resolution of 3 hours (Huffman and Bolvin, 2007). This enables the TMPA dataset to be used for the analysis of small-scale sub-daily variability.

TRMM Precipitation Radar Data The TRMM-PR is one of three instruments onboard the TRMM satellite. The TRMM-PR is an active radar, designed to observe precipitation-sized particles. Based on this instrument, surface precipitation can be estimated, together with the vertical structure of precipitation. Because of the high quality of the PR at the instantaneous scale, the PR is used for the calibration of multi-satellite based datasets like TMPA. However, the spatiotemporal coverage of the PR is very low due to the narrow instrument swath. It takes several days for the sensor to observe the same location twice. It takes even longer to observe the same location twice at the same local time (Negri et al., 2002b). Consequently, it takes several weeks to scan a full diurnal cycle at a certain location. For the validation of the mean diurnal cycle of precipitation in the tropics the data was aggregated to 3-hourly composites on a $0.5° \times 0.5°$ grid.

TRMM Microwave Imager Data The TRMM Microwave Imager (TMI) is a passive instrument with a broader swath than the TRMM-PR. The estimation of precipitation using passive sensors is more uncertain than for active instruments. While the passive microwave imager may succeed in precipitation estimation over water surfaces, it is more difficult over land. Still, precipitation estimation is possible over land with help of the scattering signal, if precipitation is mostly of convective origin and therefore contains a substantial volume of ice particles. As for the PR, the TMI data is aggregated to 3-hourly composites on a $0.5° \times 0.5°$ grid.

TRMM PR/TMI combined Data The TRMM PR/TMI combined dataset, referred to as TRMM-COMB, is a combination of data from the TRMM-PR and -TMI. The TRMM-COMB data is generated when both TMI and PR data is available and is aimed to deliver the best estimate of precipitation by using the synergy of the structural rainfall information of the TMI together with the more detailed information of the vertical structure of cloud and rain droplets by the PR

(Haddad et al., 1997).

Climate Prediction Center Morphing Technique Data

The Climate Prediction Center Morphing Technique (CMOPRH) dataset is composed of several individual passive microwave precipitation datasets which are composed into one final merged precipitation dataset. This includes, for example, datasets based on the SSM/I sensors. CMORPH is a method that relies on existing datasets and uses a morphing technique to merge those datasets with the help of high-resolution IR data from GEO (GEO-IR) satellite data (Joyce et al., 2004). The precipitation estimates are thereby not only morphed forward and backward in time but also the precipitation values itself are interpolated between the time steps with help of the GEO-IR data. Thanks to the usage of the GEO-IR data the spatial and temporal resolution of the final dataset is substantially increased compared to the original microwave-based estimates. The final CMORPH precipitation dataset is available in a spatially higher and a lower resolved version. The higher resolved version, referred to as CMORPH-hq in the following, has a spatial resolution of 5 km and a temporal resolution of 30 minutes. This corresponds approximately to the resolution of the GEO-IR data. The lower resolved version is delivered on a $0.25° \times 0.25°$ grid at a 3-hourly temporal resolution.

Precipitation Estimation from Remotely Sensed Information using Artificial Neural Networks

The Precipitation Estimation from Remotely Sensed Information using Artificial Neural Networks (PERSIANN) dataset is a global precipitation dataset delivered on a $0.25° \times 0.25°$ grid at 3-hourly temporal resolution (Sorooshian et al., 2000). The dataset is solely based on GEO-IR satellite data trained with PMW satellite data within a neural network. The fact that the dataset is mainly based on IR information makes it different from all other datasets used in this thesis. The IR-only approach may also advance on specific error characteristics of the PERSIANN precipitation dataset.

3.3 Model-based data

Three different datasets of clouds and precipitation are used in this thesis that are derived by numerical simulations: two global reanalysis, and one regional climate model that is applied in an European and an African domain. As outlined in Section 2.4, relevant processes associated to the formation of clouds and precipitation are parameterized in numerical models. The most important process responsible

for the sub-daily variability is convection, which is described in section 2.2. General aspects on how clouds and precipitation are treated within climate models are given in section 2.4.

3.3.1 European Center for Medium-range Weather Forecast Interim Reanalysis Data

The European Center for Medium-range Weather Forecast (ECMWF) - Interim Reanalysis (ERA-Interim) is a widely used re-analysis operated by the ECMWF (Dee et al., 2011). ERA-Interim is based on the Integrated Forecast System (IFS) release of 2006 and uses a 4-D VAR data assimilation system. ERA-Interim is generated on a spectral T255 grid, which corresponds to a spatial resolution of about 0.7°. Within the model system, precipitation is a variable derived by a forecast. ERA-Interim is used in the validation study in the tropical Pacific and is also used as the global driving data for the region climate model described in section 3.3.3. The convection parameterization within the ERA-Interim model system is based on the scheme by Tiedke (1989).

3.3.2 Modern-Era Retrospective Analysis for Research and Application

The Modern-Era Retrospective Analysis for Research and Application (MERRA) is a reanalysis operated by the National Aeronautics and Space Administration (NASA) and aims to have a special focus on the water-cycle of the Earth (Rienecker et al., 2011). MERRA has been developed by the Global Modeling and Assimilation Office (GMAO) and uses the Goddard Earth Observing System Model, Version 5 with the associated atmospheric data assimilation system. For many parameters, like precipitation, the data output is hourly. The native resolution of the MERRA reanalysis is $1/2° \times 2/3°$ in longitude and latitude. MERRA covers the period 1979 to present. The MERRA model system makes use of the Relaxed Arakawa-Schubert convective parameterization (Arakawa and Schubert, 1974; Moorthi and Suarez, 1992). Further information on MERRA can be found only (`http://gmao.gsfc.nasa.gov/research/merra/`).

3.3.3 Consortium for Small Scale Modelling - Climate Local Model Simulations

The Consortium for Small Scale Modelling - Climate Local Model (COSMO-CLM or CCLM) is a regional climate model that is based on the numerical weather

prediction model 'Lokalmodell' developed and operated by the Deutscher Wetterdienst (DWD). The CCLM can be used in various spatial and temporal resolutions (Rockel et al., 2008). For long term climate simulations, the typical spatial resolution of the CCLM is usually 0.44° in longitude and latitude. In this thesis such simulations are analyzed for evaluating their ability to generate reasonable diurnal cycles of clouds and precipitation. The simulations have been done for a European and a African domain. The CCLM output is available in 3-hourly or 1-hourly temporal resolution. In the used CCLM simulations, the parametrization of clouds and convection following Tiedke is applied (Tiedke, 1989).

Chapter 4

Summary of Results

In this chapter the synopsis of the main result of the thesis are presented. Most of the results are presented in more detail by one of the three peer-reviewed publications or by the additional studies given in the appendix. The results of the analysis of clouds and precipitation are separately shown for ocean and land regions. Over ocean, regions of interest are the maritime stratocumulus region off the western coast of southern Africa and the western tropical Pacific ocean. Over land, the focus is on Europe and West Africa.

4.1 Ocean

4.1.1 Clouds

Diurnal cycles of clouds and precipitation exist over land and oceans. As two thirds of the Earth are covered by oceans, systematic cloud diurnal cycles play an important role there. A global overview of mean cloud diurnal cycles for a multi-year time period is shown in Figure 4.1. In each $15° \times 15°$ grid box the mean absolute cloud diurnal cycle of different satellite and reanalysis datasets are shown. For substantial parts of the ocean, the cloud diurnal cycle shows a maximum during the night and a minimum during the day, in line with the meteorological expectations, and in line with previous studies (e.g. Cairns, 1995). The strongest oceanic cloud diurnal cycles are found in the regions of maritime stratocumulus, which are mostly located at the west sides of the subtropical regions of Africa and America (Wai, 1991). Those areas have a large negative cloud radiative effects (Raschke et al., 2005) and are hence crucial for the global climate. Figure 4.1 shows that the satellite and the reanalysis datasets reasonably agree in cloud diurnal cycles in the regions of maritime stratocumulus. However, there are substantial biases between the datasets in that regions, with the tendency of satellite data

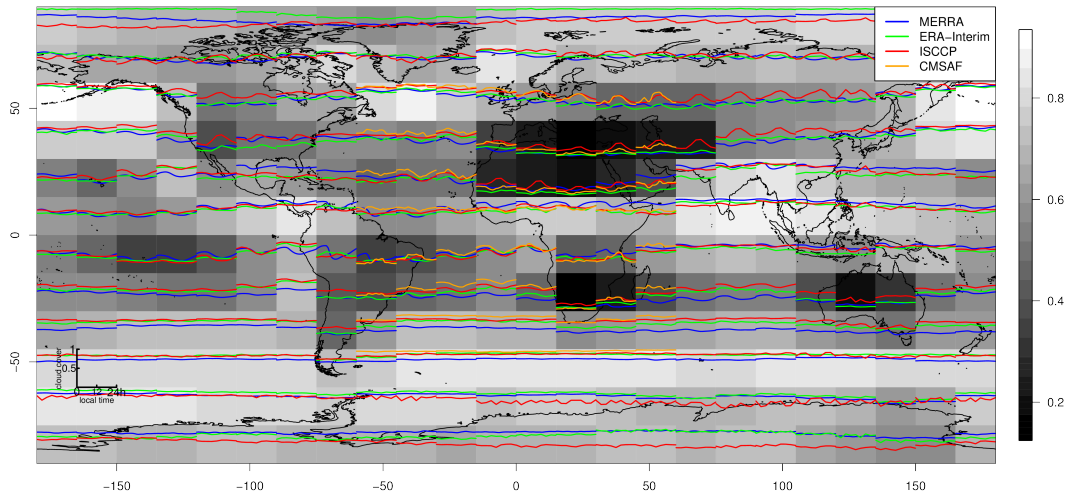

Figure 4.1: Global overview of summer season (JJA) mean diurnal cycles of cloud cover as given by MERRA and ERA-Interim reanalysis, and by the satellite-based datasets of ISCCP and CM SAF. The color scale represents the mean cloud cover of ISCCP in percentage points. The lines inside each grid box show the mean cloud cover diurnal cycle with the x-axis stand for the local time from 0 to 24 and the y-axis stand for the cloud cover from 0 to 1 (see also grid box exemplification in the lower left part of the image).

having larger cloud amounts than reanalysis data, which is also true for other atmospheric model based data (Karlsson et al., 2008). The validation of the diurnal cycle in the maritime stratocumulus regions off the west coast of southern Africa shows that not only the global reanalysis data of MERRA and ERA-Interim, but also the regional climate model COSMO-CLM is able to capture the general feature of the cloud diurnal cycle in that region (cf. Figure 4.1 and Figure A.6 and A.7). Nevertheless, a negative bias in absolute terms in the COSMO-CLM exists, too.

Over the tropical oceans the mean cloud amounts are larger and the mean cloud diurnal cycles are smaller compared to the maritime stratocumulus regions. Still, a small nighttime to early morning maximum of clouds is found over the tropical ocean, too. Owing to a lack of long-term cloud observations, a validation of cloud diurnal cycles with ground-based data is not possible over oceans.

4.1.2 Precipitation

An overview of the global distribution of precipitation and its diurnal cycles are shown in Figure 4.2. By far, the globally highest precipitation amounts occur

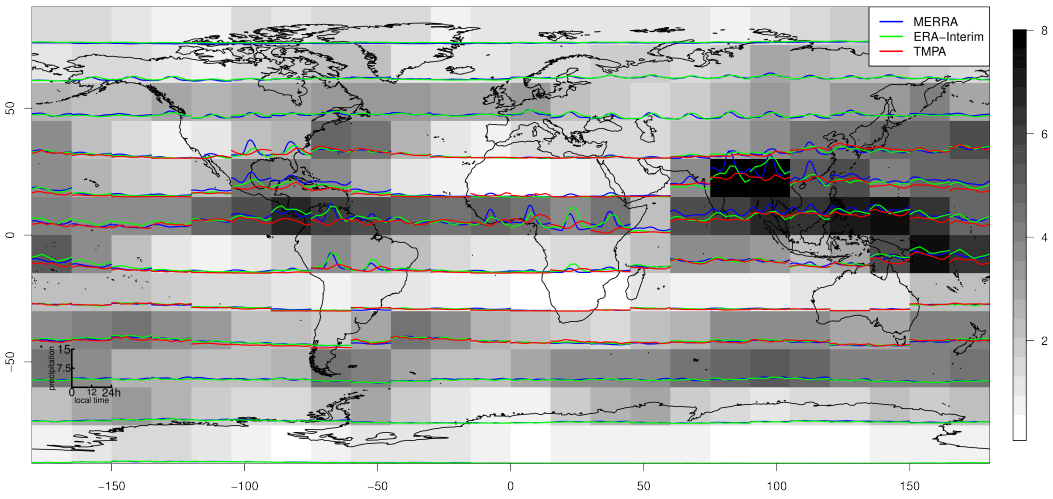

Figure 4.2: Global overview of summer season (JJA) mean diurnal cycles of precipitation as given by the reanalysis data of MERRA and ERA-Interim and by the satellite-based TMPA data. The color scale represents the mean precipitation rate in mm/day. The lines inside each grid box show the mean precipitation diurnal cycle with the x-axis stand for the local time from 0 to 24 and the y-axis stand for the precipitation rate from 0 to 15 mm/d (see also grid box exemplification in the lower left part of the image).

in the tropics, but the diurnal cycles of precipitation over oceans are relatively small compared to those over land. Like for clouds, there is a lack of long-term precipitation data over oceans, hindering the validation of satellite and model data. A unique opportunity is to use rain gauge data located on very small and flat tropical islands, so-called atolls, that exist in the tropical Pacific. Atoll rain gauge data are included in the PACRAIN database and are expected to largely represent open-ocean conditions (Sobel et al., 2011). Unfortunately, the atoll rainfall data are not available at a sub-daily temporal resolution.

However, it is still worth validating monthly means of rainfall over the tropical ocean, especially before the background of ongoing research and discussions about the closure of the Earths energy budget (Trenberth et al., 2009; Stephens et al., 2012; Wild et al., 2015). Within the budget components the latent heat flux should be balanced by the precipitation flux, that is still debated. GPCP data is regularly used for global energy budget estimations.

As part of this thesis, PACRAIN atoll data is used to validate different precipitation datasets in tropical ocean climate conditions, where globally the most precipitation occurs. The validation includes precipitation estimates by satellite

Table 4.1: GPCP, HOAPS, ERA-Interim and MERRA monthly precipitation data on a 2.5° lon/ lat grid, with reference to gridded atoll data during 1989–2005; Measures are correlation (cor) and median absolute deviation (MAD) [mm/d] and median bias [mm/d]. Boldface shows the best match to the PACRAIN reference.

Evaluation of absolute values				
	GPCP	HOAPS	ERA-Interim	MERRA
cor	**0.81**	0.77	0.76	0.71
MAD	**1.57**	1.80	1.71	1.88
bias [relative bias]	-0.91 (-12%)	-0.55 (-7%)	0.71 (+9%)	**-0.06 (0%)**
Evaluation of anomalies				
cor	**0.77**	0.72	0.71	0.70
MAD [IQR]	**1.36**	1.59	1.50	1.54

products, i.e. HOAPS and GPCP, and precipitation data by the reanalysis of ERA-Interim and MERRA. The analyzed time period is 1988 to 2005.

One major finding is that the GPCP data offers the highest correlation with the PACRAIN rain gauge data, but also shows a substantial negative bias of -10 % compared to the ground-based reference (see Table 4.1). HOAPS has a smaller bias but shows lower correlations than GPCP. ERA-Interim has a positive bias, and it was found that both reanalysis show an underestimation of high monthly precipitation amounts, which the satellite products of GPCP and HOAPS do not show. More details on the study on monthly precipitation in the western Pacific Ocean are given in Appendix C. Overall the uncertainty of satellite-based and reanalysis precipitation in the tropics is on the order of 20 to 30% on the monthly scale, with reference to atoll rain gauge stations. ERA-Interim thereby performs similar to the HOAPS precipitation data. By evaluating the HOAPS dataset separately for the time periods when HOAPS is based on one, two, and three satellites, it is shown that the uncertainties are reduced with increasing the number of satellites used. This emphasizes the importance of the spatiotemporal coverage of satellite-based datasets for its accuracy, even on the monthly scale. When HOAPS makes use of three satellites, its performance with reference to PACRAIN data is better than those of the reanalysis products, and almost in the range of GPCP. A similar uncertainty dependency on the time period chosen has not been found in the GPCP, ERA-Interim and MERRA data with reference to PACRAIN rain gauge data.

Further information on the timing of the diurnal cyles of precipitation are given in Figure 4.3 that shows the time of the maximum diurnal precipitation based on the TRMM-TMPA dataset (Rückel, 2014). Small diurnal cycles and areas of less then 200 mm annual precipitation are blanked here. As a consequence large oceanic

areas are disregarded because of the relatively small diurnal cycles observed over ocean. Larger diurnal cycles occur over oceanic regions close to coasts, probably due to the influence of land-sea interactions and precipitation systems initiated over land and then travelling over the ocean with the prevailing easterly winds in the tropics and subtropics.

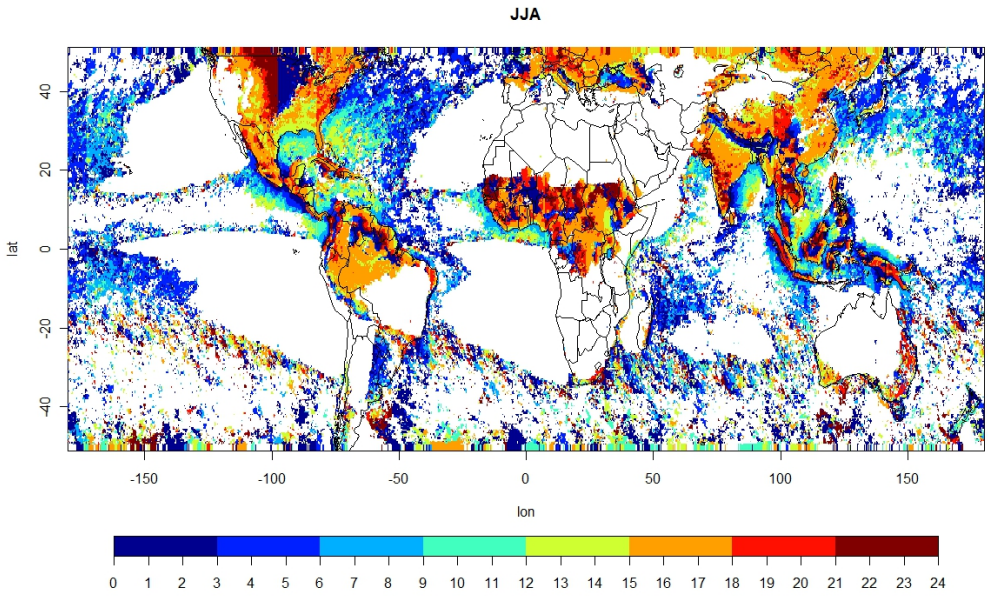

Figure 4.3: Local time of mean maximum diurnal precipitation in the summer season (JJA) based on TMPA satellite data for a 15 year period.
Source: Master Thesis of Stefan Rückel, Goethe-University, Frankfurt, 2014

4.2 Land

4.2.1 Clouds

The global distribution of cloud cover over land surfaces can also be seen in Figure 1.2 and 4.1. Analog to precipitation, the highest cloud cover amounts are found in the tropical regions. Very few clouds exist in the subtropics. Overall cloud cover is underestimated by the analyzed reanalysis products in the subtropics and in the mid-latitudes compared to the satellite data.

On average, the cloud diurnal cycle over land has a daytime maximum (cf. Figure 4.1), which can be attributed to clouds formed by convective processes (cf. Section 2.2). This behavior is most pronounced in the mid-latitude summer hemispheres, like in Europe, in large parts of Asia, and in the continental United

States. In the tropics, the diurnal cycles of cloud cover are mostly relatively smaller than they are in the mid-latitudes. Large differences between the satellite products of ISCCP and CM SAF occur in the Sahara region. This can be attributed to the increase of the cloud detection sensitivities in the ISCCP algorithm over very hot surfaces, and consequently enhanced temperature differences between clouds and the land surface. This leads to an artificially strong cloud diurnal cycle with a peak around noon in the ISCCP data (Stubenrauch et al., 1999), that does not exists in the CM SAF data.

Overall, the deviations of the cloud diurnal cycles between the datasets are larger over land than over oceans. This is related to the fact that the processes responsible for the formation of clouds are more small-scale and divers over land. Further, also the quality of the satellite products can be negatively affected by inhomogeneous surface backgrounds, i.e. ice and snow-covered regions, and strong topography.

Focus region: Europe The European climate is dominated by a strong seasonality. In the winter-half, the weather is dictated by the prevailing westerlies occurring between the sub-polar lows and the subtropical highs. Within the westerly flow, polar frontal cyclones influence the weather in Europe. In the summer-half, Southern and Central Europe gets stronger influenced by high pressure systems, which is linked to the northward shift of the Inter Tropical Convergence Zone (ITCZ) and subsequently of the whole hemispheric circulation systems (Schönwiese, 2003). As a consequence the influence of the westerlies and hence of the large scale forcing of low pressure systems is reduced in the European summer season compared to the winter season. In addition to the stronger influence of high-pressure systems, the solar incoming radiation is much stronger in summer than in winter.

In summer, the increased incident solar radiation enhances the tropospheric diurnal cycle in Europe owing to the heating of the surface during daytime by absorption. As a consequence, primarily the lower-most tropospheric layers are warmed by the sensible heat flux. The thermal energy gained is then distributed to higher tropospheric levels through turbulence and convective processes. This vertical mixing, that is in Europe most effective in summer during daytime, regularly causes the development of clouds but may also cause thunderstorms in case of the favorable atmospheric conditions.

The climatological cloud cover in Europe can be estimated to be around 60 to 70%, with higher values in winter (cf. Appendix A). But the estimation of the absolute amount of cloud cover in very much dependent on the observing system and the applied algorithms. As described in Section 2.3.1 the algorithms applied by the used CM SAF and ISCCP data are based on temperature thresholds between

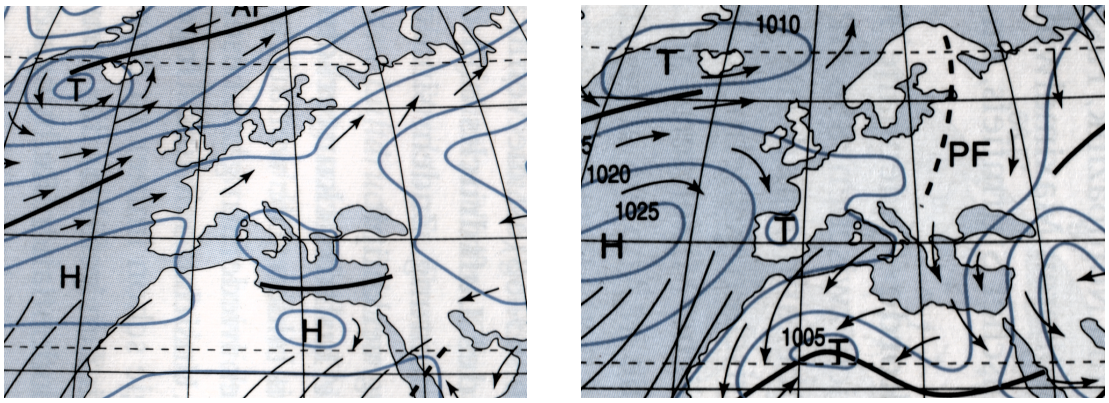

Figure 4.4: Mean circulation in Europe for (left) January and (right) July. 'T' stands for Low, and 'PF' for Polar Front.
Source: Schönwiese (2003)

the cloudy and cloud-free scenes in the individual satellite pixels. The size of those thresholds determine the cloud detection sensitivity. The ground-based reference is also not fully reliable, because these are human-eye observation. Further, the observing geometry is different between the observer at the ground, below the clouds, and the satellite, above the clouds is. Both perspectives might be not comparable one by one. This is especially true in case of scenes with broken or vertically extended clouds. The existing biases between the CM SAF, ISCCP, and the ground-based Synop observations are a consequence of the different measuring techniques and hence the different implicit definitions of clouds and cloud cover. Even though clouds can be well observed by making use of the VIS and IR spectrum of the satellite sensors, absolute values of cloud cover are not fully reliable owing to the lack of common reference data for calibration (cf. Section 2.3.1).

Therefore it is generally more reasonable to evaluate the variability of cloud cover, instead of comparing absolute values. The diurnal cycle of cloud cover is an important measure of systematic variability. In Europe, especially in the central and eastern parts, the observed cloud diurnal cycles are in the order of 13 % in the summer season, as given by ISCCP data (see Table A.1 and Figure 4.1). The cloud cover diurnal cycles agree quite well between the used satellite-based datasets in Central Europe, when analyzing relative measures (see (Pfeifroth et al., 2012), given in Appendix A)). For the comparisons to ground-based observations, Synop observations of cloud cover have been interpolated to a $0.25° \times 0.25°$ grid with a temporal resolution of 3 hours (see Appendix B). It has been found that the mean cloud diurnal cycles based on Synop observations agree reasonably with the satellite-based diurnal cycles. During the summer season, all observational data show the maximum of cloud cover in the afternoon, which shows the reliability of

the used cloud observations.

The observed cloud cover diurnal cycles are in line with the meteorological expectations as described in section 2.2, which lead to a distinct maximum of cloud cover in the afternoon and flat minimum in the morning (cf. Figure A.3). In contrast to the observational data analyzed, the regional climate model simulation by the CCLM is not able to simulate the observed diurnal cycles of cloud cover. The CCLM simulates almost no cloud cover diurnal cycle. This model deficit might have severe impacts on the radiation in the model which is mainly affected by cloud cover. In comparison to the observed cloud amounts, CCLM shows too much clouds during nighttime, which might result in an underestimation of the nocturnal thermal outgoing radiation. Indeed, by comparing the diurnal range of surface temperatures of the gridded station data by E-OBS (Haylock et al., 2008) and the CCLM simulation, an underestimation of the diurnal temperature range by the CCLM has been found in large parts of Europe (see Figure 4.5).

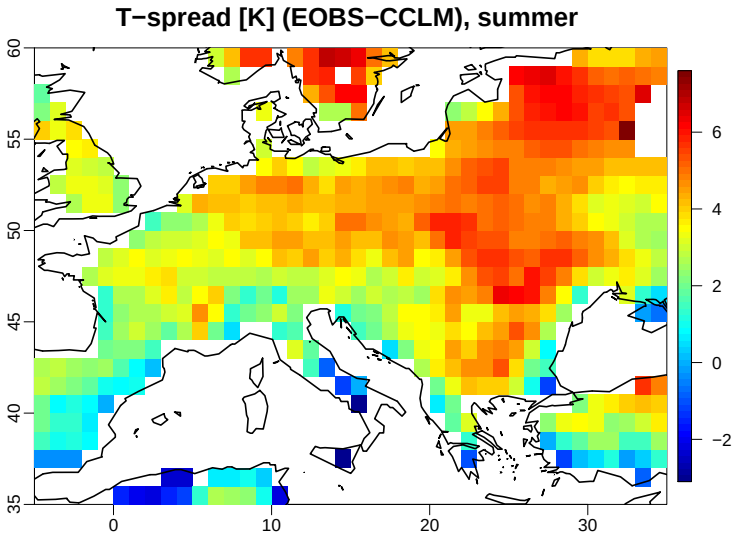

Figure 4.5: Difference of mean diurnal temperature ranges of gridded station data provided by E-OBS minus CCLM simulation, in Kelvin, for the summer season.

4.2.2 Precipitation

The global distribution of precipitation over land can be seen in Figures 1.3 and 4.2. Similar to the distribution of clouds, the highest precipitation amounts occur in the tropics and the smallest in the subtropics. In opposite to cloud cover, strong mean precipitation diurnal cycles exist over tropical land areas. The diurnal cycle given by the satellite and reanalysis data often deviate from each other. The reanalysis

data of ERA-Interim and MERRA overestimate the diurnal cycles of rainfall, with a peak around noon over most land areas, especially in the tropics. Instead, the precipitation diurnal cycles given by the TMPA satellite data show a peak that occurs in evening, a few hours later than the reanalysis data of ERA-Interim and MERRA. Owing to the limited data coverage of the TRMM satellite that does not observe latitudes higher than about 45° N/S, a validation of precipitation diurnal cycles for regions like Europe is hardly possible.

A global overview of the timing of the diurnal cycles of precipitation based on the TMPA dataset for the summer season (JJA) is shown in Figure 4.3. Over land the maximum diurnal precipitation usally occurs in the afternoon, but there are several regional exceptions, e.g. the Himalayan foothills and some tropical regions in Amazon and West Africa, where the diurnal cycle maximum occurs after midnight. These are regions of potential deficiencies in numerical models (Rückel, 2014).

Focus region: West Africa The climate of the African continent is driven by the seasonality of the ITCZ. While in the inner-tropics convective rainfall frequently occurs throughout the year, rainy and dry seasons alternate in the outer-tropics, e.g. in West Africa. Owing to the strong near-surface heating in Northern Africa and the subsequently relatively low pressure in the lower troposphere (Sahara heat low), there is a strong northward shift of the ITCZ towards the northern hemisphere during the summer season (see Figure 4.6) (Kothe et al., 2014). Consequently a low-level pressure gradient develops that let moist oceanic air flow into the West African continent (denoted by the black arrows in the right panel of Figure 4.6). This change of the general circulation during the summer half of the year, accompanied by clouds and rainfall, is called West African Monsoon (WAM).

Millions of people are affected by the WAM. Its rainfall is essential for the functioning of the social and economical life in West Africa, but the WAM may also cause large losses. The WAM is more variable and of smaller size compared to the Asian/Indian Monsoon. The WAM causes the annual rainy season in the Sahel zone - the transition zone between the inner-tropics and the Sahara dessert (see Köppen-Geiger climate zone 'BSh'='hot semiarid climate' in Figure 4.7).

Figure 4.3 denotes that there is no uniform precipitation diurnal cycle during the West African monsoon season. Instead smaller scale features of the precipitation diurnal cycles exist. It is therefore worth analyzing if various commonly used satellite-based datasets and numerical models are able to get the true diurnal cycle of precipitation.

Unfortunately, there is a lack of a meteorological measurement network in most parts of Africa, including West Africa. Because of the missing of large-scale rain gauge networks, dedicated projects like the African Monsoon Multi-Disciplinary

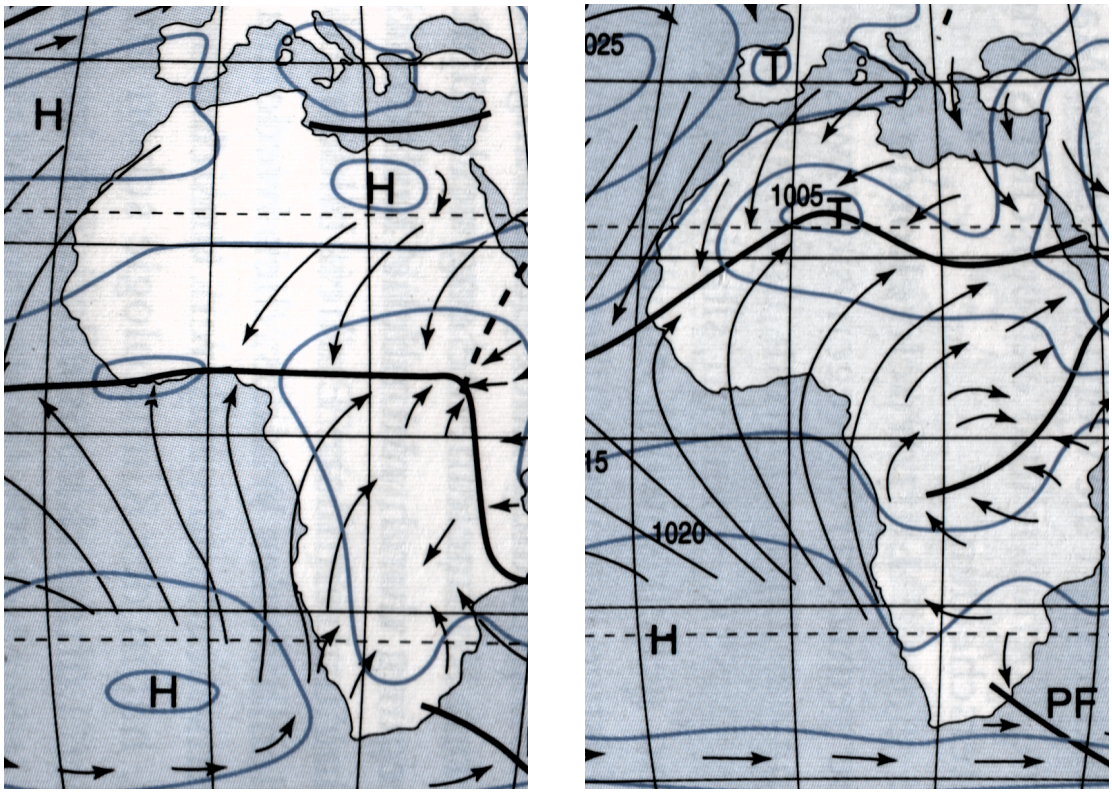

Figure 4.6: Mean circulation in Africa for (left) January and (right) July. 'T' stands for Low, 'H' for High, and 'PF' for Polar Front;
Source: Schönwiese (2003)

Analysis (AMMA) project, the AMMA-Coupling the Tropical Atmosphere and the Hydrological Cycle (AMMA-CATCH) project (Redelsperger et al., 2006; Lebel et al., 2010), and the Dynamics-aerosol-chemistry-cloud interactions in West Africa (DACCIWA) project (Knippertz et al., 2015) have been initiated to increase our knowledge on the weather and climate in Africa. Thereby the usage of satellite information plays an important role to fill the gaps in ground-based networks. However, the quality and applicability of satellite data is not fully consolidated. Further, regional weather and climate models are applied in Africa to study current and future climate conditions (Kothe et al., 2014). Moreover, these models have usually been developed to be applied in the United States or Europe and its usage in different climate regimes may cause difficulties. The model's ability to correctly simulate relevant processes is essential and requires model validations. One of the most relevant processes, especially in a tropical climate, is convection that controls the diurnal cycle of precipitation.

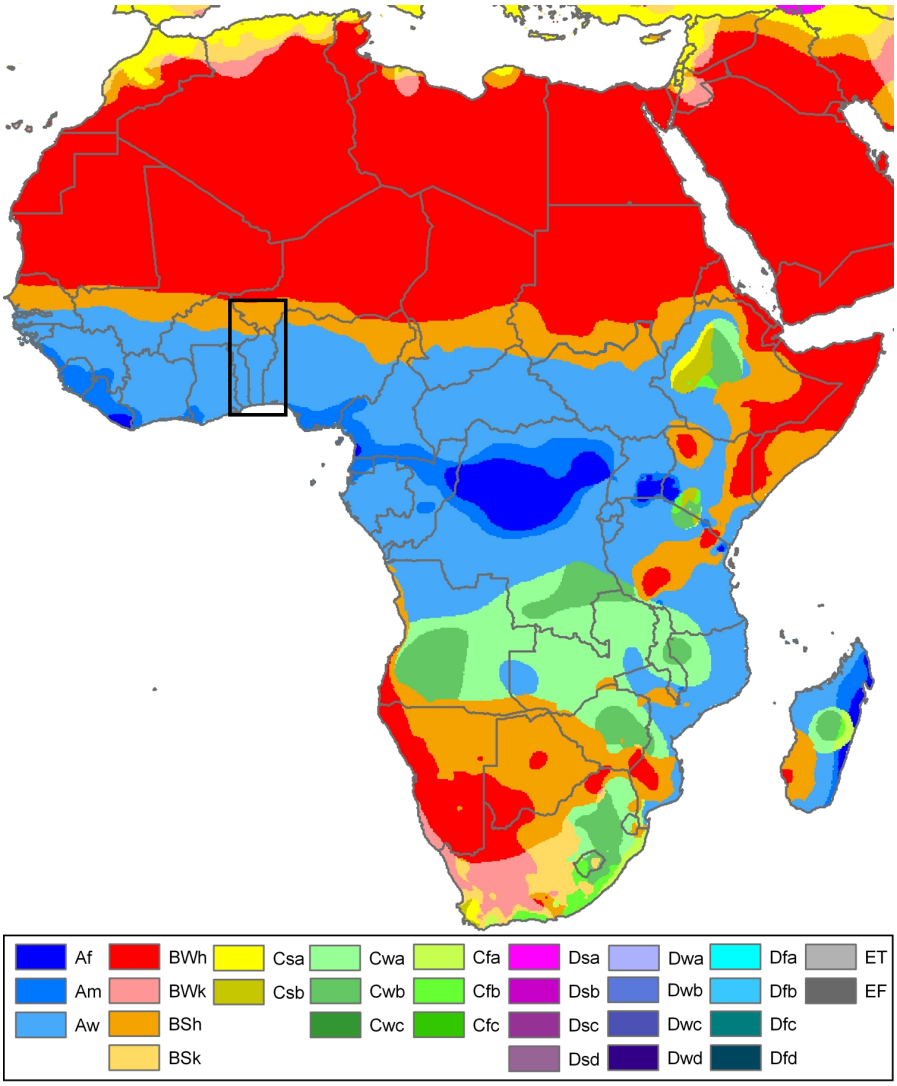

Figure 4.7: Climate zone classification of Africa by Köppen-Geiger; The black box shows the region of interest, which includes the used AMMA-CATCH rain gauges networks. Source: `https://commons.wikimedia.org/wiki/File:Africa_Koppen_Map.png`

The focus is now on the diurnal cycle of precipitation in West Africa. As satellite data is the only data source in many tropical regions, it is essential to evaluate if current satellite-based datasets can capture the true diurnal cycles of rainfall in a that regime. Therefore rain gauge stations of 1-hourly precipitation data from the AMMA-CATCH database have been used as the ground-based reference. The used AMMA-CATCH data is located at two meso-sites in Benin (Ouémé) and in Niger (Niamey) (cf. Figure D.1). At both mesosites the satellite products of TMPA, TRMM-TMI, TRMM-PR, TRMM-COMB, PERSIANN, CMOPRH and

CMORPH-hq (see Section 3.2 for data descriptions) are validated during a common 12-year time period of 2000–2011.

Even though the climate of both mesosites in Ouémé and Niamey are controlled by the WAM, they have different diurnal cycles of precipitation. The southern Ouémé site exhibits a diurnal cycle with a double peak structure, while the late afternoon peak is more pronounced when averaged over the full monsoon season (May–September) (see Figure 4.8). Instead the Niamey mesosite has on average a diurnal cycle with a broader maximum of rainfall in the early morning. However the precipitation diurnal cycles vary from month-to-month and year-to-year, which is especially true for the Ouémé mesosite in Benin (see Appendix D for more details).

At the Ouémé mesosite the diurnal peak precipitation changes between a morning peak at the beginning and the end of the monsoon season, and a distinct evening peak during the central monsoon months of July and August. Different rainfall characteristics for the pre-monsoon and full-monsoon season have also been found by Gounou et al. (2012). While the rainfall originates mainly from westward propagating MCSs at the beginning and end of the WAM, rainfall during the central monsoon months is mainly caused by locally initiated convection (Fink et al., 2006; Koster et al., 2004). The Year-to-year diurnal cycle characteristics are most likely controlled by the dominating rainfall regime in the respective year. The prevailing rainfall regime may vary with the varying location of the ITCZ in West Africa.

At the Niamey meso-site rainfall is less frequent compared to the Ouémé mesosite and the diurnal cycle of rainfall is driven by rare rainfall events. Those events mostly occur due to MCSs that are initiated in mountains east of Niamey in the evening and travel toward Niamey, where the MCSs usually arrive in the early morning hours. Consequently, a mean diurnal rainfall peak in the morning is observed. The analyzed satellite products capture this early morning peak. However the variability between the different datasets is relatively large owing to the limited number of rainfall events each year in the outer-tropics.

Overall, the analyzed satellite-based datasets are able to capture the general properties of the diurnal cycle of precipitation at both the Ouémé and the Niamey mesosites. Especially the TRMM-TMPA and CMORPH data performs well in getting the true diurnal cycle of rainfall, while the TRMM satellite-only based datasets suffer from their weak spatiotemporal coverage, when analyzed at shorter time scales.

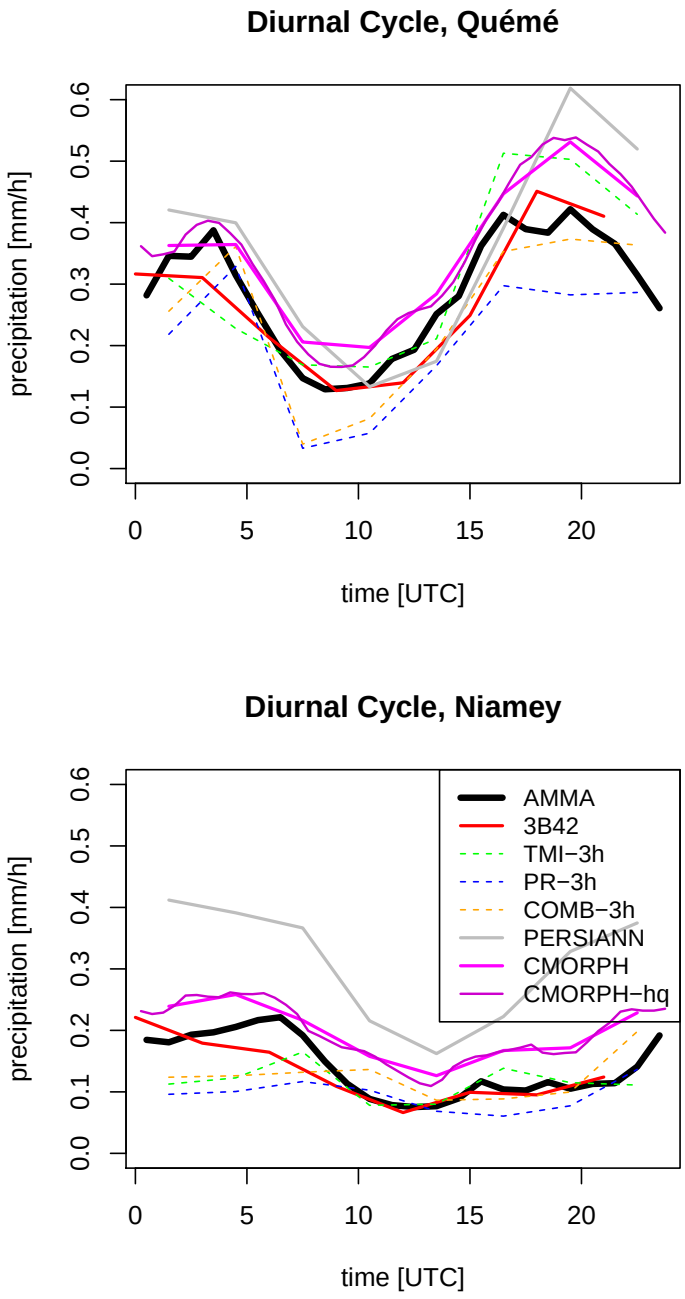

Figure 4.8: Mean diurnal cycles of the satellite-based datasets and the AMMA-CATCH reference data at the West African Niamey meso-site (upper part) and Ouémé mesosite (lower part) during the monsoon season (MJJAS), during 2000 to 2011

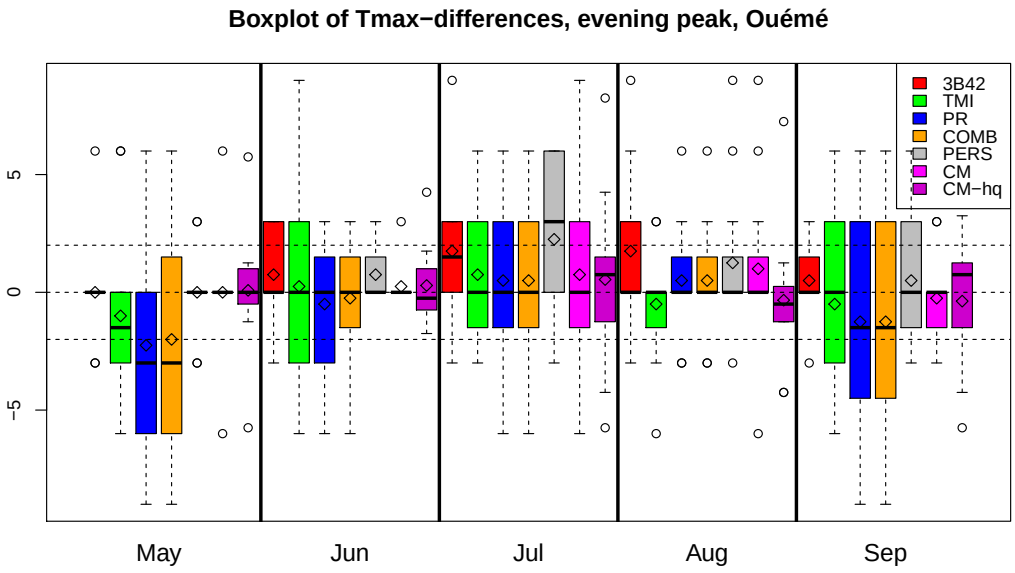

Figure 4.9: Time differences [h] (satellite datasets minus station data) in the evening peaks of monthly mean diurnal rainfall in the monsoon months at the Ouémé mesosite. Time differences are shown by box-plots, mean values are plotted by diamond-signs

The satellite-based datasets get the diurnal cycles of rainfall reasonably well, but there is the tendency of estimating the distinct evening peak of rainfall at the Ouémé mesosite a little too late. Figure 4.9 shows that during the main monsoon months the satellite products show mean delays of 1 to 2 hours that are quite systematic. The delay is largest for the PERSIANN data, which might be owing to the fact that PERSIANN is mainly based on IR information that are only sensitive to cloud top temperatures. However, following the study by Futyan and Del Genio (2007), most rainfall in tropical convective storms appear at an early stage, while the cloud and its anvil is still growing in height and coverage. This may cause IR-based satellite precipitation estimates peak too late in the diurnal cycle, in case of locally initiated convective rainfall. However a slight delay is seen for most analyzed satellite products, probably as a result of the use of IR-information in generating the datasets. Another reason might be the large fall velocities of rain as often graupel is involved in the generation of convective precipitation in West Africa (Cetrone and Houze, 2009). These fall velocities might be underestimated by the applied rainfall algorithms.

The numerical model based precipitation data by CCLM and MERRA show deficiencies in getting the correct diurnal rainfall variability. As shown in Ap-

pendix E, the analyzed CCLM simulations are neither able to get the correct mean precipitation diurnal cycle nor the observed year-to-year and month-to-month variabilities with reference to the CMOPRH-hq satellite data, at the Ouémé mesosite. The same is true for the MERRA reanalysis. Both CCLM and MERRA show a too strong and too early diurnal peak of rainfall, occurring around noon. The early peak in precipitation diurnal cycles is a known model deficiency (e.g. Hohenegger et al., 2008), caused most likely by the usage of convective parameterizations that initiate convection too early, e.g. owing to the missing of a reasonable convective inhibition in the model. However, at least at the Niamey mesosite the CCLM is able to simulate a weak morning peak of rainfall, which is in rough agreement with observations.

Chapter 5

Conclusions and Outlook

The diurnal cycle of clouds and precipitation is of high importance for understanding the energy- and water cycle of the earth. Despite its relevance, the diurnal cycle is often disregarded while the focus is usually limited to the daily, monthly or seasonal time scale. In meteorology, small scales influence the larger scales and vise versa. In order to better understand the large scales, it is essential to know about the small scale in a best possible way. To do so, it is important to analyze the best possible data available. As it is shown in this thesis, finding the best possible meteorological data for a certain purpose is not straightforward and requires detailed data analysis, including the validation with reference data, if available.

Clouds and precipitation are essential climate variables that are subject to considerable diurnal variability that control the local and global climate. Clouds directly effect radiation fluxes and precipitation further affect energy fluxes, especially through latent heat. Both clouds and precipitation can only be observed with a global coverage by making use of satellite data. Further, models, including model-based reanalysis, deliver regional and global information about various meteorological parameters on the sub-daily temporal scale.

Because of unknown feedbacks, clouds are a major uncertainty factor concerning the current and the future climate (Bony et al., 2015). The analysis of satellite based cloud datasets showed an overall reasonable data quality concerning cloud variability. For cloud diurnal cycles, the analyzed ISCCP and CM SAF datasets reasonably agree with ground-based Synop observations. Nevertheless, because of data source and algorithm dependent cloud detection sensitivities, and a missing a common definition of cloud cover, biases regularly occur. For the European summer season, all observational cloud products agree for the cloud diurnal cycle with a minimum of cloud cover in the morning and a maximum in the afternoon. Instead, the CCLM fails to simulate the observed climatological cloud diurnal cycle in Europe in summer (cf. Figure A.5). A possible reason for this failure is the issue of small-scale processes that are responsible for the initiation of convection, but

not resolvable by the model. The erroneous cloud cover diurnal cycle introduces errors in the radiative transfer calculations in the model. As there are too much clouds during nighttime, the nocturnal emission of longwave radiation might be underestimated. In accordance, the diurnal temperature range is underestimated in the CCLM simulation in central and eastern Europe as a consequence, compared to E-OBS gridded station data.

In opposite to the results in Europe, the CCLM is able to simulate the distinct cloud cover diurnal cycles in the maritime stratocumulus region off the west coast of southern Africa. There, the cloud diurnal cycle is not related to deep convection. The reasons for the diurnal formation and breakup of the low-level maritime clouds are a continuous oceanic moisture flux from below a low-level inversion, and a strong solar insolation during daytime that causes the cloud breakup (e.g. Rozendaal et al., 1995). These processes seem to be better simulated by the model, probably because they are more large-scale. As in Europe, there are substantial biases in the stratocumulus regime between all analyzed data, with a large cloud cover underestimation by the CCLM with reference to the satellite data.

Classical rain gauge data is the reference for the precipitation measurement. Unfortunately, the rain gauges are globally irregularly distributed and satellite-based data is often the only data source available, especially in the tropics and over oceans. Further, model-based reanalysis datasets deliver global information of the full range of climate variables including precipitation.

The evaluation of monthly precipitation given by satellite and reanalysis datasets revealed a relatively similar performance of both data sources, showing anomaly correlations in the order of 0.65 to 0.75 and mean absolute errors in the order of 20 to 30 %. These numbers show the quite large uncertainties of current precipitation datasets, either satellite- or model-based. Based on the detailed analysis of the HOAPS dataset it is concluded that higher spatiotemporal coverage is a key to higher data quality—given a reasonable algorithm performance at the instantaneous time scale. The deviations of HOAPS are reduced when its spatial resolution is reduced, likely as a result of the cancellation of errors at smaller scales. It is concluded that HOAPS suffers from a combination of low spatiotemporal coverage and a relatively high spatial resolution, which constitutes a suboptimal combination for highly variable tropical precipitation. It is remarkable that the precipitation data from the reanalysis datasets of ERA-Interim and MERRA perform almost in the range of the satellite-based precipitation datasets for anomaly correlations on the monthly scale. This shows that current global reanalysis products are a valuable data source, at least when larger temporal scales are considered. This is also a result of the extensive data assimilation efforts made by modern reanalysis systems, where satellite data play an important role.

The analysis in the tropical Pacific also showed that the GPCP satellite data,

which makes use of LEO and GEO satellites, performed best despite of its coarse spatial resolution. The higher-resolved HOAPS satellite and ERA-Interim and MERRA reanalysis data do not offer a higher data performance in the tropical oceanic climate regime analyzed. Despite of its good performance concerning correlations, the GPCP data has a negative bias of $-9\,\%$ with reference to the PACRAIN atoll data. This negative precipitation bias corresponds to the global energy budget analysis by Stephens et al. (2012), who suggests to increase the global precipitation flux to better close the Earths energy budget.

A disadvantage revealed for the analyzed reanalysis data is its underestimation of high precipitation and overestimation of small precipitation amounts, which have been found in both the ERA-Interim and MERRA reanalysis data. Such systematic over- and underestimations are not observed for the analyzed satellite-based datasets. As a consequence, the usage of reanalysis precipitation data is hindered for certain purposes, including the analysis of extreme events. A reason for the overestimation of small rainfall amounts might be related to the too frequent initiation of convection by the responsible parametrization schemes—an issue that has already been found by Dai (2006) for global climate models.

The validation of precipitation diurnal cycles in West Africa showed that the satellite-based datasets overall perform well in capturing the observed precipitation diurnal cycles as measured by rain gauges on the ground. The rain gauge data given by the AMMA-CATCH database are available for two mesosites located in the inner- and outer tropics of the West African monsoon region. Especially at the inner-tropical Ouémé mesosite in Benin, where monsoonal rainfall is more frequent than at the outer-tropical Niamey mesosite, the measured mean rainfall diurnal cycles at the surface are well captured by the analyzed satellite-based datasets.

At the Niamey mesosite located northward in the outer-tropics, the validation results are more divers. The main reason for the larger deviations is that rainfall is less frequent in the West African outer-tropics. There, the diurnal cycle is mostly dominated by only few rainfall events during the monsoon season, which originate from MCSs that usually arrive in the early morning at the Niamey mesosite. Still, the resulting diurnal cycle of rainfall that shows a scattered maximum in the morning is overall captured by the satellite products. The largest deviations are observed for the TRMM-only satellite datasets (TRMM-PR, TRMM-TMI and TRMM-COMB), which have a weak spatiotemporal coverage and therefore likely miss some of the anyway rare rainfall events.

A more detailed analysis of diurnal cycles was possible for the Ouémé mesosite, where rainfall is more frequent during the monsoon season and hence the precipitation statistics are more robust. Overall, the analysis at the Ouémé mesosite during a 12 year time period revealed monsoonal mean diurnal cycles with a double peak structure, consisting of a weaker early morning and a stronger evening

peak of rainfall. This general behavior is consistent with findings by Fink et al. (2006) during a one year period in 2002. The satellite products also capture the intra-monsoonal rainfall regime shift from a subtropical MCS dominated regime toward a local convection dominated regime during the central monsoon months, and back to a MSC regime at the end of the monsoon season. Also a year-to-year variability of the diurnal cycle is found, likely depending on the precipitation regime dominating, being either more MCS or more local convection controlled. Outstanding in this respect are the years of 2004 and 2009, when MCSs and local convection is dominating, respectively.

For the Ouémé mesosite both the morning and the afternoon peak of the diurnal cycle have been analyzed concerning its timing. For the locally initiated convective rainfall that mainly occurs in the evening during the central monsoon months, most satellite products show a delayed rainfall peak relative to the ground reference of about 1 to 2 hours. The observed delay in diurnal peak precipitation can be attributed to the use of IR-based estimates of precipitation, which are only sensitive to cloud top information. Futyan and Del Genio (2007) showed that local tropical convective storms produce maximum rainfall in an early stage—before the convective cloud has reached its maximum extent and its minimum cloud top temperatures. But only the latter two cloud properties are usable as proxies by applying IR-sensors for the estimation of rainfall. Therefore the delay is most likely a result of the misinterpretation of high and cold but non-precipitating clouds as still raining—like ice shields from dissipating thunderstorms. Further, graupel is often involved in thunderstorms in West Africa (Cetrone and Houze, 2009), which might additionally contribute to the timing mismatch as the satellite algorithms might underestimate the precipitation fall velocities. The delay is quite systematic and most pronounced (up to 2 hours) for the used PERSIANN data that is solely based on IR information.

Owing to their reduced spatiotemporal coverage, the TRMM-only products need to be analyzed on long—ideally multi-year time scales to get a reasonable mean diurnal cycle, while the data coverage in not sufficient for analyzing the diurnal cycle on shorter time scales. Overall, the analyzed satellite-based precipitation datasets perform well in capturing the diurnal cycle and its variability during the West African monsoon season. The TMPA and the CMORPH products overall perform best, while the TMPA dataset also gets the mean amounts quite well, and the high-resolved CMORPH-hq product correctly captures the diurnal cycles timings. The results shows that the CMIORPH method of using microwave sensors onboard LEO satellites to derive absolute precipitation amounts, and the downscaling of those values with spatiotemporally high resolved GEO-IR satellite data performs well in the tropical climate regime.

Two regional climate model simulations by the CCLM and the MERRA re-

analysis are subsequently evaluated for rainfall diurnal cycles in West Africa with reference to the CMOPRH-hq satellite data (cf. Appendix E), which has been shown to be of good quality concerning diurnal cycles by Pfeifroth et al. (2016). It is revealed that both the CCLM simulations and the MERRA reanalysis do not provide the correct rainfall diurnal cycle at the inner-tropical Ouémé mesosite. Instead, they produce a rainfall diurnal cycle with a single pronounced peak at around noon. This is a typcal problem of many weather and climate models that have to use convective parametrizations. Nevertheless, it is worth mentioning that also the treatment of energy fluxes between the soil and the atmosphere plays a role for the initiation of rainfall; An improved treatment of the heat conductivity formulation in the TERRA soil model used by the CCLM (Schulz et al., 2016), at least slightly improved the simulated diurnal cycle, leading to a peak rainfall that is about one hour later than before. Still, the simulated precipitation diurnal cycles deviate from the observations. At the Niamey mesosite, where rainfall is mainly originating from MSCs, the CCLM seems to better simulate the diurnal cycle than the MERRA reanalysis that shows a similar behavior than at the inner-tropical site. A possible reason for the improved diurnal cycle of the CCLM in the MCS-regime is that MCSs are much larger than the local convective storms in the inner-tropics (e.g. at the Ouémé mesosite) and can therefore be better resolved by the model. Furthermore, a substantial part of MCSs rainfall is also of stratiform nature (Houze Jr., 2004).

Overall, current satellite-based cloud and precipitation datasets are valuable data sources for analyzing the global distribution and the variability of clouds and precipitation from the monthly to the sub-daily scale. Nevertheless, users should be aware that satellite data can be subject to substantial uncertainties, and its quality is often dependent on location and time span, and finally on the actual application. Therefore, satellite data should be used with care, and, if there are justified doubts about its reliability, the satellite data should be validated with reference data if available, or existing profound data validation studies should be considered.

Weather and climate models, including reanalysis products, have been improved in recent years. But accurate simulations of the diurnal cycle requires very-high resolved simulations to reduce the usage of parametrizations for sub-grid scale processes (Brisson et al., 2016). But convective-permitting simulations are at the moment computationally too expensive for longer-term applications. As a consequence, for the analysis of sub-daily variability of clouds and precipitation, satellite-based observations are preferred, and can also be used for model validations from the global to the regional scale. Anyway, each meteorological data source of clouds and precipitation has its strengths and weaknesses and are not ideal on for any purpose, also because of the limited data availability. Individual

data characteristics, as analyzed in this thesis, should be considered when using cloud and precipitation data on the monthly to sub-daily scale.

Appendices

Appendix A

Paper 1: Cloud Cover Diurnal Cycles in Satellite Data and in Regional Climate Model Simulations

published as:

Pfeifroth, U., Hollmann, R. and Ahrens B. (2012): Cloud Cover Diurnal Cycles in Satellite Data and Regional Climate Model Simulations. *Meteorologische Zeitschrift*, 21(6):551-560.

abstract

The amount and diurnal cycle of cloud cover play an important role in the energy and water cycle of the earth-atmosphere system and influence the radiation budget of the earth. Due to its importance and the challenging nature of its quantification, cloud cover is considered the biggest uncertainty factor in climate modeling. There is a clear need for reliable cloud datasets suitable for climate model evaluation studies.

This study analyzes two datasets of cloud cover and its diurnal cycle derived from satellite observations by the International Satellite Cloud Climatology Project (ISCCP) and by EUMETSAT's Satellite Application Facility on Climate Monitoring (CM SAF) in Africa and Europe. Two regions, Europe and the subtropical southern Atlantic Ocean, were identified as offering distinct cloud cover diurnal cycles reasonably observed by both satellite datasets. In these regions, simulations by the regional climate model COSMO-CLM (CCLM) were evaluated in terms of cloud cover and its diurnal cycle during the time period of 1990 to 2007.

Results show that the satellite derived cloud diurnal cycles largely agree, while discrepancies occur under extreme conditions like in the Sahara region. The CCLM is able to simulate the diurnal cycle observed consistently in the two satellite datasets in the South-Atlantic ocean, but not in Europe. CCLM misses the afternoon maximum cloud cover in Summer in Europe, which implies deficiencies in the parameterization of convection and in the treatment of surface-atmosphere interactions. The simulation of the diurnal cycle of the more stratiform cloud cover over the subtropical Atlantic was satisfactory in CCLM.

Zusammenfassung

Die Wolkenbedeckung und dessen Tagesgang spielen eine wichtige Rolle im Wasser- und Energiekreislauf der Erde in dem sie beispielsweise die Strahlungsbilanz der Erde beeinflussen. Wolken gelten zudem als eine der größten Unsicherheitsfaktoren in der Klimamodellierung. Trotz dieser Wichtigkeit, sind Wolken eine schwer zu quantifizierende Größe, und es gibt Bedarf an möglichst global verfügbaren und verlässlichen Wolkendaten, beispielsweise für Modellevaluierungen.

In dieser Arbeit werden Satellitendaten der Wolkenbedeckung und dessen Tagesgang vom International Satellite Cloud Climatology Project (ISCCP) und von EUMETSAT's Satellite Application Facility on Climate Monitoring (CM SAF) in Afrika und Europa bezüglich ihrer Verlässlichkeit verglichen. Es zeichnen sich hierbei zwei Regionen mit deutlichen Tagesgängen der Wolkenbedeckung und guter Übereinstimmung aus: Mitteleuropa und der subtropische Südatlantik, westlich von Afrika. Die Satellitendaten werden schließlich genutzt um Simulationen des regionalen Klimamodells COSMO-CLM bezüglich der Wolkenbedeckung und dessen Tagesgang in jenen Regionen zu evaluieren.

Die Vergleiche zeigen, dass die Satellitendaten bezüglich der Tagesgänge der Wolkenbedeckung insgesamt gut übereinstimmen und bis auf regionale Ausnahmen eine relativ verlässliche Datenquelle darstellen. Im subtropischen Süd-Atlantik zeigen die Satellitendaten große Tagesgänge in der Wolkenbedeckung, welche auch relativ gut vom Klimamodell CCLM simuliert werden. In Europa im Sommer zeigen beide satellitenbasierten Datensätze übereinstimmend ein Bewölkungsmaximum am Nachmittag, welches vom Modell aber nicht simuliert wird. Gründe dafür liegen möglicherweise in der Parametrisierung von Konvektion und in Problemen mit Landoberflächenflüssen.

A.1 Introduction

The global radiation budget of the earth-atmosphere system determines our climate (e.g. Trenberth et al., 2009). The absorbed shortwave radiation acts as a heat source while the emitted longwave radiation counteracts by cooling the planet. Clouds play a major role in impacting radiation in both the longwave and shortwave spectral ranges. There are two important radiative effects of clouds: the cloud albedo effect and the cloud greenhouse effect. The cloud albedo effect causes incoming solar radiation to be reflected back to space. Since less solar radiation reaches the earth surface, this has a cooling effect. The cloud greenhouse effect causes outgoing terrestrial radiation to be partly absorbed and reemitted by clouds - a warming effect (Stuhlmann, 1995). These counteracting effects have globally averaged radiative forcings of the order of $+50W/m^2$ and $-30W/m^2$, respectively, as roughly estimated in several studies (Sohn and Robertson, 1993; Stuhlmann, 1995; Kiehl and Trenberth, 1997; Raschke et al., 2005; Loeb et al., 2009). The magnitude of cloud radiative effects depends on the spatio-temporal distribution of clouds and their properties. The systematic diurnal variability of cloud cover, referred to in this study as cloud diurnal cycle, has a significant radiative impact (Arkin, 1991).

Increased attention is paid to climate reanalysis and simulation in the era of climate change. Numerical atmospheric models have difficulties in simulating quantities, such as cloud cover, which depend on small scale processes not resolved by the models. This includes cloud formation and breakup processes, which are often controlled by minor changes in atmospheric conditions. The simulation of cloud cover and its variability are essential to do reasonable climate simulations because cloud radiative effects are significant. Moreover various feedback processes may disturb simulation results owing to severe problems in modelling cloud cover. Therefore clouds are generally considered the biggest uncertainty factor in weather and climate modelling (Dybbroe et al., 2005).

In order to evaluate climate models with respect to cloud cover diurnal cycles, reliable cloud data offering a suitable spatio-temporal coverage are required. Satellite data may deliver the required cloud information but reliable cloud detection from satellites is challenging (e.g. Schulz et al., 2009). Due to the relatively long history of infrared (IR) and visible (VIS) radiometers in satellite meteorology, often these spectral ranges are used for the generation of satellite based cloud datasets. For the satellite data used in this study this is also the case.

In many earlier comparison studies satellite based cloud data was usually analyzed on a daily or monthly basis (e.g. Rossow and Garder, 1993; Jin et al., 1996; Ahrens et al., 1998; Jaeger et al., 2008; Stubenrauch et al., 2010). A validation of monthly and daily mean cloud cover data by the Satellite Application Facility on Climate Monitoring (CM SAF) showed an overestimation of clouds over ocean,

while the data was acceptable in Europe (Reuter et al., 2009). In desert regions, usually having high surface albedo, large daily temperature variations and high aerosol loads, cloud detection using VIS and IR measurements is more difficult and uncertain (Stubenrauch et al., 1999). Marine stratiform clouds, present over large ocean areas, are easily detectable e.g. by International Satellite Cloud Climatology Project (ISCCP) data (Stubenrauch et al., 1999) and measurements are in good agreement with surface observations (Rozendaal et al., 1995).

Diurnal cycles of cloud cover by ISCCP data were analyzed by Cairns (1995). He found that diurnal cycles in ISCCP data agreed with synoptical observations in a six year period. Moreover diurnal cycles were overall regarded as reasonable and in accordance with known atmospheric conditions. Bergman and Salby (1996) also analyzed ISCCP data and found that diurnal cycles over oceans are quite distinct and primarily related to the daily cycle of insolation. Moreover Minnis et al. (1992) and Meskhidze et al. (2009) found that over large ocean areas a strong diurnal cycle of low clouds can be well observed. These low clouds have a significant impact on the radiation budget (Karlsson et al., 2008).

It has been seen in various studies that numerical models have difficulties in simulating clouds. Meinke (2006) evaluated simulations by the Regional Model (REMO) in climate mode with satellite observations by ISCCP in Europe and found that the simulated diurnal cycles of cloud cover were too small. Roebeling and van Meijgaard (2009) used satellite data to evaluate daytime cycles of cloud cover simulated by the Regional Atmospheric Climate Model (RACMO) and found that the model performs better over ocean than over land, which is attributed to shortcomings in the parameterization of convection in the model. A comparison of simulations by the regional climate model COSMO-CLM (CCLM) and observational data revealed general overestimations of cloud cover in Central Europe in summer (Jaeger et al., 2008), with especially nighttime cloud cover too high. Further, the analysis of cloud resolving CCLM simulations revealed that problems in modeling the diurnal cycle of clouds and precipitation are primarily caused by deficiencies in the convection parameterizations (Hohenegger et al., 2008). The high relevance of cloud cover in model simulations is emphasized by Hohenegger et al. (2008) and Kothe et al. (2010), who found that radiative flux errors in CCLM simulations are mainly caused by deficiencies in modeling cloud cover. CCLM simulations are also evaluated in this study.

This study compares satellite based cloud cover datasets of the International Satellite Cloud Climatology Project (ISCCP) and of EUMETSAT's Satellite Application Facility on Climate Monitoring (CM SAF) in order to evaluate their reliability in monitoring diurnal cycles of cloud cover (section A.4). We found two regions, Europe and the subtropical South-Atlantic ocean, offering distinct diurnal cycles of cloud cover and high data reliability. Consequently we evaluated cloud

cover diurnal cycles as simulated by CCLM with ISCCP data in those two regions, during the time period of 1990 to 2007 (section A.5). The results are summarized and discussed in section A.6

A.2 Data

A.2.1 Satellite data

ISCCP

The International Satellite Cloud Climatology Project (ISCCP) started in 1982 as the first project of the World Climate Research Programme (WCRP). It generates global cloud datasets derived from measurements of several geostationary and polar orbiting operational weather satellites. ISCCP data is widely used to improve the understanding of the role of clouds in the climate system.

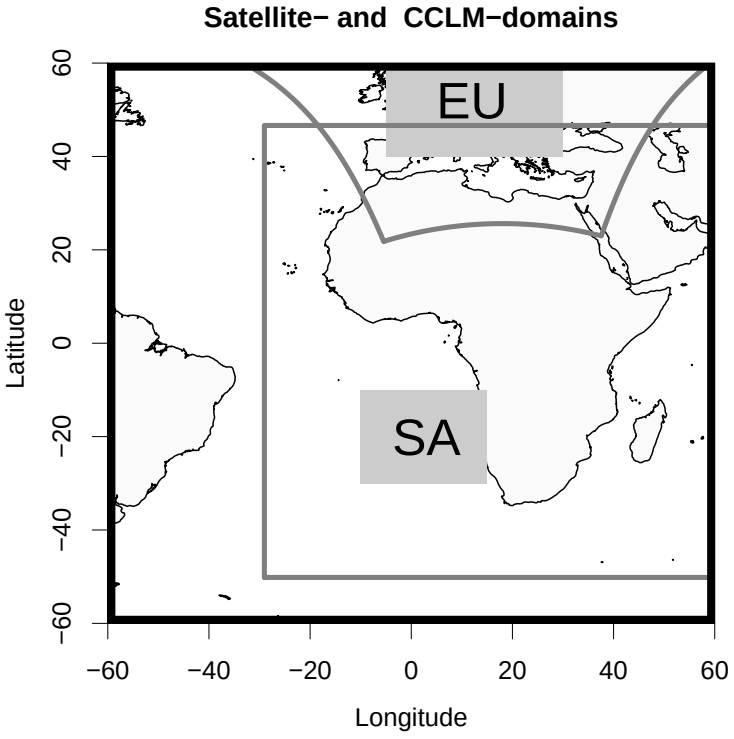

Figure A.1: Domains of the comparison of satellite data (big black box), domains of the CCLM simulations in Europe and Africa (grey) and regions of interest (EU and SA) for the evaluation of CCLM simulations (grey shaded regions)

In this study, monthly mean diurnal cycles of cloud cover data of the ISCCP climatological summary product (ISCCP-D2) are used. The diurnal cycle is sampled 3-hourly and offers a spatial resolution of 2.5°. In the analysis domain (cf. Fig. A.1) the ISCCP-D2 data is based on the SEVIRI (Spinning Enhanced Visible and Infrared Imager) instrument onboard the geostationary METEOSAT satellites, while one infrared (IR) and one visible (VIS) channel is used.

The main challenge for the ISCCP cloud detection algorithm is to get clear-sky background values in both channels. Therefore variability tests are performed to check for radiance variations in space and time to detect clear-sky situations (Rossow and Garder, 1993; Rossow and Schiffer, 1999). The actual radiance measurement for each pixel is then compared to the corresponding clear-sky value. If the clear-sky value and the actual measurement differ by more than a certain detection threshold (Rossow and Schiffer, 1999), the pixel is classified as cloudy. Otherwise it is classified as cloud-free. The clear sky value, which is derived for each time slot separately, is kept constant for 5 to 30 days, depending on cloud cover frequency. Hence cloud detection uncertainties increase in case of rapid variations of local surface or atmospheric conditions. Inside each 2.5 °gridbox, the individual pixels are averaged to get cloud fractional cover. More detailed information about the ISCCP data and its retrieval methods can be found online at http://isccp.giss.nasa.gov or in various scientific publications (e.g Rossow and Garder, 1993; Rossow and Schiffer, 1999).

CM SAF

The EUMETSAT Satellite Application Facility on Climate Monitoring (CM SAF) is continuously developing capabilities for a sustained generation and provision of Climate Data Records derived from operational meteorological satellites (Schulz et al., 2009). In particular the generation of long-term data sets is pursued. The ultimate aim is to make the resulting data sets suitable for the analysis of climate variability and potentially the detection of climate trends. To achieve this goal CM SAF works in close collaboration with the international science community and liaises with other satellite operators to advance the availability, quality and usability of Fundamental Climate Data Records (FCDRs) as defined by the Global Climate Observing System (GCOS). The major task of the CM SAF is to utilize FCDRs to produce records of Essential Climate Variables (ECVs) as defined by GCOS. Thematically, the focus is on ECVs associated with the global energy and water cycles. The CM SAF was initiated in 1999 and is led by the Deutscher Wetterdienst (DWD).

The CM SAF cloud cover product used (CFC) is based on the SEVIRI instrument, just like the ISCCP product. The principle method to derive the product is a threshold method, in principle similar to the ISCCP approach, except that clear-

sky background values are derived with the help of a radiative transfer scheme. The cloud detection method was developed in EUMETSAT's Nowcasting SAF (NWC SAF) and is described in Derrien and Le Gléau (2005). The algorithm uses individual threshold tests to find cloudy or cloud-free pixels. Several SEVIRI channels are used, enabling the method to be adapted for local atmospheric and surface conditions. The calculated clear-sky background values are updated in each time step, in contrast to the ISCCP algorithm. Within processing, native SEVIRI pixels are classified depending on cloud contamination and averaged inside areas of $(15\,km)^2$ to calculate cloud fractional cover. The SEVIRI data (15 min temporal resolution) is sampled hourly to generate the monthly mean diurnal cloud cover product (Version 300) (Karlsson et al., 2011) obtained through the CM SAF web user interface at http://www.cmsaf.eu. Both detection algorithms of ISCCP and CM SAF are sensitive to the applied radiance thresholds. More detailed information about the data, data quality and its retrieval methods can be found in the CM SAF documentation available at http://www.cmsaf.eu.

A.2.2 CCLM simulations

Simulations by the regional climate model (RCM) COSMO-CLM (CCLM) in model version 4.8_CLM8 were evaluated using satellite data during the period of 1990 to 2007. The COSMO-CLM (CCLM) is a non-hydrostatic regional model, developed for climate simulations (Rockel et al., 2008). It is based on the COSMO-model (http://www.cosmo-model.org), which was developed for operational weather forecasting at the Deutscher Wetterdienst. The CCLM is now further developed and supported by the CLM-Community (www.clm-community.eu). It can be used on spatial resolutions ranging from 1 to 50 km and on time scales up to several decades. As driving dataset for the CCLM simulations, reanalysis data by the European Centre of Medium-range Weather Forecasts (ERA-Interim; see www.ecmwf.int/research/era/, Dee et al. (2011)) has been used. The CCLM was set up in a European domain and a African domain (see grey boxes in Fig. A.1). The simulations ran with a horizontal resolution of 0.44° and with 32 vertical atmospheric layers. More detailed information about the model and its setup are given in Dobler and Ahrens (2010) and Kothe et al. (2010).

In this study, seasonal mean diurnal cycles of the model parameter CLCT (total cloud cover) are evaluated. Cloud cover in the model is calculated by a combination of grid-scale cloud cover and subgrid-scale convective cloud cover. Grid-scale cloud cover in a certain model layer is unity if the relative humidity reaches 100%. If the relative humidity is below 100% cloud cover is not simply set to zero but is calculated as a fractional cloud cover between zero and unity by an empirical function of relative humidity. This accounts for some heterogeneity of clouds within grid boxes. The convective cloud cover is parameterized based on

convective activity, which is described by the Tiedtke mass-flux scheme (Tiedke, 1989). The convective cloud cover is dependent on the vertical extent of the convective cloud. Moreover cloud-top anvils can be considered resulting in a doubling of the convective cloud cover.

A.3 Methods

In order to make useful intercomparisons, the spatially finer resolved CM SAF and CCLM data is regridded to a common regular 2.5 °longitude/ latitude grid equal to that of ISCCP by applying a standard mean-conservative remapping method using a Climate Data Operator (see https://code.zmaw.de/projects/cdo).

A procedure necessary to ensure the comparability of diurnal cycles in different time zones, is the transformation of data from Universal Time (UTC) to Local Solar Time (LST). This entails a linear interpolation keeping the time resolution constant. Thereby a smoothing of the diurnal amplitude is unavoidable. The lower the temporal resolution of data the stronger the smoothing when interpolating to LST. In consequence, diurnal cycles of ISCCP data (3-hourly resolution) are smoothed more than diurnal cycles of CM SAF and CCLM data (both in hourly resolution).

As described in section A.2, cloud cover is dependent on the radiance thresholds used to distinguish between cloudy and cloud-free situations. Slightly different detection thresholds result in different cloud detection sensitivities which in turn lead to systematic differences in cloud cover. Nevertheless the diurnal cycle of cloud cover should be unaffected by general biases and was therefore chosen as the object of investigation in this study. The diurnal cycles of cloud cover are shown (e.g. in Fig. A.2, A.3) with the all-day mean subtracted, referred to as the 'relative' diurnal cycle in the following. Absolute diurnal cycles are also shown (eg. in Fig. A.4, A.5, A.6 and A.7).

To check the consistency of diurnal cycles between the satellite datasets in different regions an intercomparison of data is done on the full domain ranging from 60 °W to 60 °E and from 60 °S to 60 °N (see Fig. A.1) for the year 2007. To get an overview, ISCCP and CM SAF data are analyzed on a regular 15 °longitude/ latitude grid. Seasonal averaged relative diurnal cycles of cloud cover in each grid box of both datasets are shown in Figure A.2 and A.3.

In the model evaluation in section A.5, results are presented with the help of some statistical measures, including the bias, the diurnal cloud cover range (defined as diurnal maximum minus diurnal minimum) and the local times of maximum and minimum cloud cover. The CCLM simulations are evaluated in the the European (EU) area and in the Subtropical South Atlantic ocean (SA) area (Fig. A.1) during the time period of 1990 to 2007.

A.4 Intercomparisons of ISCCP and CM SAF cloud cover products

The satellite based cloud cover products of ISCCP-D2 and CM SAF are compared in the domain shown in Fig. A.1 for 2007 to get an overview of the consistency between the two datasets. The CM SAF cloud cover is higher by 3.7 percent over ocean and lower by 1.8 percent over land compared to the ISCCP cloud cover in 2007.

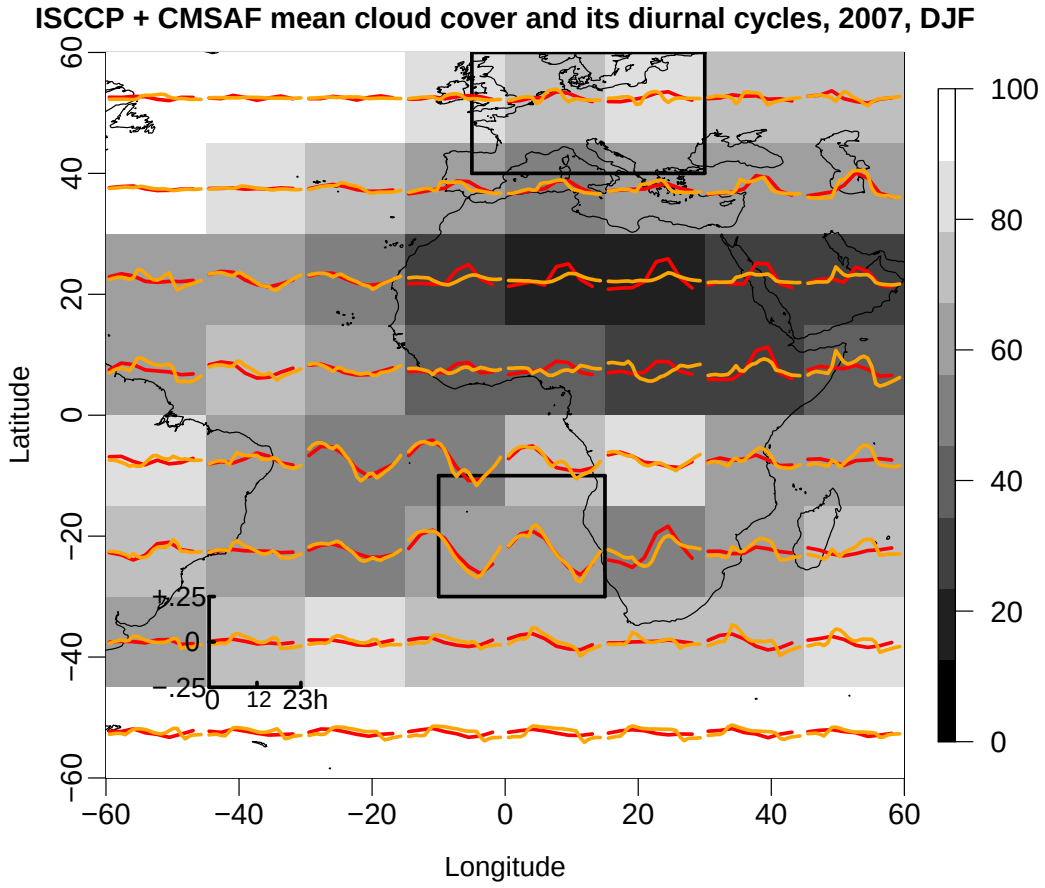

Figure A.2: Seasonal (DJF) averaged cloud cover (greyscale grid boxes) and relative diurnal variability of cloud cover of ISCCP (red lines) and CM SAF (orange lines) in each grid box. Exemplary axis (daytime (x-axis), relative cloud cover (y-axis)) are shown in a grid box in the lower left part of the image.

Main results of the comparison of diurnal cycles are shown in Figures A.2 and A.3. These figures contain various information: the greyscale of the grid boxes

indicates the average cloud cover and the lines inside each grid box show the mean relative diurnal variability of cloud cover. Figure A.2 shows results for the winter season (DJF (December, January, February)) and Figure A.3 for the the summer season (JJA (June, July, August)).

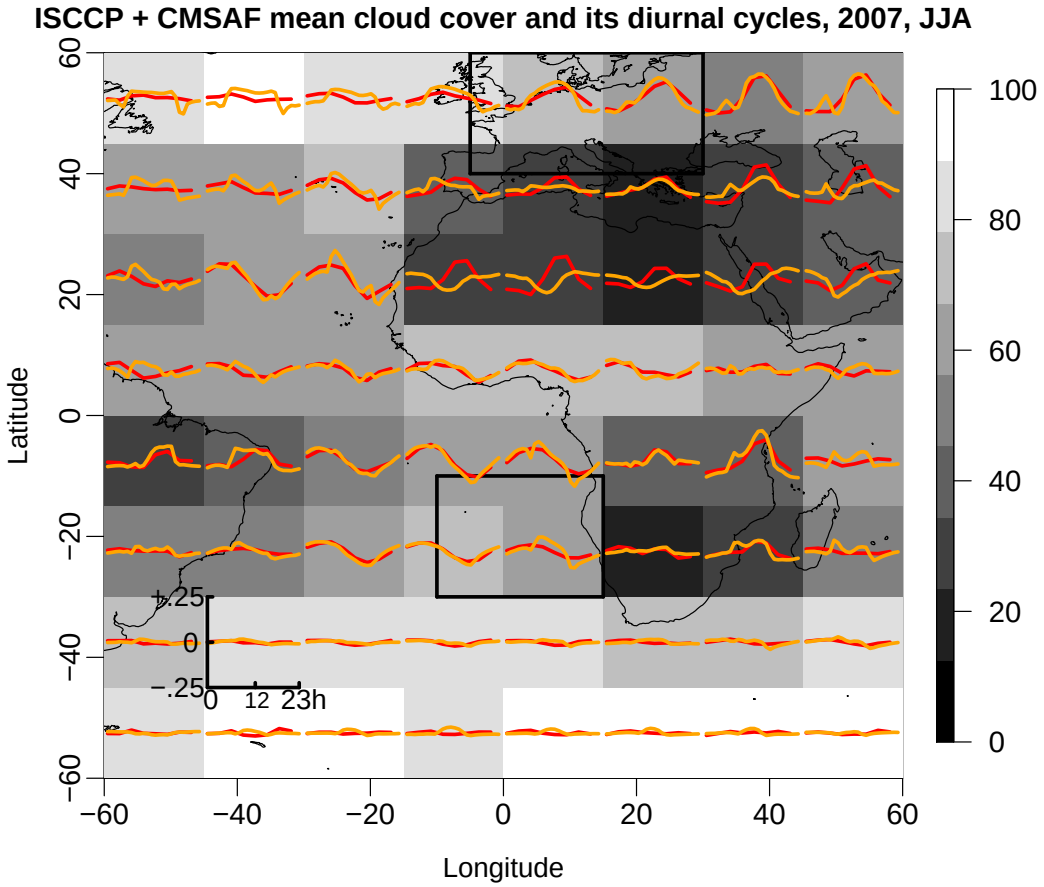

Figure A.3: Seasonal (JJA) averaged cloud cover (greyscale grid boxes) and relative diurnal variability of cloud cover of ISCCP (red lines) and CM SAF (orange lines) in each grid box. Exemplary axis (daytime (x-axis), relative cloud cover (y-axis)) are shown in a grid box in the lower left part of the image.

Overall the cloud cover diurnal cycles of ISCCP and CM SAF data agree, but there is one clear exception: the Sahara and Sahel region (see Fig. A.2 and A.3). The reason for this disagreement is the extraordinary climate conditions in this area with the strong near surface daytime heating together with high surface albedo. As detection algorithms of ISCCP and CM SAF are applied to various climate conditions, deficiencies have to be expected under extreme conditions like in desert

regions. There, ISCCP does show a clear diurnal cycle of cloud cover with a daytime maximum, while the CM SAF product does not. An explanation for the relatively large diurnal cycles in the ISCCP data is an increased cloud detection sensitivity in case of hot surface backgrounds (Bergman and Salby, 1996). The increase in sensitivity is due to increasing temperature differences between surface background and cloud top. In addition, temporarily very high aerosol concentrations, e.g. due to dust storms, may disturb the cloud detection, particularly in ISCCP (Stubenrauch et al., 1999). In contrast, cloud diurnal cycles in the Sahara region do not exist in the CM SAF cloud cover product. This may be due to the fact that the CM SAF cloud detection algorithm makes use of various combinations of SEVIRI spectral channels depending on climate conditions. Moreover a special test for dust is applied. Nevertheless, in the Sahara and Sahel region cloud detection is expected to be quite uncertain and inhomogeneous throughout the day. A cross-check with a climatology of synoptical observations showed the diurnal variability to be different to ISCCP and CM SAF data respectively (not shown).

Apart from the Sahara region, the relative cloud diurnal cycles agree reasonably well. Over land cloud cover usually peaks at or after noon, and over ocean the maximum cloud cover occurs in the early morning. Hence, the satellite derived cloud diurnal cycles agree with the meteorological expectations. The diurnal variations of cloud cover are generally larger in the summer hemisphere as primarily solar insolation controls cloud formation and breakup processes. This is obvious, for example, in Europe and in the subtropical South-Atlantic west of South Africa (Fig. A.2 and A.3). As both algorithms make use of spectral channels in the visible range when available, the detection algorithms are slightly more sensitive to clouds during daytime in both satellite products. This causes the algorithm to systematically detect more clouds during daytime than during nighttime. In case of ISCCP, differences between daytime and nighttime cloud cover due to algorithm differences have been found to be on the order of 3% (Meinke, 2006), which is small compared to observed diurnal cycles. In the CM SAF product the switching between nighttime and daytime algorithms regionally causes jumps in the averaged diurnal cycle of cloud cover (Fig. A.2 and A.3), especially over ocean. So far the CM SAF team has tackled this misfeature by smoothing. Nevertheless these jumps can be regarded as small relative to the natural diurnal variability of cloud cover in many regions.

A.4.1 European (EU) area

In winter there is almost no diurnal variability in either dataset (Fig A.2) as the weather is dominated by the westerlies. In the EU area in summer there is a clear peak in cloud cover in the afternoon and flat minimum in the nighttime (Fig. A.3).

The characteristic of the diurnal cycle of cloud cover in the summer season is primarily caused by convective clouds which occur frequently when the surface heats up in the afternoon and the troposphere becomes layered unstable. Deep convective clouds usually develop in the afternoon, too. Therefore there is a clear diurnal cycle of cloud cover the EU area in summer. There is no bias between ISCCP and CM SAF annual average cloud cover in this area.

A.4.2 Subtropical South-Atlantic ocean (SA) area

The SA area is characterized by a strong diurnal cycle of cloud cover in the winter and summer season (Fig. A.2 and A.3), consistently seen in both satellite products. The SA area offers the most distinctive cloud diurnal cycles in the analyzed domain. The long-term top of atmosphere radiative effect of these low-level clouds is about $-50\,\mathrm{W/m^2}$ (Raschke et al., 2005), indicating a strong cooling. The persistent stratus and stratocumulus clouds in this area feature a minimum of cloud cover in the evening and a maximum in the morning. This diurnal variability is caused by a daytime breakup of the consistent stratus cloud cover located at the top of a strong low-level inversion. The cloud breakup is a consequence of a decreasing inversion strength due to solar insolation and thus easier entrainment of dry air from above into the moist, cloudy layer (Wai, 1991; Rozendaal et al., 1995). During night, cloud cover rebuilds again. This diurnal cycle exists throughout the year, but it is most striking during the southern hemisphere summer (DJF) when insolation is strongest (Fig. A.2 and A.3). There is a bias in the SA area between ISCCP and CM SAF annual averaged cloud cover of 4%, with higher values in the CM SAF data.

The focus in the following model evaluation is on the EU and SA area (see Fig. A.1), where both satellite datasets offer large cloud cover diurnal cycles, which are in agreement with the meteorological expectations.

A.5 Evaluation of CCLM simulations

Two CCLM simulations for the time period of 1990 to 2007 are evaluated in this section. ISCCP serves as data reference due to its long time series. As mentioned, the chosen regions of interest are the EU and SA areas (Fig. A.1). There is a distinct diurnal cycle of cloud cover observed in both regions, especially in the summer season. The meteorological mechanisms responsible are different in the two areas, dominated by a primarily convective regime in EU and a stratiform regime in SA, as described in section A.4. The evaluation is done by the comparison of absolute and relative diurnal cycles of cloud cover together with some quantitive measures.

A.5.1 European (EU) area

It has already been shown that the diurnal cycle of cloud cover on the Eurasian continent in summer (JJA) is characterized by maxima at noon and in the afternoon and minima during nighttime (Fig. A.3). This cloud diurnal cycle is primarily controlled by convective activity. CCLM completely failed to simulate the observed diurnal cycle of cloud cover in the EU area in the summer season (Fig A.5). In contrast ERA-Interim, the driving dataset, was able to simulate a diurnal cycle with an afternoon maximum (not shown).

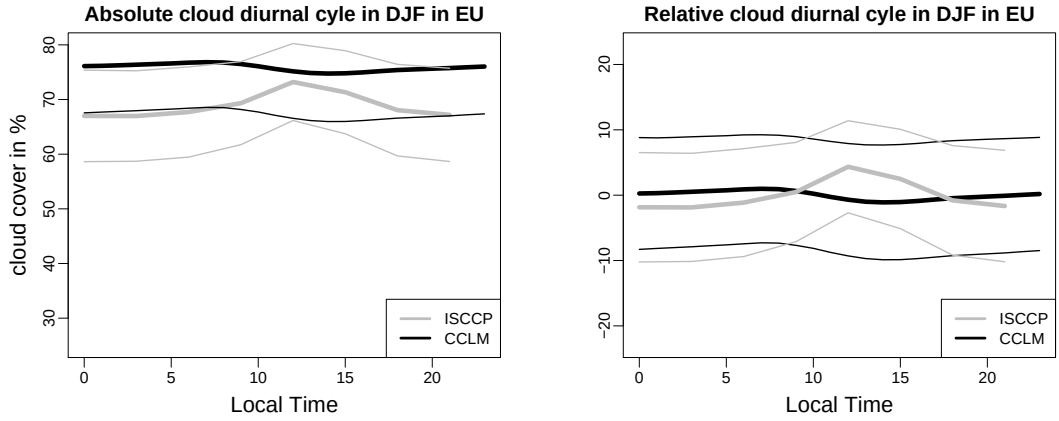

Figure A.4: Mean diurnal cycles of absolute (left) and relative (right) cloud cover in winter (DJF) in the EU region of ISCCP and CCLM including plus/minus its standard deviations (thin lines)

The evaluation of absolute cloud amounts shows that the CCLM simulated too much cloud cover (+10% compared to ISCCP, see Tab. A.1), especially during nighttime (Fig. A.5 right), which is in agreement with findings by Jaeger et al. (2008). Table A.1 summarizes the model evaluation and shows that the CCLM overestimated cloud cover and underestimated its mean diurnal cycle, especially in JJA. Diurnal cycles of cloud cover are absent in the winter season (Fig. A.4 and Tab. A.1) in observational and model data. Overall the results show that model deficiencies in simulating reasonable cloud diurnal cycles are likely associated with issues related to the parameterization of the diurnal cycle of convective activity and the simulation of surface-atmosphere interactions.

A.5.2 Subtropical South-Atlantic Ocean (SA) area

The diurnal cycle of cloud cover in the SA area is characterized by the afternoon breakup of low-level clouds owing to solar insolation and the nighttime rebuilding

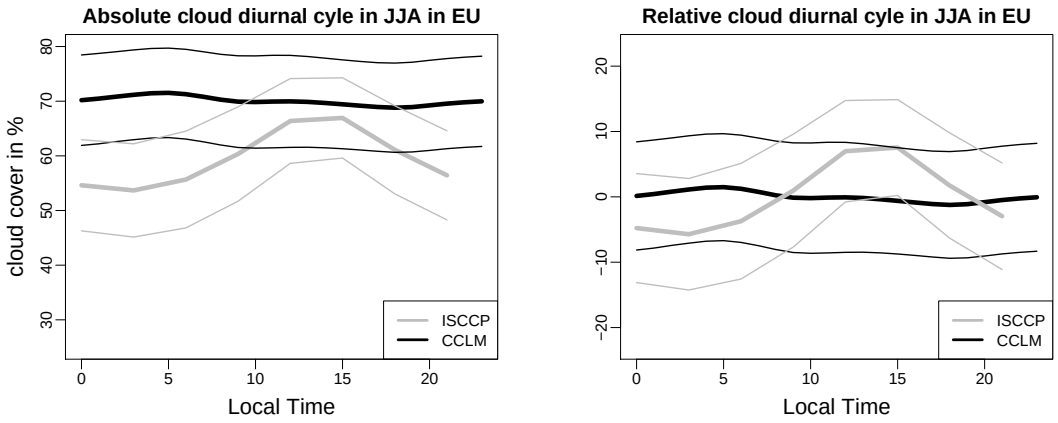

Figure A.5: Mean diurnal cycles of absolute (left) and relative (right) cloud cover in summer (JJA) in the EU region of ISCCP and CCLM including plus/minus its standard deviations (thin lines)

	mean [%]		amp [%]		LT of min. clouds		LT of max. clouds	
season	DJF	JJA	DJF	JJA	DJF	JJA	DJF	JJA
CCLM	76	70	2	3	14	18	7	5
ISCCP	68	60	6	13	3	3	12	15
diff	+8	+10	-4	-10	11 h	9 h	5 h	10 h

Table A.1: Results of the evaluation of CCLM simulations in the European (EU) region for the winter (DJF) and summer (JJA) season. Measures shown: mean cloud cover (mean), diurnal amplitudes of cloud cover (amp), local times (LT) of minimum (min) and maximum (max) cloud cover and its differences (diff) in percentage points or hours (h)

of cloud cover over the cold ocean (cf. section A.4). Diurnal cycles in the SA area are most distinct in the southern hemisphere summer season (DJF) (Fig. A.2), when insolation is maximal. In contrast to the results for the EU area, the diurnal cycles of cloud cover of the satellite and simulation data agree fairly well in the SA region. There is maximum cloud cover in the early morning (ca. 6 am LT) and a minimum cloud cover in the afternoon (15 to 18 pm LT) in both seasons (see Tab. A.2, Figs. A.6 and A.7). While the simulated relative diurnal cycles of cloud cover were correct (Figs. A.6 and A.7), there was a strong negative bias in average cloud cover in the winter season (JJA), when the cloud cover simulated by the CCLM is about 20 percent lower than the cloud cover observed by the ISCCP (Fig. A.7 left and Tab. A.2). That agrees with the finding of Karlsson et al. (2008) that atmospheric models usually underestimate subtropical low level cloud cover.

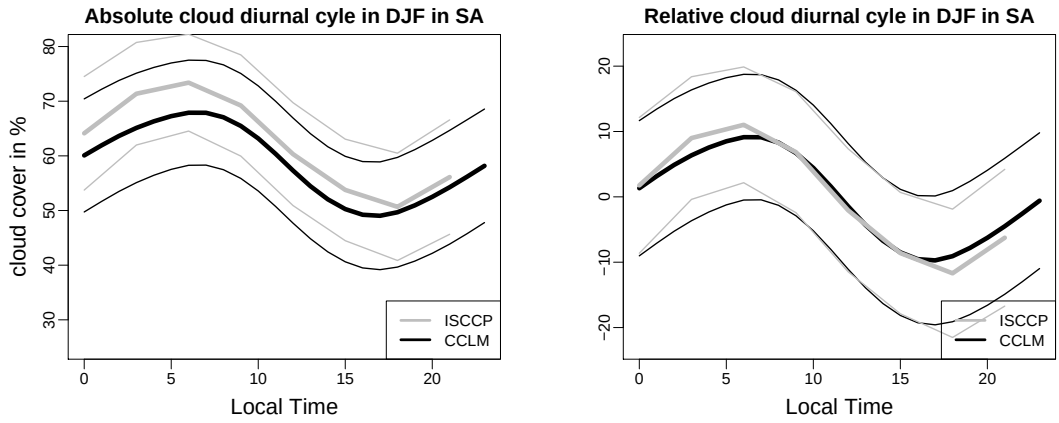

Figure A.6: Mean diurnal cycles of absolute (left) and relative (right) cloud cover in winter (DJF) in the SA region of ISCCP and CCLM including plus/minus its standard deviations (thin lines)

	mean [%]		amp [%]		LT of min. clouds		LT of max. clouds	
season	DJF	JJA	DJF	JJA	DJF	JJA	DJF	JJA
CCLM	59	41	19	7	17	16	6	7
ISCCP	62	63	23	9	18	15	6	6
diff	-3	-22	-4	-2	1 h	1 h	0 h	1 h

Table A.2: Results of the evaluation of CCLM simulations in the sub-tropical South-Atlantic Ocean (SA) area for the winter (DJF) and summer (JJA) season. Measures shown: mean cloud cover (mean), diurnal amplitudes of cloud cover (amp), local times (LT) of minimum (min) and maximum (max) cloud cover and its differences (diff) in percentage points or hours (h)

A.6 Discussion and Summary

On the one hand there is need for reliable cloud data, e.g. to evaluate models, and on the other hand satisfactory cloud detection is challenging. Satellite data provides suitable spatio-temporal data coverage but cloud detection by satellites may be hindered by inhomogeneous surface properties and inappropriate cloud detection sensitivities, which may additionally depend on the time of day. Hence, we first analyzed satellite based cloud products for data reliability before using them for the evaluation of CCLM simulations.

The comparison of the satellite based cloud cover products of ISCCP and EUMETSAT's CM SAF showed that relative cloud diurnal cycles largely agree and meet meteorological expectations (Figs. A.2 and A.3). Nevertheless there are bi-

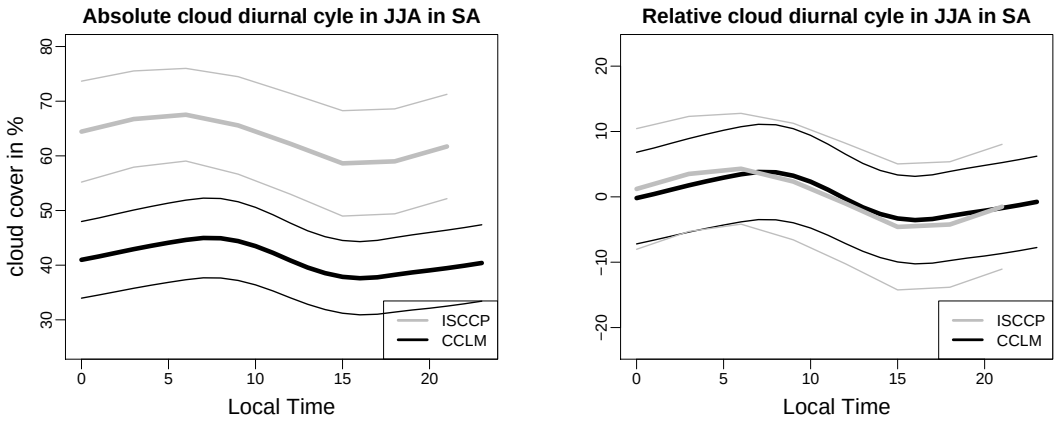

Figure A.7: Mean diurnal cycles of absolute (left) and relative (right) cloud cover in summer (JJA) in the SA region of ISCCP and CCLM including plus/minus its standard deviations (thin lines)

ases between the datasets as cloud detection algorithms are sensitive to individual brightness temperature thresholds used for cloud detection (sections D.2 and A.4). Actually these thresholds predefine clouds from the satellite point of view. Regions of extreme climate conditions, like deserts or high mountain areas, are regions of reduced data quality in satellite products (Stubenrauch et al., 1999). This is especially true for the ISCCP data which is based on two spectral channels only. Hence the possibility for the individual adaption of the algorithm to local conditions is limited. This became obvious in the Sahara and Sahel region where the satellite products offer large discrepancies (Fig. A.4). In contrast, the satellite based cloud cover products agree reasonably well in most other regions, including the EU and SA areas. These regions of interest offer distinct diurnal cycles which meet meteorological expectations. Therefore these regions were chosen for evaluating the CCLM simulations.

In the EU area during summer, cloud cover diurnal cycles are induced mainly by convection. Modeling convection is challenging as it occurs on spatial scales not resolved by climate models. As the CCLM simulations applied a grid spacing of 0.44°, convection had to be parameterized, which induced uncertainty. Moreover convection depends on additional processes which are also not fully resolved. For instance the small scale vertical profiles of temperature and humidity are crucial for the initiation of convection, as is the inhomogeneity of land surface properties which are not very well resolved in the models. Especially the interaction between the surface and the atmosphere which influences the stability of the lower atmosphere should be analyzed in terms of its diurnal variability. The failure of the model to simulate the cloud diurnal cycle over land is crucial as cloud cover acts

as an important input parameter to the calculation of radiative processes inside the model (Kothe et al., 2010). Hence error propagation will occur through the various feedback processes involved. One possible consequence might be an underestimation of the diurnal surface temperature amplitude in Europe in summer. Actually this underestimation has been seen by comparisons with station based data and might likely be associated to model issues concerning cloud cover and its diurnal cycle.

The diurnal cloud formation and break-up process in the SA area is reasonably well simulated by CCLM (Figs. A.5 and A.6). Nevertheless there is a strong underestimation of mean cloud cover during the southern hemisphere winter, which has an impact on the radiation budget. It should be mentioned that biases in cloud cover might also be introduced by unavoidable inconsistencies owing to different definitions of cloud cover in satellite data and model output. The presented evaluation results for the EU and SA areas are different, which is likely to be caused by the different processes responsible for cloud formation in the two areas. While the SA area is dominated by low-level stratus and stratocumulus clouds over an homogeneous surface background, the amount of mid-level and high-level clouds is increased in the afternoon owing to convection over the European continent in summer.

A correct simulation of the diurnal cycle of clouds in a climate model is important for overall model performance. For example, Hohenegger et al. (2008) found that problems of CCLM simulations in Europe are probably due to deficiencies in the parameterizations of convection and sub-grid clouds. Increasing the resolution of model simulations towards cloud resolving scales reduces the dependency on parameterizations of physical processes. This might improve the performance of CCLM simulations (Hohenegger et al., 2008, 2009), but also computational costs increase with increased model resolution. Finally it has to be pointed out that the analyzed CCLM simulations depend on the driving dataset, which is ERA-Interim in this case. Sea surface information in CCLM is prescribed by the driving dataset while land surface parameters and fluxes are calculated within CCLM itself. Hence a review of the land-atmosphere interaction, which is also relevant for the initiation of convection, might be another key to model improvements (see e.g. Asharaf et al., 2012).

Acknowledgement

ISCCP data was obtained from the International Satellite Cloud Climatology Project data archives at NOAA/NESDIS/NCDC Satellite Services Group. Thank for data provision and support goes to the EUMETSAT Satellite Application Facility on Climate Monitoring (CM SAF) group at the Deutscher Wetterdienst, Offenbach, Germany. Further we thank the CLM-Community (www.clm-community.eu),

especially Steffen Kothe and Andreas Dobler for providing CCLM and general support. Bodo Ahrens acknowledges funding from the Hessian initiative for the development of scientific and economic excellence (LOEWE) at the Biodiversity and Climate Research Centre (BiK-F), Frankfurt/Main.

Appendix B

Using Synop observations for the evaluation of cloud diurnal cycles in Europe

B.1 Motivation

Clouds are of major relevance for the Earth's climate due to its direct influence on various radiation fluxes. In Pfeifroth et al. (2012) (see Appendix A) it is shown that satellite based cloud observation can be used for model evaluations, as their quality is sufficiently high. On the other hand cloud observation are have been done since several decades by human eye observations, so-called Synop observations. Both satellite and Synop observations may become more uncertain under certain circumstances, e.g during nighttime or in case of very thin or very low clouds. To enable the prolongation of human-eye observations of cloud cover with help of satellite based observations, both need to be inter-compared. Validations of satellite-based diurnal cycles of cloud cover with Synop observation are rare. It is further important to compare the diurnal cycle of cloud cover of satellite and Synop observation, as the former is often used to do model evaluations or climate studies in remote areas, where no other cloud informations are available. In this study cloud cover diurnal cycles of Synop observations are compared to satellite data by the ISCCP. Individual Synop stations have been gridded to a global and a European domain.

Data and Methods

The satellite data used here is data from the International Cloud Climatology Project (ISCCP-D2) (Rossow and Schiffer, 1999). The data is identical to the one

used in Pfeifroth et al. (2012) (see also section 3.2.1 in this thesis for more details). Only data over is used for the comparison.

The Synop based data which is used as a reference, has been gridded to allow for better comparison to the satellite data that is also natively available on grids. To generate the gridded Synop dataset all available Synop cloud cover observations have been used during the time period of 1980 to 2011. The Synop cloud observations are done at the 3-hourly UTC times (0,3,etc.) in octas, with '9'-values (cloud estimation not possible) disregarded. All stations have been interpolated by using inverse-distance weighted interpolation onto a global 2.5°2.5° grid and to a 0.25° × 0.25° grid for central Europe (-10 to +30 W and +40 to + 60 N), as for Central Europe the much higher observational density allows for a higher resolution grid. An alternative Synop-based dataset of cloud cover is made available by Eastman and Warren (2013), but at the time of analysis this data was not yet available. Moreover the generation of an own dataset allowed to have full data control and to generate the data in individual resolutions. The mean summertime Synop cloud cover in octa is shown in Figure B.1 globally and in Figure B.2 for Europe. The Synop data has been converted from UTC to LT as described in Pfeifroth et al. (2012) (see Appendix A). The same is done with the ISCCP data. The summer and winter season (JJA and DJF respectively) are analyzed separately.

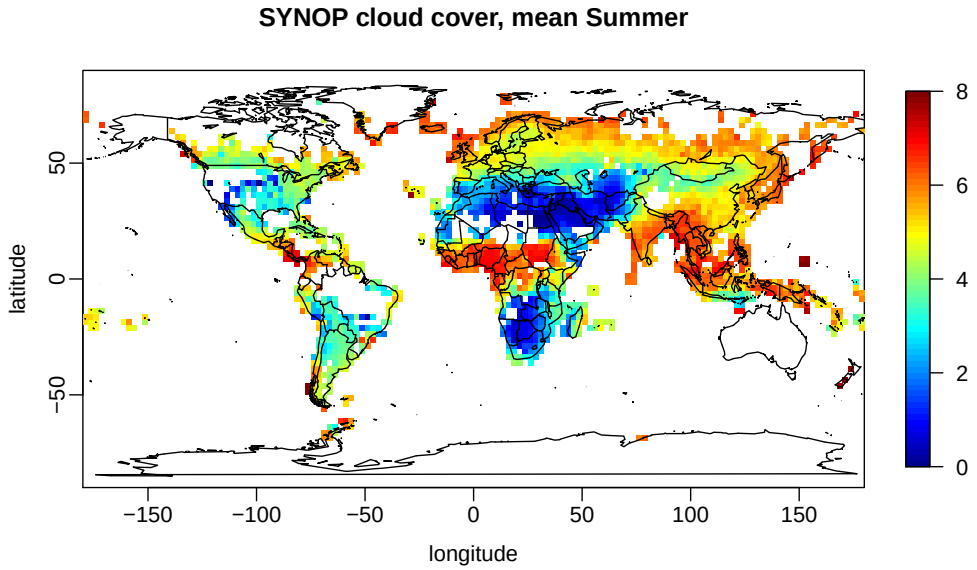

Figure B.1: Mean cloud cover [octa] of gridded Synop observation during 1980 to 2011

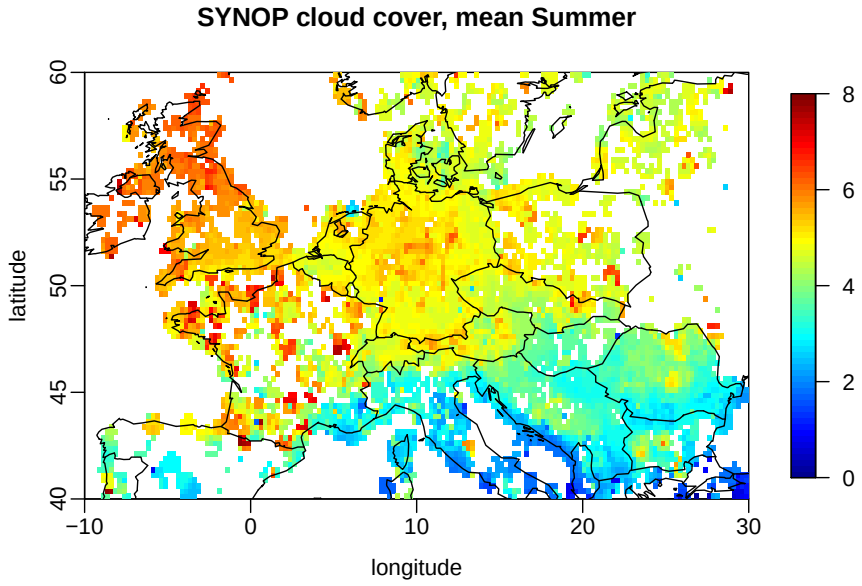

Figure B.2: Mean cloud cover [octa] of gridded SYNOP observation during 1980 to 2011

Results

For the evaluation with the ISCCP-D2 data is conducted for the European domain as defined in Pfeifroth et al. (2012). Figure B.3 shows the validation of the mean cloud diurnal cycles for the winter and summer season. Both the ISCCP and Synop data capture a small diurnal cycle in the winter season (see Figure B.3,left). As solar insolation is quite in Europe in winter, one might even expect no diurnal cycle at all. This might also hold before the background of large scale low-pressure systems often controlling the weather in European winter. Both the satellite and the Synop data observe a maximum of cloud cover during daytime, but the relative diurnal cycles are with 4 to 6 % quite small.

In summer, the observed diurnal cycles of cloud cover are in the order of 10 to 15 % and hence much larger than in winter (see Figure B.3, right), while the mean cloud cover is smaller in summer. Owing to the larger solar insolation, tropospheric convection occurs more frequently in case of favorable atmospheric conditions. The Synop and ISCCP satellite data agree quite well for the timing of the maximum cloud cover that is observed at about 15 local time. The ISCCP diurnal cycle is slightly stronger than the one based on Synop observations. Overall there is positive bias of ISCCP cloud cover in summer with reference to Synop.

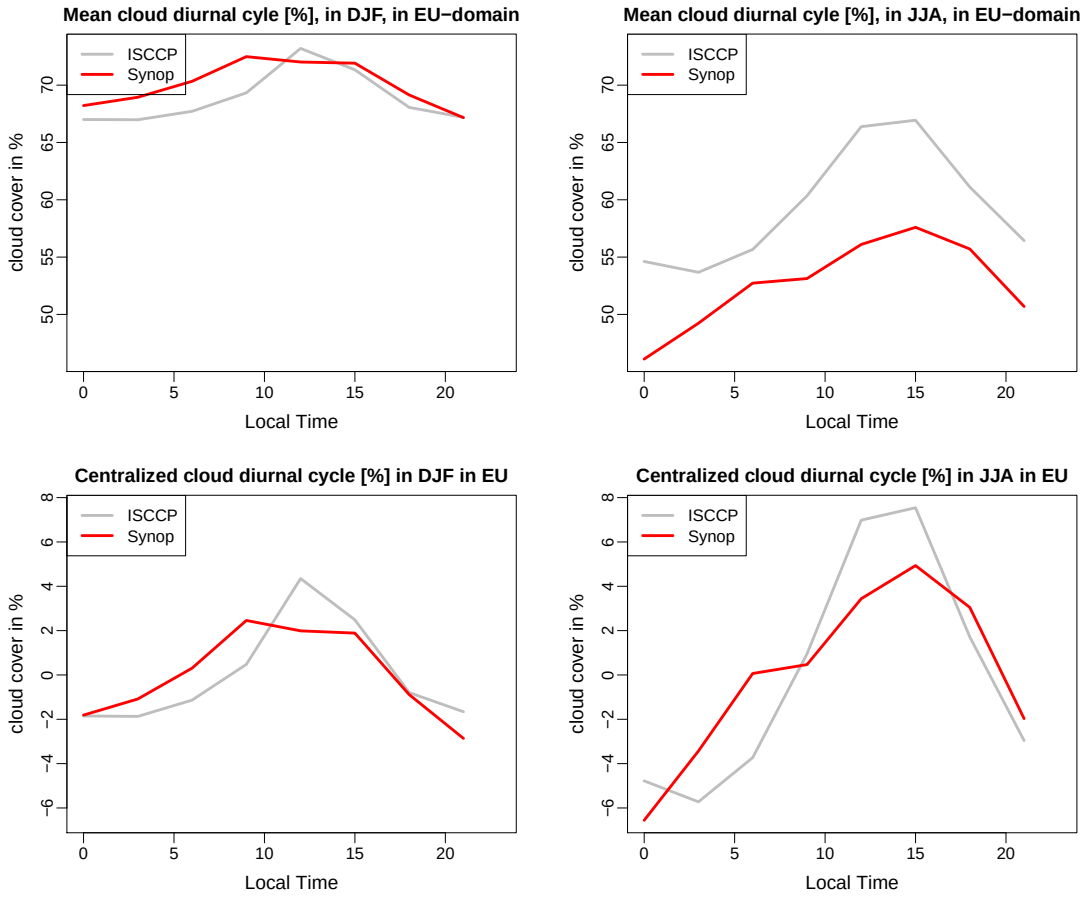

Figure B.3: Absolute (top) and centralized (bottom) mean cloud cover diurnal cycles of ISCCP-D2 (red) and Synop (grey) data in Central Europe in the winter (left) and summer season (right)

Further both data sets slightly disagree in the timing of the minimum cloud cover in nighttime in summer by about 3 hours. This is likely a result of the reduced ability of both the human observer and the satellite sensor to estimate the cloud cover.

Conclusions

It has been shown that the satellite-based observation of cloud cover are in good agreement with the Synop observations in Central Europe. The satellite data by ISCCP slightly overestimates the diurnal cycle of cloud cover and has a positive bias in summer compared to the Synop observations. The latter is relevant when

trying to merge satellite and Synop cloud cover data. During nighttime larger discrepancies have to be expected owing to the absence of sunlight which is used by both the human observer and some satellite sensors. These results confirm the quality of satellite-based cloud cover observations and the possible usage of satellite data to evaluate cloud diurnal cycles as simulated by models. However, as biases are omnipresent when analyzing cloud cover, the analysis focus should primarily be on the variability of cloud cover.

Appendix C

Paper 2: Evaluation of Satellite-based and Reanalysis Precipitation Data in the Tropical Pacific

published as:

Pfeifroth, U., Mueller, R. and Ahrens B. (2013): Evaluation of Satellite-based and Reanalysis Precipitation Data in the Tropical Pacific. *Journal of Applied Meteorology and Climatology*, 52(3):634-644.

Abstract

Global precipitation monitoring is essential for understanding the earth's water and energy cycle. Therefore, usage of satellite-based precipitation data is necessary where in situ data are rare. In addition, atmospheric-model-based reanalysis data feature global data coverage and offer a full catalog of atmospheric variables including precipitation. In this study, two model-based reanalysis products obtained by the interim reanalysis by the European Centre for Medium-Range Weather Forecasts (ERA-Interim) and NASA's Modern Era Retrospective Analysis for Research and Applications (MERRA) as well as two satellite-based datasets obtained by the Global Precipitation Climatology Centre (GPCP) and Hamburg Ocean Atmosphere Parameters and Fluxes from Satellite Data (HOAPS) are evaluated. The evaluation is based on monthly precipitation in the tropical Pacific during the time period of 1989 to 2005. Rain-gauge atoll station data provided by the Pacific Rainfall Database (PACRAIN) are used as ground-based reference. It is

shown that the analyzed precipitation datasets offer temporal correlations ranging from 0.7 to 0.8 for absolute amounts and from 0.6 to 0.75 for monthly anomalies. Average monthly deviations are in the range of 20%–30%. GPCP offers the highest correlation and lowest monthly deviations with reference to PACRAIN station data. The HOAPS precipitation data perform in the range of the reanalysis precipitation datasets. In high native spatial resolution, HOAPS reveals deficiencies owing to its relatively sparse temporal coverage. This result emphasizes that temporal coverage is critical for controlling the performance of precipitation monitoring. Both reanalysis products show similar systematic behaviors in overestimating small and medium precipitation amounts and underestimating high amounts.

C.1 Introduction

Tropical precipitation plays an important role in the global freshwater balance and is sensitive to large-scale disturbances in the atmosphere and the oceans. In addition, accurate observation of tropical precipitation is crucial for monitoring anomalies such as El Niño–Southern Oscillation (ENSO), which has global impacts (New et al., 2001).

Monsoon systems are another important climatic feature that can be monitored with global precipitation datasets. Such systems transport moisture and precipitation from the oceans toward the continents (Dobler and Ahrens, 2010). Because of the lack of ground-based observations over the ocean and other isolated parts of the world, satellite-based and reanalysis datasets are an important data source. The high spatiotemporal variability of tropical precipitation complicates the evaluation of precipitation products in the analyzed region.

The usage and diversity of satellite-based precipitation datasets has grown in recent years (Kidd and Levizzani, 2011; Kidd and Huffman, 2011). The availability of long time series of data together with good data homogeneity is essential for the analysis of climate and its variability. The lifetimes of satellites are limited, which make changes in the observing system within a data time series unavoidable. Moreover, the number of satellite sensors used to generate time series of data is not fixed, influencing temporal coverage. Since satellite data are also widely assimilated into atmospheric reanalysis, it is not safe to assume that both satellite-based and reanalysis will be homogeneous a priori. Precipitation data from satellites face problems owing to limited temporal sampling, especially when low-Earth-orbiting satellite platforms are used, as sites close to the equator are scanned only once or twice per day. Precipitation datasets are usually based on measurements by passive microwave sensors, since they are able to detect precipitation-sized particles in a relatively direct manner. Emission by liquid drops and scattering on ice particles are signals in the microwave spectrum that were proved to be convert-

ible into precipitation amounts (Wilheit et al., 1977; Ferraro et al., 1996; Ferraro, 1997). One prominent, widely used series of microwave sensors are the Special Sensor Microwave Imager (SSM/I) instruments flying on board the Defense Meteorological Satellite Program satellite series (`http://www.ngdc.noaa.gov/dmsp/`). The precipitation datasets evaluated in this study make use of SSM/I data, either directly or through data assimilation, as in the case of reanalysis products.

Independent reference data used to evaluate satellite estimates and numerical models are rare, especially over the ocean, where the major portion of global rainfall takes place. Whereas ship measurements may provide data only along the ship route, buoy rain-gauge measurements deliver time series from fixed positions over the ocean. Tropical buoy rain-gauge data have been used to validate satellite-derived precipitation datasets over tropical and subtropical oceans (Bowman et al., 2003; Bowman, 2005). Bowman et al. (2009) compared long-term averages of buoy and satellite data during the time period 1997–2006 and found biases of up to 25%. An evaluation of the Hamburg Ocean Atmosphere Parameter and Fluxes from Satellite Data (HOAPS) shows that its mean precipitation amounts in the western tropical Pacific Ocean are lower than those in the current interim reanalysis of the European Centre for Medium-Range Weather Forecasts (ERA-Interim) and higher than those in the Global Precipitation Climatology Project (GPCP) dataset (Andersson et al., 2011). A comparison of HOAPS precipitation data with instantaneous ship measurements has proven that the HOAPS algorithm can detect small-scale convective rainfall reasonably well (Klepp et al., 2003). The ability of HOAPS to monitor monthly precipitation will be analyzed in this study.

Another oceanic precipitation study focuses on intercomparisons between satellite-based and reanalysis-based precipitation datasets. This results in relatively good agreement over the ocean concerning variability patterns but substantial disagreement in intensities (Shin et al., 2011). Tian and Peters-Lidard (2010) analyzed various multisatellite-based precipitation datasets in a 2-yr period and showed that relative uncertainties can be considered small over tropical oceans. A study of seasonal and interannual variations found that the western South Pacific is a region that exhibits large differences among all analyzed data, including data from the GPCP and HOAPS. Precipitation products using a composite of various data sources perform best (Béranger et al., 2006). Adler et al. (2012) estimated the climatological bias of the GPCP to be from $-10\,\%$ to $-15\,\%$ in the tropical western Pacific. Data from the GPCP have been validated with the Comprehensive Pacific Rainfall Database (PACRAIN) atoll station data, which are also used as reference data in this study. The result of this validation was a negative bias of $-16\,\%$ during a time period from 1979 to 2001 (Adler et al., 2003). One year of PACRAIN atoll station data have also been used within the Third Precipitation Intercomparison Project. Results revealed that the temporal coverage of polar-orbiting satellites

seems to be a limiting factor for the correlation and that atmospheric models are less accurate than satellite products (Adler et al., 2001).

In precipitation validation studies, the PACRAIN database has received relatively less attention because the influence of the atoll land mass on oceanic precipitation was seen with skepticism. A recent study on rain on small tropical islands indicates that the influence of atoll-sized islands on precipitation is negligibly small (Sobel et al., 2011), motivating our use of PACRAIN as a reliable reference.

The objective of the present study is to evaluate the ability of satellite-based and reanalysis precipitation datasets to observe regional variability and anomalies on a monthly time scale. The evaluation takes place in a climatic zone that is characterized by heavy convection-induced precipitation events, contributing disproportionately to global precipitation amounts. Hence, tropical precipitation plays an important role in the global freshwater balance. Further, precipitation in the tropical Pacific is sensitive to atmospheric and oceanic disturbances (e.g., from ENSO), which have large-scale impacts on precipitation amounts and distribution patterns. The high temporal and spatial variability of tropical precipitation poses a major challenge for precipitation datasets.

In this study, satellite-based precipitation data from the GPCP and HOAPS and reanalysis-derived precipitation data from ERA-Interim and from the National Aeronautics and Space Administration (NASA) Modern-Era Retrospective Analysis for Research and Applications (MERRA) are evaluated. As reference data, in situ rain gauge measurements on atoll stations extracted from the PACRAIN database (Greene et al., 2008) are used. The validation covers a variety of data sources ranging from those adopting the single-sensor approach (HOAPS) to those based on the multisatellite-multisensor approach (GPCP) to reanalysis products. The latter assimilates various satellite data and generates precipitation data that are based on numerical model parameterizations. The time period of validation is between 1989 and 2005, according to the overlapping period of the analyzed data.

C.2 Data

C.2.1 GPCP V2.2

The GPCP is part of the World Climate Research Programme and of the Global Energy and Water Cycle Experiment (GEWEX). It provides global estimates of monthly precipitation using a multisatellite approach; that is, it combines the data from various satellites into a final merged precipitation product. The GPCP data used in this study are from version 2.2 of the monthly precipitation analysis, with a spatial resolution of 2.5° (latitude) × 2.5° (longitude). Over-ocean GPCP data incorporate precipitation estimates based on different geostationary infrared (IR)

sensors operated by the United States, Europe, and Japan; however, for filling gaps, passive Earth-orbiting microwave sensors (e.g., SSM/I) and sounders (e.g., Television and Infrared Observation Satellite (TIROS) Operational Vertical Sounder (TOVS)) are also used. The temporal coverage of GPCP data is improved by integrating multiple satellite data sources rather than single-sensor-based datasets. A detailed description of the data basis included in the GPCP dataset and a description of the merging and combining methods used can be found in Adler et al. (2003), Huffman et al. (2009) and in the dataset documentation available online (`ftp://precip.gsfc.nasa.gov/pub/gpcp-v2.2/doc/V2.2_doc.pdf`).

C.2.2 HOAPS

HOAPS delivers precipitation and evaporation data over global, ice-free oceans (Andersson et al., 2011). The approach of HOAPS differs from that of the GPCP, because solely intercalibrated SSM/I data are used as a basis for deriving the HOAPS parameters. The algorithm used to estimate precipitation is based on a neural network, which was trained with SSM/I brightness temperatures and dedicated European Centre for Medium-Range Weather Forecasts (ECMWF) precipitation data (Andersson et al., 2010). The data used in this study are the HOAPS-G Version 3 precipitation data, which are delivered on a monthly time scale with a spatial resolution of 0.5° (latitude) × 0.5° (longitude) (obtained online from `www.hoaps.org`).

C.2.3 ERA-Interim reanalysis by ECMWF

The ERA-Interim reanalysis is the latest global atmospheric reanalysis operated by ECMWF (obtained at `http://www.ecmwf.int`). ERA-Interim makes use of an extensive data assimilation effort. It uses a wide variety of available observations, including satellite data, to obtain a global state of the atmosphere (Dee et al., 2011). The analyzed monthly precipitation is calculated based on 12–24-h forecasts within the ERA-Interim model system. Assimilated satellite data, including SSM/I, act as an important input for water vapor profiles and, thus, implicitly influence precipitation forecasts. The native grid resolution of ERA-Interim is T255, which corresponds to about 0.75° in longitude and latitude.

C.2.4 MERRA

MERRA is a recently launched NASA reanalysis of the atmosphere for the era of satellite observations (Rienecker et al., 2011). A state-of-the-art data assimilation system was developed and applied by the Global Modeling and Assimilation Office to synthesize various observations. MERRA covers the time period

from 1979 onward and has a special focus on the analysis of the hydrological cycle. MERRA is based on the Goddard Earth Observing System (GEOS-5) general circulation model and offers a native spatial resolution of 1/2° (latitude) × 2/3° (longitude). The data assimilation system also integrates rain-rate estimates from passive microwave measurements. The MERRA variable used is the diagnostics of total precipitation, time averaged at surface level. The MERRA monthly mean total precipitation was downloaded via the MDISC Data Subsetter (`http://disc.gsfc.nasa.gov`). The product used is the monthly incremental analysis update (IAU) 2d land surface diagnostics.

C.2.5 PACRAIN

PACRAIN was developed under a research grant from the National Oceanic and Atmospheric Administration. It collects ground-based rainfall data in a data-poor region of the world—the tropical Pacific (see `http://pacrain.evac.ou.edu/` for database information and data access). The input data to PACRAIN consist of daily and monthly rain-gauge data from inland, coastal, island, and atoll stations, and the database is updated monthly. The data undergo a rigorous quality control process. Detailed information about the PACRAIN database is given in Greene et al. (2008). We used a subsample of the atoll stations in this study (cf. Fig. C.1). The PACRAIN atoll station data used are not included in any of the evaluated satellite or reanalysis datasets, which makes it an independent validation dataset. Atoll stations are fairly representative of open-ocean conditions owing to their small size and flat orography (Sobel et al., 2011). The atolls used are of a size assumed not to significantly influence relevant satellite precipitation algorithms.

C.3 Methods

Daily PACRAIN atoll station data have been used to calculate mean precipitation for each month, if at least 25 days per month were available. Finally, 34 atoll stations offering data times series as complete as possible have been chosen manually (see Fig. C.1). The evaluation in this study takes place on a monthly time scale. PACRAIN monthly means are compared with the monthly means of the satellite and reanalysis datasets as given by the data provider. Because the time series of PACRAIN stations vary in terms of their completeness, this ensures common evaluation time periods. It should be noted that the more inhomogeneous a variable is in space and time, the larger the deviations between the gridded data and the point data will be (Ahrens and Beck, 2008), since gridded data represent grid-box area-averaged data and the real small-scale spatial distribution is unknown. To counteract this issue of data comparability, all data are analyzed

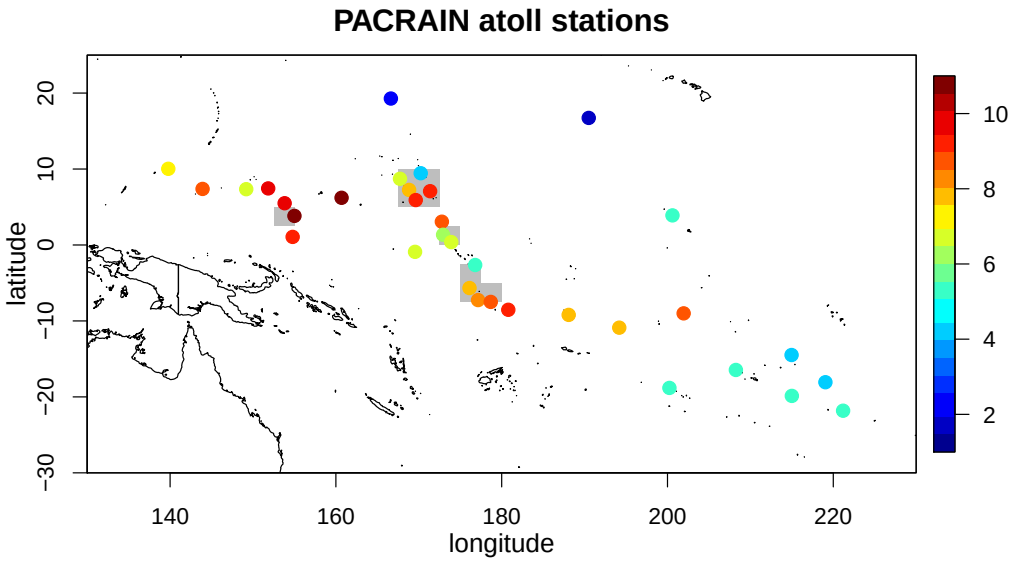

Figure C.1: PACRAIN atoll stations and their average precipitation (mm/d; color bar) during 1989–2005, and grid boxes (gray) showing the gridded PACRAIN data.

in terms of monthly precipitation averages. For monthly PACRAIN atoll station data, Morrissey (1991) found correlation lengths of hundreds of kilometers. Additionally, spatial averaging is applied by gridding PACRAIN atoll stations, where the station density is sufficient.

The evaluation is applied in four steps. First, satellite and reanalysis data are compared to the respective PACRAIN atoll stations located inside the grid box. Thereby satellite and reanalysis datasets are kept in their native spatial resolutions (cf. Table C.1). This evaluation gives information about the ability of the dataset to reproduce monthly precipitation amounts on local scales. Overall, 4682 months distributed over 34 PACRAIN stations and spanning the time period from 1989 to 2005 were used for this part of the precipitation evaluation. The average monthly precipitation of the PACRAIN stations used is 6.6 mm/d. In the second step, HOAPS, ERA-Interim, and MERRA data are interpolated to onto a common regular 2.5° latitude–longitude grid with first-order conservative remapping (Jones, 1999) applied with the help of a Climate Data Operator (`https://code.zmaw.de/projects/cdo`) to analyze the effects of the different spatial resolutions of the dataset.

data	GPCP	HOAPS	ERA-Interim	MERRA
spat. resolution	2.5° lon/lat	0.5° lon/lat	∼ 0.75° lon/lat	(2/3)° lon x (1/2)° lat

Table C.1: Native spatial resolutions of analyzed datasets

In the third step, spatial interpolation of atoll stations to grid boxes of 2.5° latitude–longitude resolution is applied to account for the quite inhomogeneous spatial distribution of precipitation in the tropics. Therefore, an inverse-distance-weighted interpolation is used when at least two stations are available close (1.5°) to the grid-box center. Nine grid boxes fulfilled this condition and were used to perform an evaluation on individual common 2.5° latitude–longitude grid boxes (cf. Fig. C.1). Overall, 1154 observations are used in the last part of the evaluation. Hence, there is a reduced data basis for this validation step.

Finally, to analyze the evaluation of the data, various statistical measures and scatterplots are used. Thereby, focus is placed on Pearson's correlation coefficient, referred to as correlation hereafter, and on the median of absolute deviations (MAD) between datasets and the PACRAIN reference. The measure of absolute deviations is highly relevant, especially when evaluating climate data and its anomalies. Data offering strong variability, such as precipitation, cannot be evaluated by using the bias alone, which might deliver misleading results as errors can cancel out. Hence, whenever the bias is used, scientists should at least deliver another measure—the average absolute deviation—as an add-on. The interpretation of the MAD for the user is simple since deviations are treated linearly. Confidence intervals are added to the measures of correlation of absolute values and anomalies. These intervals help us to interpret the results as they support statements of correlations being significantly different or not. Additionally, to measure the scatter of deviations, the interquartile range of MAD is used.

To evaluate possible systematic under- or overestimations in different ranges of precipitation amounts, we used a piecewise linear regression model to visualize existing relationships. This segmented linear regression model is able to estimate slopes and multiple breakpoints (Muggeo, 2008). The applied method enables a universal regression that is not dependent on specific fitting functions (e.g. linear function). Hence, it performs well for nonlinear distributions whereby it would lead to a linear regression if the scattering would exhibit a linear pattern of behavior (see Figure C.3, top right). The applied method is therefore more sophisticated and preferable compared to simple linear regression when nonlinear behavior is or might be apparent. The regression model was set to fit the regression using up to three breakpoints between the piecewise linear regressions. Because of the large scatter of data, the regression model is fit after some smoothing of the scatterplots by using a least squares method (Cleveland, 1981).

C.4 Evaluation of precipitation data

C.4.1 Evaluation of datasets in native resolution with PACRAIN stations

As described in Section C.3, datasets are kept at their native resolutions (see Table C.1) during this part of the evaluation process. Dataset grid boxes are compared with the respective PACRAIN atoll stations located within the grid box. In general, the evaluation is performed on monthly data.

Evaluation of absolute values				
	GPCP	HOAPS	ERA-Interim	MERRA
cor [90% CI]	**0.77** [0.76;0.78]	0.70 [0.69;0.72]	0.75 [0.74;0.76]	0.73 [0.72;0.75]
MAD [IQR]	**1.75** [2.63]	1.98 [3.18]	1.89 [2.59]	1.87 [2.78]
bias [relative]	-0.79 (-12%)	-0.62 (-9%)	0.52 (8%)	**-0.04 (0%)**
Evaluation of anomalies				
cor [90% CI]	**0.71** [0.69;0.72]	0.62 [0.60;0.63]	0.64 [0.630;0.66]	0.68 [0.67;0.69]
MAD [IQR]	**1.55** [2.24]	1.87 [2.85]	1.65 [2.31]	1.63 [2.28]

Table C.2: Evaluation of GPCP, HOAPS, ERA-Interim and MERRA precipitation data at native resolution with single PACRAIN stations during 1989–2005; Measures are correlation (cor) and 90% confidence interval (CI), MAD and interquartile range (IQR) [mm/d], and median bias [mm/d]; Boldface shows the best match to the PACRAIN reference.

Results of this evaluation are shown in Fig. C.2. In general, it is evident that all analyzed precipitation datasets exhibit a large scatter with reference to the PACRAIN atoll stations. In Table C.2, additional statistical measures are shown. The mean correlation ranges between $r = 0.70$ and $r = 0.77$. MAD values range from 1.75 to about 2 mm/d,, which stand for relative MAD values of about 25%–30% (cf. Table C.2). The correlation between HOAPS and PACRAIN is lowest with $r = 0.7$, while the segmented regression line is closest to the one-to-one line over the full range of precipitation amounts (see Fig. C.2, top right). Only a small systematic underestimation of high monthly precipitation amounts can be found in HOAPS data, whereas both low and medium precipitation amounts almost match the one-to-one line. GPCP offers the highest correlation (0.77) and the smallest monthly MAD (1.75 mm/d) with respect to PACRAIN station data, whereas higher precipitation amounts are somewhat more strongly underestimated compared to HOAPS (see Fig. C.2, top left). The correlations for the reanalysis datasets of ERA-Interim and MERRA rank in between GPCP and HOAPS, but similar systematics are exhibited: small and medium precipitation amounts are overestimated, whereas high amounts are underestimated (see regression lines in

Fig. C.2, bottom left and bottom right). The large scatter of absolute monthly precipitation with reference to PACRAIN station data is reflected in the large interquartile ranges (IQRs) in the range of 2.6–3.2 mm/d. HOAPS thereby has the highest IQR and GPCP the lowest (cf. Table C.2). The satellite products of GPCP and HOAPS show negative biases of about 10%, whereas ERA-Interim has a positive bias and MERRA has almost no bias to PACRAIN.

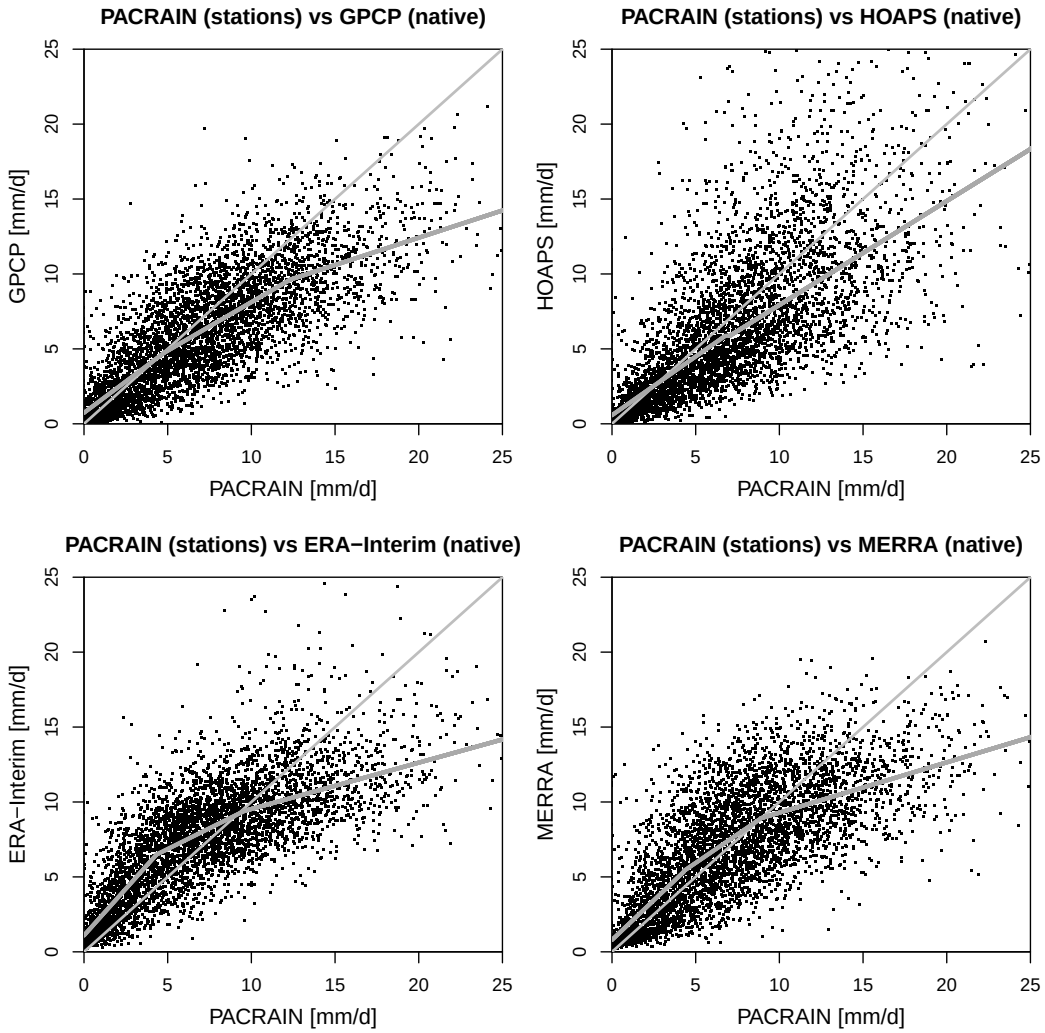

Figure C.2: Scatterplots of monthly absolute precipitation of (top left) GPCP, (top right) HOAPS, (bottom left) ERA-Interim, and (bottom right) MERRA against PACRAIN stations in 1989–2005, with segmented regression line.

Correlations of monthly precipitation anomalies are generally smaller (see Table C.2, bottom) relative to absolute values (see Table C.2, top). This is be-

cause the seasonal cycle of precipitation positively affects correlations of absolute amounts. In contrast, the seasonal cycle of precipitation is not included in time series of monthly anomalies of the corresponding long-term monthly average. Again, GPCP delivers the highest correlation (0.71) and the smallest MAD (1.55 mm/d) for precipitation anomalies (see Table C.2, bottom). As in the case of absolute values, HOAPS has the lowest correlation (0.62) and largest MAD (1.87 mm/d) for precipitation anomalies in native data resolution. Some interpretations and discussion of these results are presented in section C.5.

C.4.2 Evaluation of datasets with PACRAIN data on a common grid

After the evaluation of precipitation datasets in their native resolution in section C.4.1, datasets are now evaluated on a common 2.5° latitude–longitude grid with individual PACRAIN stations and with gridded PACRAIN data.

Evaluation of absolute values				
	GPCP	HOAPS	ERA-Interim	MERRA
cor [90% CI]	**0.77** [0.76;0.78]	0.75 [0.74;0.76]	0.74 [0.73;0.75]	0.73 [0.71;0.74]
MAD [IQR]	**1.75** [2.63]	1.81 [2.84]	1.97 [2.64]	1.88 [2.78]
bias [relative bias]	-0.79 (-12%)	-0.42 (-6%)	0.65 (10%)	**-0.01 (0%)**
Evaluation of anomalies				
cor [90% CI]	**0.71** [0.69;0.72]	0.68 [0.67;0.70]	0.66 [0.65;0.68]	0.68 [0.67;0.70]
MAD [IQR]	**1.55** [2.24]	1.62 [2.43]	1.65 [2.35]	1.63 [2.30]

Table C.3: Evaluation of GPCP, HOAPS, ERA-Interim, and MERRA precipitation data at 2.5° lat–lon resolution with single PACRAIN stations during 1989–2005. Measures are correlation (cor) and 90% confidence interval (CI), MAD and interquartile range (IQR) [mm/d], and median bias [mm/d]. Boldface shows the best match to the PACRAIN reference.

The results of the dataset evaluation of absolute values and monthly anomalies on the common grid with single PACRAIN stations are presented in Table C.3. The effects of spatial averaging on the evaluation result are varied. Whereas the reanalysis datasets of ERA-Interim and MERRA perform similarly, the correlation of HOAPS improves from 0.70 to 0.75, resulting in a correlation not significantly lower than that of GPCP (0.77) (cf. evaluation of absolute amounts in Tables C.2 and C.3). For MAD, values range between 1.8 and 2 mm/d. The improvement of the HOAPS correlation and MAD might be explained by the cancellation of small-scale deviations as a result of spatial averaging. These small-scale deviations are likely a result of the relatively low temporal coverage of HOAPS, owing to the

Evaluation of absolute values				
	GPCP	HOAPS	ERA-Interim	MERRA
cor [90% CI]	**0.81** [0.79;0.83]	0.77 [0.75;0.79]	0.76 [0.73;0.78]	0.71 [0.68;0.73]
MAD [IQR]	**1.57** [2.20]	1.80 [2.50]	1.71 [2.31]	1.88 [2.47]
bias [relative]	-0.91 (-12%)	-0.55 (-7%)	0.71 (9%)	**-0.06 (0%)**
Evaluation of anomalies				
cor [90% CI]	**0.77** [0.75;0.79]	0.72 [0.70;0.74]	0.71 [0.69;0.73]	0.70 [0.68;0.72]
MAD [IQR]	**1.36** [1.94]	1.59 [2.17]	1.50 [2.07]	1.54 [2.10]

Table C.4: Evaluation of GPCP, HOAPS, ERA-Interim, and MERRA precipitation data on 2.5° lat–lon grid with gridded PACRAIN data during 1989–2005; Measures are correlation (cor) and 90% confidence interval (CI), MAD and interquartile range (IQR) [mm/d] and median bias [mm/d]. Boldface shows the best match to the PACRAIN reference.

SSM/I–only approach. Especially in the tropics, which exhibit large spatiotemporal variability of rainfall, temporal coverage is crucial to monitoring precipitation. To evaluate this hypothesis, a separate analysis of the HOAPS time series is done in the native spatial resolution, during successive time periods in which one, two, and three SSM/I sensors are used for data generation.

The results presented in Table C.5 confirm that correlation increases when temporal coverage is increased. MAD values do decrease slightly. During the period when the temporal coverage of HOAPS is best (three SSM/I sensors used), the HOAPS correlation is similar to the correlations of the reanalysis precipitation data (cf. Tables C.2 and C.5). To eliminate the effects of analyzing HOAPS during different time periods, HOAPS monthly precipitation amounts generated by the combination of one, two, and three sensors are additionally analyzed in a common time period. The effect of temporal coverage on the evaluation results, as seen in Table C.2, is confirmed by evaluating HOAPS while piecewise increasing the number of SSM/I sensors used for data generation during the time period that goes from 2000 through 2005 (cf. Table C.6).

# SSM/I	1 (1989-01 to 1990-12)	2 (1991-01 to 1995-08)	3 (1995-09 to 2005-12)
cor [90% CI]	0.62 [0.58;0.66]	0.70 [0.68;0.72]	**0.74** [0.72;0.75]
MAD [IQR]	2.11 [3.59]	2.09 [3.26]	**1.89** [2.99]
bias	**-0.32**	-0.68	-0.59

Table C.5: Evaluation of HOAPS absolute monthly precipitation with 34 PACRAIN stations during three successive periods when HOAPS is based on one, two and three SSM/I sensors. Measures are correlation (cor) and 90% confidence interval (CI), MAD and IQR [mm/d], and median bias [mm/d]. Boldface shows the best match to the PACRAIN reference.

The biases between the precipitation products and the PACRAIN reference are almost independent of the dataset resolution. Hence, biases on the coarser grid are in the same range as those in the native resolution (cf. Tables C.2 and C.3).

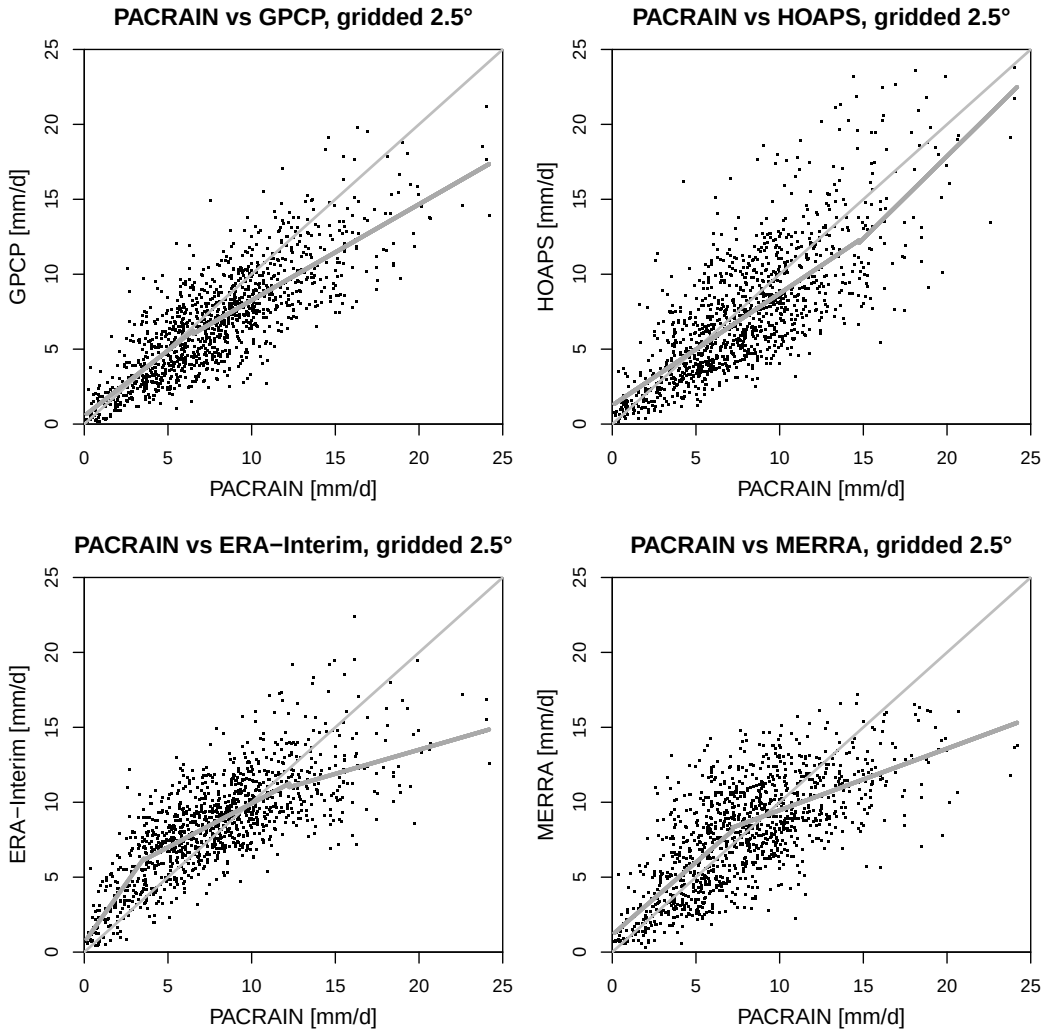

Figure C.3: Scatterplots of monthly precipitation of GPCP (top left), HOAPS (top right), ERA-Interim (lower left) and MERRA (lower right) in 1989 to 2005 against PACRAIN gridded data, on a 2.5° lon/ lat grid

The precipitation data from GPCP, HOAPS, ERA-Interim, and MERRA are also compared with gridded PACRAIN data. Datasets are compared on individual common 2.5° latitude–longitude grid boxes. Therefore, individual PACRAIN stations are spatially interpolated to grid boxes, where station density is sufficient. Hence, only a reduced PACRAIN database, as seen in Fig. C.1 (gray boxes), is used

in this part of the evaluation. The average monthly precipitation of the reduced PACRAIN data is 6.9 mm/d.

Results show that correlations of absolute precipitation amounts of GPCP, HOAPS, and ERA-Interim with the PACRAIN reference slightly increase when the data are evaluated on common grid boxes (cf Tables C.4 and C.3), relative to the evaluation with individual stations. The correlation of GPCP and PACRAIN grid boxes reaches 0.81, which is the highest correlation among all analyzed datasets. Correlations of HOAPS and ERA-Interim with PACRAIN are similar (0.77 and 0.76, respectively), while MERRA has a correlation with PACRAIN of 0.71. MAD values of the analyzed precipitation products and PACRAIN gridded data range from 1.6 to 1.9 mm/d, corresponding to relative MAD values of about 23%-28%, with GPCP having the lowest MAD of 1.57 mm/d. For the median bias, results are diverse but similar to the results obtained by using single PACRAIN stations. GPCP has a negative bias of about 12%, which is in accordance with the findings of Adler et al. (2012) in the tropical Pacific. ERA-Interim has a positive bias of about 9% and HOAPS has a negative bias of 9%, but MERRA has no bias with respect to the PACRAIN atoll station data. Hence, relative biases are not influenced by the reduction of the reference database. As in the case of the evaluation of reanalysis products in native resolution, in this evaluation too, the reanalysis datasets of ERA-Interim and MERRA both show underestimations of high precipitation amounts, which the satellite datasets obtained by HOAPS and GPCP can avoid (cf. Fig. C.3 top and bottom). Again, an overestimation of low and medium precipitation amounts using the reanalysis data, especially ERA-Interim, is found.

For the evaluation of anomalies on the common grid boxes, GPCP offers the highest anomaly correlation (0.77) to the gridded reference data, which is an important measure for climate datasets. HOAPS, ERA-Interim, and MERRA give lower correlations of anomalies within the range of 0.70–0.72 (see Table C.4). MAD values of monthly anomalies range from 1.35 to 1.6 mm/d, with IQR values of about 2 mm/d.

C.5 Discussion and Summary

Tropical precipitation is characterized by high spatiotemporal variability and originates primarily from convective events, which can be very short-lived. In addition, the tropical climate is characterized by systematic diurnal cycles of precipitation (Sato et al., 2009). The evaluation of four precipitation datasets in the period of 1989–2005 showed that GPCP performs best for correlation of absolute values and of anomalies, evaluated either with single PACRAIN stations or with gridded PACRAIN data. This can be attributed to the fact that GPCP uses the synergy effect of relatively direct derivations of precipitation by microwave sensors and the

high temporal coverage of geostationary infrared observations, calibrated with the microwave measurements. This increases the temporal sampling and seems to compensate for the disadvantage of a larger spatial resolution relative to the HOAPS dataset, emphasizing the importance of high temporal coverage in observing tropical precipitation and demonstrating the power of the chosen approach relative to the SSM/I–only approach applied to generate HOAPS. In native spatial resolution, the reanalysis datasets of ERA-Interim and MERRA outperform HOAPS precipitation data in terms of correlation, when compared with the individual PACRAIN stations.

However, GPCP exhibits the largest negative bias in the analyzed domain (–12%) of the used datasets, which is a disadvantage when studying tropical precipitation. Because of the high variability of tropical rainfall, median absolute deviations between the datasets and PACRAIN are generally quite large, with values of 20%–30%. MAD values of HOAPS, ERA-Interim, and MERRA, which offer higher spatial resolutions than GPCP, are in the same range (25%–30%). Hence, the usage of the reanalysis products to analyze precipitation in high spatial resolution would be favored in conjunction with higher correlations at small scales. Further, it reflects improvements in reanalysis datasets in recent years (e.g., more sophisticated data assimilation schemes, inclusion of data from multiple satellites, and improved parameterizations of precipitation and relevant processes). In light of additional atmospheric variables that reanalysis datasets can provide, reanalysis products can be a useful tool for studying the climate system.

The HOAPS correlation is significantly improved if the evaluation is done on the coarser 2.5° latitude–longitude grid with PACRAIN stations. The results of the evaluation on the common coarser grid revealed that the HOAPS monthly precipitation data suffer from a combination of a high spatial resolution and a relatively rare temporal sampling. This is why the reanalysis products of ERA-Interim and MERRA offer higher correlations with PACRAIN than does HOAPS at high resolution. HOAPS, ERA-Interim, and MERRA MAD values are within the same range of about 25%, while deviations in GPCP are somewhat smaller. Biases of the analyzed datasets are within the same range, with the strongest underestimations being those of GPCP data (–12%) and the strongest overestimations being those of ERA-Interim data (+9%). In addition, results show that the bias is not influenced by the spatial resolution of the datasets in the analyzed domain.

For the regression lines shown in the scatterplots, HOAPS is closest to the one-to-one line of all analyzed data at any data resolution (see Figs. C.2 and C.3), indicating that there are no systematic under- or overestimations of precipitation on a monthly time scale. In contrast, there exists a systematic pattern of behavior in both reanalysis products with reference to the PACRAIN atoll station data: high precipitation amounts are underestimated, whereas small and medium

amounts are overestimated, which is especially true for ERA-Interim. This is a disadvantage when using the data for climate studies and might be due to the difficulties numerical prediction models have in simulating precipitation. This in turn might hint at drawbacks in the parameterizations of precipitation in the models. However, it is notable that despite this disadvantage, the differences in the error measures of the satellite datasets and reanalysis products are relatively small, which is likely a result of the extensive assimilation of satellite radiances into the reanalysis.

The separate analyses of the HOAPS time series in native spatial resolution when one, two, and three SSM/I sensors are available for data generation show that temporal coverage is a crucial factor when monitoring tropical precipitation. The correlation significantly increases if temporal coverage is increased. This in turn might result in a better resolution of diurnal cycles of precipitation. In the period when three SSM/I sensors are available for data generation, the correlation of HOAPS is similar to the correlation of the reanalysis products at high resolution. In addition, we analyzed the coherence between temporal coverage and correlation during a common time period for HOAPS data. It is shown that correlation increases with increasing temporal coverage (cf. Table C.6). This relation has to be regarded as being especially true for tropical precipitation.

# SSMI	1	2	3
cor [90% CI]	0.61 [0.57;0.63]	0.68 [0.65;0.71]	**0.71** [0.69;0.74]
MAD [IQR]	2.29 [3.62]	2.33 [2.92]	**2.23** [2.70]
bias	-0.61	-0.36	**-0.33**

Table C.6: Evaluation of HOAPS absolute monthly precipitation with 34 PACRAIN stations. HOAPS data used based on one, two and three satellites during the common time period from 2000 through 2005. Measures are correlation (cor), 90% confidence interval (CI), MAD and interquartile range (IQR) [mm/d], and mean bias [mm/d]. Boldface shows the best match to the PACRAIN reference.

Even though GPCP, ERA-Interim, and MERRA also make use of the SSM/I data, which vary in temporal sampling, no major jumps in the correlation could be found by comparisons with PACRAIN. The reason for this might be that GPCP uses only one SSM/I sensor at a given time and that reanalysis precipitation is strongly dependent on model microphysics and parameterizations, in addition to the assimilation of SSM/I and other satellite data.

Because the HOAPS precipitation algorithm performs well on an instantaneous basis (Klepp et al., 2003), it could be improved when temporal coverage is increased. HOAPS is a single-source dataset, which is its strength and also its weakness. High stability and homogeneity owing to the well-calibrated SSM/I data

come along with a relatively low degree of spatiotemporal coverage. This became clear especially at high spatial resolution. Nevertheless, there is a need for such datasets (e.g., for model-independent studies or just for comparison).

The results gained from the evaluation of datasets with gridded PACRAIN data should not be regarded in direct relation to the dataset evaluation with single PACRAIN stations, because in the gridding procedure, only a reduced number of stations have been used. Nevertheless, the precipitation regime is similar. The results presented in Fig. C.3 and Table C.4 show that GPCP, HOAPS, and ERA-Interim are in better agreement with the PACRAIN grid boxes than is MERRA in terms of correlation of absolute values. Concerning the correlation of monthly anomalies, GPCP has the highest value (0.77), while the other datasets are within the same, lower range (0.70 to 0.72). Hence, it can be concluded that GPCP best represents the variability on the 2.5° latitude–longitude resolution. Deviations of monthly anomalies range from 1.35 mm/d (GPCP) to 1.60 mm/d (HOAPS), with IQR values on the order of 2 mm/d.

The relatively large deviations of 20%–30% between analyzed precipitation datasets and the PACRAIN reference are also a consequence of the climate regime in the analyzed domain, which is dominated by convective, highly variable rainfall. The uncertainties in the monthly precipitation datasets are significantly higher compared to other essential climate variables derived by satellites (e.g., cloud albedo or radiation). In recent years the spatiotemporal resolution of satellite-based precipitation datasets could be increased, for example, with help of the Tropical Rainfall Measuring Mission satellite (`http://trmm.gsfc.nasa.gov`), but time series of high-resolution precipitation datasets are still short. Despite the use of combined satellite precipitation products, the use of global precipitation datasets for regional climate monitoring and analysis is rather limited owing to the relatively large uncertainties at small scales. New satellite missions, such as the Global Precipitation Measurement Mission (`http://pmm.nasa.gov/GPM`), are planned, promising improved spatial and temporal data resolutions and a higher degree of data accuracy. The validation performed here demonstrates that there is need for improved precipitation datasets. High spatial resolution in line with increased temporal coverage is one key to attaining these improvements. This study shows that the quality of precipitation datasets can be improved by increasing their spatiotemporal resolution.

acknowledgment

The research leading to these results has received funding from the European Union, Seventh Framework Programme (FP7/2007-2013), under grant agreement 242093. The authors acknowledge dataset provisions by PACRAIN, GPCP, HOAPS,

ERA-Interim, and MERRA. We thank Michael Klatt for some extra information about PACRAIN and Karsten Fennig and Axel Andersson for useful information about HOAPS and data support. Author BA acknowledges funding from the Hessian initiative for the development of scientific and economic excellence (LOEWE) at the Biodiversity and Climate Research Centre (BiK-F), Frankfurt am Main, Germany.

Appendix D

Paper 3: Evaluating satellite-based diurnal cycles of precipitation in the African tropics

published as:

Pfeifroth, U., Trentmann, J., Fink, A. H. and Ahrens B. (2016): Evaluating satellite-based diurnal cycles of precipitation in the African tropics. *Journal of Applied Meteorology and Climatology*, 55(1):23-39.

abstract

Precipitation plays a major role in the energy and water cycles of the earth. Because of its variable nature, consistent observations of global precipitation are challenging. Satellite-based precipitation datasets present an alternative to in situ–based datasets in areas sparsely covered by ground stations. These datasets are a unique tool for model evaluations, but the value of satellite-based precipitation datasets depends on their application and scale. Numerous validation studies considered monthly or daily time scales, while less attention is given to subdaily scales. In this study subdaily satellite-based rainfall data are analyzed in West Africa, a region with strong diurnal variability. Several satellite-based precipitation datasets are validated, including Tropical Rainfall Measuring Mission (TRMM) Multisatellite Precipitation Analysis (TMPA), TRMM 3G68 products, Precipitation Estimation from Remotely Sensed Information Using Artificial Neural Networks (PERSIANN), and Climate Prediction Center (CPC) morphing technique (CMORPH) data. As a reference, highly resolved in situ data from the African Monsoon Multidisciplinary Analysis—Couplage de l'Atmosphere Tropical

et du Cycle Hydrologique (AMMA-CATCH) are used. As a result, overall the satellite products capture the diurnal cycles of precipitation and its variability as observed on the ground reasonably well. CMORPH and TMPA data shows overall good results. For locally induced convective rainfall in the evening most satellite data show slight mean delays in peak precipitation of up to 2 h.

D.1 Introduction

In meteorology and climatology the spatial and temporal variability of precipitation is of great importance. The key to further understanding precipitation variability at various spatial and temporal scales is having the best possible precipitation database available. Especially in the tropics, which globally receive maximum rainfall, precipitation plays a major role for scientific analysis, but it is also of high relevance for the economy and the society as a whole. Large tropical and subtropical regions like India, East Asia, or West Africa are affected by monsoon systems, which are responsible for rainy seasons. Even though those rainfall events may cause severe flooding, they are essential for human life. The tropical monsoon systems do not only exhibit annual and seasonal variability, but are also subject to large diurnal variations (e.g. Lau et al., 2007; Kikuchi and Wang, 2008). Heavy rainfall usually falls in convective events, which poses a challenge for observation and modeling. The diurnal cycle of precipitation systematically impacts atmospheric properties like humidity and temperatures (e.g. through evaporation) and therefore is a prominent feature of the tropical climate (Yang and Slingo, 2001).

Unfortunately, there is a lack of ground-based meteorological measurements in parts of the earth and in particular in tropical regions. The sparse distribution of rain gauge stations in the tropics and the lack of a dense measuring network are problematic because of the high spatiotemporal variability of tropical precipitation. In recent years efforts have been made to retrieve precipitation estimates through remote sensing from satellites to fill the gaps in the station network. Tapiador et al. (2012) and Kidd and Levizzani (2011) give thorough overviews on currently available satellite-based precipitation datasets. These datasets are unique in delivering precipitation with quasi-global spatiotemporal coverage, which make these datasets valuable in increasing our knowledge of precipitation distribution and variability (Kucera et al., 2013). Satellite-based high-resolution precipitation datasets are commonly used to study precipitation diurnal cycles (e.g. Sato et al., 2009; Dirmeyer et al., 2012; Birch et al., 2014; Pohl et al., 2014). Moreover these datasets are an important tool to evaluate precipitation as simulated by numerical weather prediction and climate models, which often have deficiencies in modeling precipitation (e.g. Dobler and Ahrens, 2008; Sato et al., 2009; Kothe et al., 2014). Concerning subdaily variability, models still have difficulties in simulat-

ing the proper timing and size of the precipitation diurnal cycles because of the necessity to parameterize small-scale processes (Dirmeyer et al., 2012). Recently, however, Bechtold et al. (2014) substantially improved the diurnal cycle of precipitation in the global model of the European Centre for Medium Range Weather Forecasts by improved parameterizations with reference to, among others, Tropical Rainfall Measuring Mission (TRMM) satellite data in Africa. Satellite-based precipitation datasets can help to further identify and understand model deficiencies.

Even though there has been progress in developing satellite-based precipitation datasets in recent years, it is problematic to use them unevaluated as reference for any purpose. It is challenging to correctly estimate precipitation reaching the ground by means of satellite remote sensing, as it is not a direct measurement and relies on assumptions like temperature profiles or droplet sizes. Moreover the data quality is dependent on the precipitation regime. Data uncertainties at a certain location have to be expected because of the algorithm itself but also owing to the limited spatiotemporal coverage (Negri et al., 2002a; Kidd and Levizzani, 2011; Pfeifroth et al., 2013). The latter is especially problematic for tropical regions often affected by convective rainfall events (Yang and Slingo, 2001). Weak temporal coverage may reduce data quality, especially when looking at subdaily rainfall variability. To overcome this deficiency, efforts have been made to improve the spatiotemporal coverage by combining data from different satellites into merged products (Kidd and Levizzani, 2011). In particular, these datasets make use of infrared measurements by geostationary satellites to improve the spatiotemporal sampling of low-earth-orbiting satellites. But precipitation estimates based on infrared measurements are more indirect and hence more uncertain than those based on microwave measurements. Overall, it is known that precipitation estimates by satellites perform better in the tropics than in high latitudes, as described by Ebert et al. (2007). This is due to the fact that tropical precipitation is mostly convective, which implies a clearer signal in satellite measurements as result of heavy rainfall from thick clouds rather than precipitation from shallow clouds. The difficulties involved with accounting for the time lag between maximum rainfall and the maximum development of a convective cloud have already been addressed by Reed and Jaffe (1981). This is still one of the issues that infrared (IR)-based rainfall algorithms have to deal with. Nevertheless thanks to the incorporation of high-resolution IR data, current satellite-based precipitation datasets deliver their observations at 3-hourly (or in even higher) temporal resolution. As a result of the fact that high-resolution reference data are very rare in tropical regions, systematic validations of subdaily variations as provided by satellite-based precipitation data are infrequent.

Various studies have evaluated satellite-based precipitation datasets on different scales. Different satellite-based precipitation datasets are intercompared to

check for consistency and to reveal deficiencies, as has been done by Andersson et al. (2011). Some studies used rain gauge data to evaluate differences between the ground-truth and satellite-based precipitation estimates (e.g. Pfeifroth et al., 2013). Usually it is monthly or daily means that are considered, while some studies also validated subdaily data. Sapiano and Arkin (2009) evaluated different high-resolution satellite-based datasets, including TRMM Multisatellite Precipitation Analysis (TMPA) and Climate Prediction Center (CPC) morphing technique (CMORPH) data, with rain-gauge data and found correlations of about 0.5 for 3-hourly data in the southern United States and concluded that CMORPH is best suited to studying precipitation variability. Janowiak et al. (2005) evaluated one summer season of CMORPH precipitation diurnal cycles with weather radar data for the United States and found reasonable agreement for the mean diurnal cycle.

Thanks to the African Monsoon Multidisciplinary Analysis - Couplage de l'Atmosphère Tropical et du Cycle Hydrologique (AMMA-CATCH) project some longer-term high-resolution rain-gauge data are now available, which is used as a precipitation reference for the African tropical climate in this study. Also Roca et al. (2010) and Gosset et al. (2013) used station data provided by the AMMA database for West Africa to validate different satellite-based and rain-gauge based datasets in West Africa. By comparison with AMMA data Roca et al. (2010) concluded that TMPA data are best suited for analyzing diurnal cycles. Gosset et al. (2013) found temporal correlations between satellite estimates and rain gauge data in the range of 0.5–0.7 for daily time steps. He et al. (2015) used TMPA and AMMA station data to improve model simulations in West Africa and also evaluated the diurnal cycle of rainfall. They found a pronounced evening peak and a weaker morning peak for 2005. Sane et al. (2012) analyzed the diurnal cycle of precipitation in Senegal in two months of 2006 using rain gauge and TMPA satellite data and found a secondary peak of rainfall in the morning.

In this study we provide information on the ability of state-of-the-art high-resolution satellite-based precipitation datasets to observe systematic diurnal variations. Therefore, we evaluate, overall, seven different satellite-based precipitation products with at least 3-hourly temporal resolution with reference to in-situ observations in the African tropics. We focus on the mean diurnal cycles of precipitation and also analyze its mean month-to-month and year-to-year variability. We used rain gauge data from the AMMA-CATCH station network to evaluate satellite-based precipitation datasets including the TMPA, the TRMM 3G68 datasets, two CMORPH datasets and the Precipitation Estimation from Remotely Sensed Information using Artificial Neural Networks (PERSIANN). In Section 2 and 3 we describe the data and the methods used. The evaluation results are presented and discussed in Section 4 and 5.

D.2 Data

D.2.1 AMMA rain gauge data

The African Monsoon Multidisciplinary Analysis project is an international interdisciplinary program dealing with the West African Monsoon, its variability, and its impacts on human life. Within the AMMA project, three so-called mesosites with enhanced surface measurements were set up, two of which were the Ouémé mesosite in central Benin and the Niamey mesosite in southern Niger (Lebel et al., 2010). Within these two sites rain gauge networks were maintained until recent by the Institut de recherche pour le Développement (IRD) funded AMMA-CATCH program. Rainfall data at high temporal resolution and for more than a decade are freely available from the AMMA-CATCH database (see `http://bd.amma-catch.org`; data accessed in June 2015).

Overall, we used hourly observations from 37 stations covering the monsoon seasons (May–September) during the time period 2000–11. The chosen stations are mainly located in the Ouémé mesosite in Benin and in the Niamey meso-site in Niger (see Figure D.1). The two mesosites have different rainfall characteristics (Gosset et al., 2013) and are therefore analyzed separately in this study. We use the AMMA-CATCH station data as the reference to validate the satellite products. Therefore, the stations have been gridded as described in section D.3.

D.2.2 TRMM 3G68 dataset

The Tropical Rainfall Measuring Mission is a joint venture between the National Aeronautics and Space Administration and the Japan Aerospace Exploration Agency designed to monitor and study tropical precipitation. The TRMM satellite covers the area from 35°N to 35°S; its sensor package is described in Kummerow et al. (1998). The TRMM satellite's orbit is circular and non-sun-synchronous, which means that each location is covered at different local times each day. This makes the TRMM satellite especially interesting for analyzing the diurnal cycle of precipitation.

The TRMM 3G68 dataset in Version 7 is used, which consists of three different products based on two different instruments aboard the TRMM satellite. Product 2A12 is based on the TRMM Microwave Imager (TRMM-TMI), 2A25 is based on the TRMM Precipitation Radar (TRMM-PR) and the 3B31 product is a combination of the 2A12 and 2A25 products, referred to as TRMM-COMB in the following. All TRMM 3G68 products consist of 1-hourly instantaneous rainfall estimates gridded to a $0.5° \times 0.5°$ grid and cover the global tropics (40°N–40°S).

The TRMM-PR sensor is an active instrument and delivers the most direct measure of precipitation, which implies that the PR should give the best measure

of precipitation. Contrary to the PR, the TMI sensor is a passive microwave imager that relies on emission and scattering signals due to precipitation-sized particles. The TMI sensor swath is wider than that of the PR, but its measure of precipitation is more indirect. The TRMM-COMB combines TMI-calibrated brightness temperatures and PR reflectivities to generate a best-of-TRMM-only product at the instantaneous time scale. The TRMM-COMB algorithm is designed to make use of the strengths of both sensors (Haddad et al., 1997). A drawback of the TRMM-only datasets is its limited spatiotemporal sampling, as analyzed by Negri et al. (2002b). On average, the 1-hourly PR and TMI version-7 datasets on the $0.5° \times 0.5°$ grid are based on 13–15 and 37–40 overpasses per month in the target region, respectively. To improve the spatiotemporal coverage, we aggregated the 1-hourly instantaneous TRMM G68 data to 3-hourly data by averaging. This is close to the ideal aggregation interval of 4 h, as proposed by Negri et al. (2002b)

D.2.3 TRMM 3B42 dataset

The TRMM 3B42 dataset in version 7 is a multisatellite precipitation dataset. It incorporates numerous different satellite sources including microwave and infrared sensor data from polar-orbiting and geostationary satellites (Huffman and Bolvin, 2007) into a final product on a $0.25° \times 0.25°$ grid. The algorithm for generating the TRMM 3B42 dataset consists of three main steps. First, the TRMM-COMB (cf. section D.2.2) product is used to calibrate the different microwave data sources. Then, the infrared-based datasets are converted into precipitation estimates using the calibrated microwave data. Finally, the microwave and infrared data are merged into 3-hourly precipitation estimates.

D.2.4 CMORPH datasets

The Climate Prediction Center morphing technique developed by the National Oceanic and Atmospheric Administration produces a quasi-global precipitation dataset with high spatiotemporal resolution. This technique uses precipitation estimates derived from passive microwave observations and transports these estimates via spatial propagation information obtained from geostationary satellite IR data (Joyce et al., 2004). The morphing technique makes use of 30-min-resolution IR data to propagate and morph the microwave precipitation estimates. It not only transports the spatial rainfall features but also interpolates the rainfall intensities both forward and backward in time to get the best estimate. These precipitation estimates are available in a very high resolution of 30 min in time and 8 km in space, corresponding to the resolution of the geostationary IR data used. A lower-resolution CMORPH data version is available as 3-hourly averaged precipitation estimates, on a $0.25° \times 0.25°$ grid. Both datasets are provided online

(http://rda.ucar.edu). In this study we are using both the lower- and higher-resolution CMORPH version-1.0 data, referred to as CMORPH and CMORPH-hq, respectively.

D.2.5 PERSIANN dataset

The Precipitation Estimation from Remotely Sensed Information using Artificial Neural Networks dataset is an effort coordinated by the Center for Hydrometeorology and Remote Sensing (CHRS) of the University of California (Sorooshian et al., 2000; Ashouri et al., 2015). PERSIANN data are available 3 hourly on a $0.25^\circ \times 0.25^\circ$ grid. To generate the PERSIANN precipitation data, IR measurements from global geostationary IR composites are used to estimate precipitation by applying a neural network trained with various passive microwave based precipitation estimates. The data and more information are available online (http://chrs.web.uci.edu/persiann).

D.2.6 CLAAS dataset

The Cloud Property Dataset using SEVIRI (CLAAS) is generated within the EUMETSAT Satellite Application Facility on Climate Monitoring (CM SAF) (Stengel et al., 2014). The CM SAF generates and provides datasets on various essential climate variables with a focus on the earth's energy cycles. The CLAAS dataset contains several cloud property parameters including cloud-top informations at high spatial and temporal resolutions. The dataset is well suited to study diurnal cycles (Kniffka et al., 2014). We used 1-hourly monthly mean diurnal cycles of cloud-top temperatures (CTT) during a 4-yr period for the three central monsoon months of June–August. CLAAS is used in this study to analyze the correspondence of diurnal cycles of rainfall and cloud-top temperatures.

D.3 Methods

We are using hourly rain gauge data in West Africa as obtained from the AMMA-CATCH database as ground-based reference when comparing with different gridded precipitation datasets during the time period 2000–11. The AMMA-CATCH station data has proven to be of reasonable quality, especially when aggregating in space and time, for example, to 1° daily data (Gosset et al., 2013). While setting up the validation, we were facing the issue of different datasets having different spatiotemporal resolutions. Further, the difficulty of comparing point data to gridded data is addressed by spatial and temporal averaging.

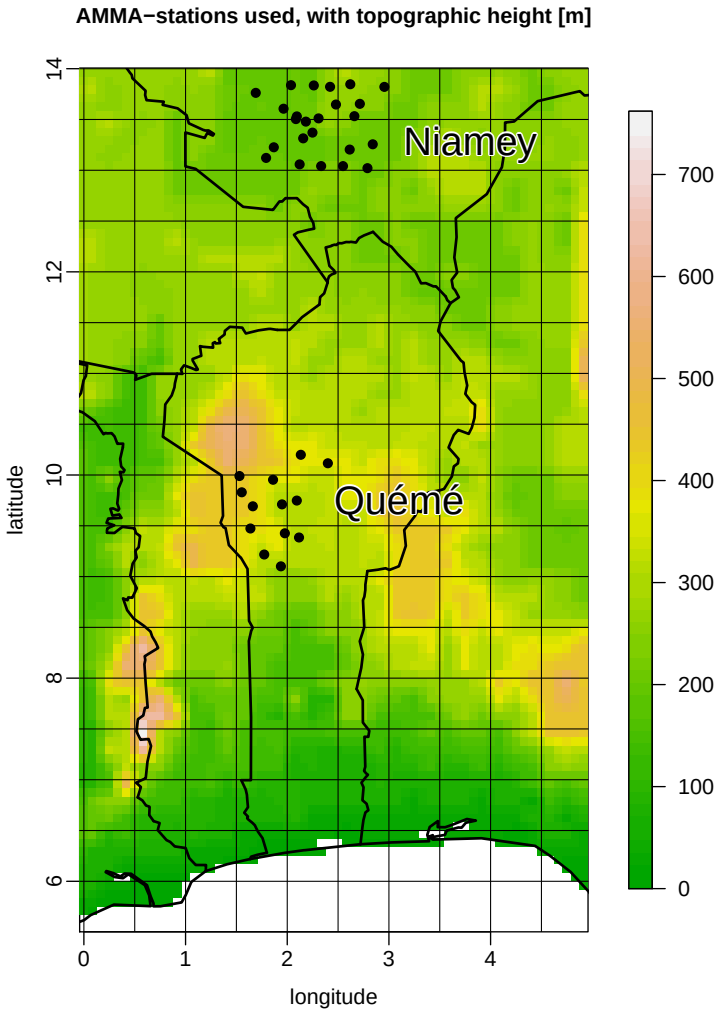

Figure D.1: Topographic map of the analysis region in West Africa, including the AMMA stations used at the Niamey (northern) and Ouémé (southern) mesosites.

As the AMMA-CATCH stations used are distributed relatively dense in some areas, multiple stations could be merged into grid boxes. The stations were aggregated into grid boxes with a size of $0.5° \times 0.5°$ by averaging of the respective stations located in the same grid box. By doing so, the problem of station representativeness could be reduced. All the satellite datasets are also analyzed on the same $0.5° \times 0.5°$ grid. The regridding, if necessary, was performed by conservative remapping. We thereby also aggregated the 1-hourly instantaneous TRMM G68 data into 3-hourly data to be in line with the other satellite data and to account

for the lower sampling rate. This brings the TRMM-3G68 data close to the ideal aggregation interval of 4 h, as proposed by Negri et al. (2002a).

Further improvement of the station data representativeness is achieved by temporal averaging. First, of all monthly mean diurnal cycles for each grid box are computed by averaging the rainfall amounts for the individual hours. These monthly diurnal cycles are then further regionally averaged and then further averaged to multiyear monthly diurnal cycles (see Figures D.5 and D.6), to multimonth yearly diurnal cycles (see Figures D.3 and D.4), and to overall mean diurnal cycles (see Figure D.2). Especially when comparing station data and gridded data at smaller temporal scales than in this study, one should explicitly account for the temporal and spatial sampling errors, as proposed, for example, by Kirstetter et al. (2013) and Roca et al. (2010).

resolution	AMMA	TRMM-3B42	-PR	-TMI	COMB	PERSIANN	CMORPH	CMORPH-hq
native								
lon/lat	/	0.25°	0.5°	0.5°	0.5°	0.25°	0.25°	8 km
temporal	1 h	3 h	1 h	1 h	1 h	3 h	3 h	30 min
timestamp	end	central	begin	begin	begin	begin	begin	begin
used for the validation								
lon/lat	0.5°	0.5°	0.5°	0.5°	0.5°	0.5°	0.5°	0.5°
temporal	1 h	3 h	3 h	3 h	3 h	3 h	3 h	30 min
timestamp	central	central	central	central	central	central	central	central

Table D.1: Spatial and temporal resolutions and time stamp information of all data used as given by the data provider and as used in the validation.

Moreover, we have to consider that the different datasets not only have different spatial resolutions but also different temporal resolutions. As the analyzed datasets are mostly incorporating multiple satellites, the individual single-sensor-based estimates are usually aggregated and finally averaged over a certain time interval during data processing. Accounting for those aggregating time intervals is necessary to compare the actual diurnal timings of precipitation. For the validation of the mean diurnal cycles we used the satellite data at 3-hourly temporal resolution and the AMMA-CATCH reference at hourly resolution. The CMORPH-hq satellite dataset was kept in its native temporal resolution of 30 min to check if there is an added value on the standard CMORPH dataset. A summary of the datasets used, including relevant information on the resolutions, is given in Table D.1.

In most of the analyzed satellite datasets the time stamp given in the data corresponds to the starting point of the accumulation interval (see Table D.1). In the TRMM 3B42 dataset each 3-hourly precipitation value given at a certain UTC time corresponds to the mean precipitation estimated in the interval of ± 1.5 h relative to the time stamp. The time stamps of all other satellite-based datasets have

been adjusted to represent the central time of the summation interval. Thereby, we account for the different starting points of the aggregation intervals. The data are evaluated on the common $0.5° \times 0.5°$ grid.

The evaluation focusses on two main characteristics of the diurnal cycle of precipitation: the diurnal timing of the maximum precipitation value and the size of the diurnal peaks. The analysis is limited to the monsoon season defined as the five months of May, June, July, August and September, when, except for the coastal strip along the Guinea Coast, the majority of the annual rainfall occurs in West Africa. The results are separately shown for the Niamey and Ouémé mesosites, as well as its month-to-month and year-to-year variability. Especially when analyzing the diurnal cycle for individual years, larger uncertainties occur as a result of the shorter averaging interval, visible by a larger scatter and a less smooth diurnal cycle.

At the Ouémé mesosite two diurnal rainfall peaks were found, which are analyzed in more detail. Therefore, all data including the AMMA-CATCH stations were used with a 3-hourly time step, to avoid any resolution effect on the results. To distinguish between the diurnal rainfall peaks, the timing and the size of the rainfall peaks (defined as the mean maximum rainfall amount) are evaluated separately for morning (0000–1200 UTC) and evening (1200–0000 UTC) hours, when the peaks occur.

D.4 Evaluation results

The West African monsoon season is characterized by large rainfall amounts with substantial diurnal cycles (Fink et al., 2008; Birch et al., 2014). Moreover, the rainfall diurnal cycles vary spatially (He et al., 2015). This tropical rainfall regime poses a challenge for satellite-based precipitation datasets because of its high spatiotemporal variability. In the following, the monsoonal mean rainfall is analyzed and the mean diurnal cycles of rainfall are described. Then, the focus is shifted to the precipitation diurnal cycle variability in the different datasets.

D.4.1 Monsoonal mean precipitation

To assess the overall quality of the analyzed datasets, it is useful to validate the monsoonal mean rainfall amounts in comparison with the AMMA-CATCH station data. The monsoonal mean is the mean of the five months (May–September) when the majority of rainfall occurs in West Africa north of $8°N$. The results are shown in Table D.2. There is a negative gradient of rainfall from south to north. The Ouémé mesosite in central Benin ($\sim 9.5\,°N$) gets about 1000 mm of rain while the Niamey mesosite ($\sim 13.5\,°N$) in southern Niger gets on average 500 mm of rain.

	AMMA	TRMM-3B42	-TMI	-PR	-COMB	PERSIANN	CMORPH	CMORPH-hq
Ouémé meso-site								
mean	1051	1018	1153	767	928	1326	1302	1300
rel. bias [%]		**-3.1**	+9.7	-27.0	-11.7	+26.2	+23.9	+23.7
Niamey meso-site								
mean	515	486	423	348	455	1135	719	719
rel. bias [%]		**-5.6**	-17.9	-32.4	-11.7	+120.4	+39.6	+39.6

Table D.2: Monsoonal mean precipitation (mm) and relative biases (%) of the analyzed datasets with reference to the AMMA-CATCH station data during 2000–11 for the Ouémé and Niamey the mesosites. Best values are shown in boldface.

Because of different rainfall dynamics (Gosset et al., 2013; Fink et al., 2006), the validation results in Table D.2 are shown separately for the Niamey and Ouémé mesosites.

The precipitation amounts vary, especially for the Niamey mesosite, where rainfall is less frequent than at the Ouémé mesosite (Gounou et al., 2012); hence single rain events have a large impact on the rain amounts. At the Niamey mesosite the PERSIANN data shows more than twice the rainfall amount compared to the ground reference, which is in line with findings by Gosset et al. (2013), while the PR data show the largest underestimations (–27 %). For the Ouémé mesosite the monsoonal mean rainfall amounts are in better agreement. The values range from about 750 to 1300 mm with the highest values given by PERSIANN and CMORPH data. An overestimation of CMORPH has also been found by Pierre et al. (2011) in Senegal in West Africa. We find negative biases of the PR product to be in the order of 20%–30%, which is consistent with the negative biases found in convective storms in South America by Rasmussen et al. (2013). Overall, the TRMM 3B42 data are closest to the reference, with deviations of only 5% on average in both analyzed regions.

D.4.2 Mean diurnal cycles

The overall monsoonal mean diurnal cycles of rainfall at both mesosites are shown in Figure D.2. At the Ouémé mesosite there is a distinct diurnal cycle with a maximum of rainfall in the evening at around 1800 UTC and a minimum in the morning at about 0800 UTC. A secondary maximum occurs in the early morning at around 0400 UTC. The analyzed satellite datasets reasonably agree with the AMMA-CATCH reference, with a slight tendency toward a delayed peak in the evening. Because of its high temporal resolution, the CMOPRH-hq dataset also nicely captures the secondary peak in the morning. Overall, the rainfall amount during the evening peak are overestimated by most of the satellite datasets. In terms of the size of the evening peak the three TRMM 3G68 data products sub-

stantially deviate from each other, as shown in Figure D.2.

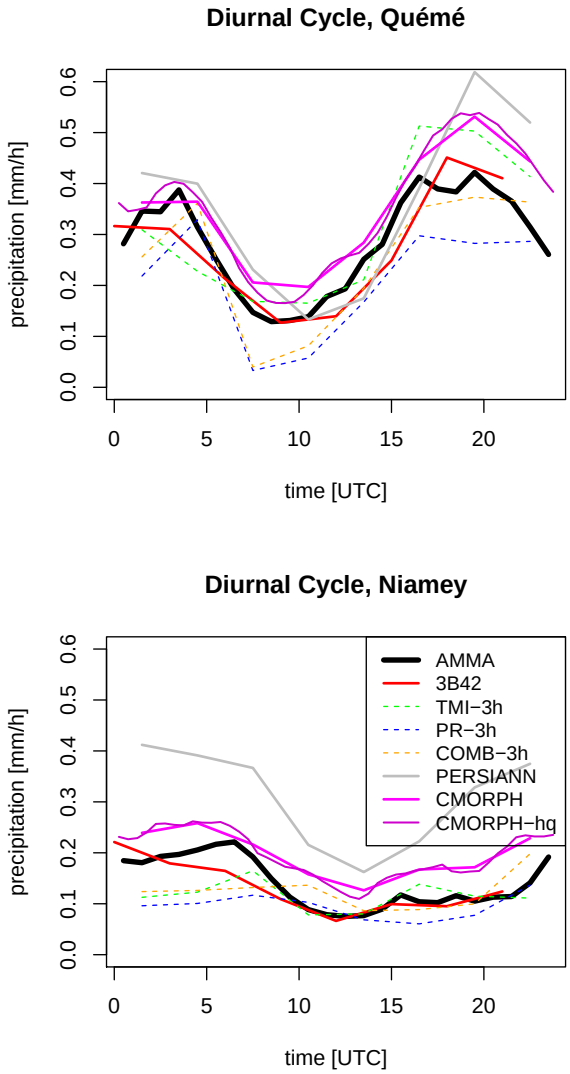

Figure D.2: Mean diurnal cycles of the satellite-based datasets and the AMMA-CATCH data at the (top) Ouémé and (bottom) Niamey mesosites during the monsoon season (MJJAS).

The monsoonal mean diurnal cycle of rainfall is less pronounced at the Niamey mesosite (see Fig. D.2). The diurnal cycle as measured by the rain gauges peaks in the morning at about 0600 UTC, and a minimum is observed around noon. During the late evening the rainfall amounts increase again. At the Niamey mesosite the

satellite products have more difficulties in capturing the diurnal cycle. It is further obvious that CMORPH, and in particular PERSIANN, overestimate the rainfall while the PR underestimates the rain, as described in the previous subsection. The morning peak is best captured by the CMORPH-hq data but is also visible in the TMI data. Overall, at the Niamey mesosite the satellite products show larger differences from the AMMA-CATCH reference than are seen at the Ouémé mesosite.

D.4.3 Year-to-year variability of the diurnal cycle

The monsoonal mean diurnal cycles of rainfall from each of the years from 2000 to 2011 are shown in Figures D.3 and D.4 for the Ouémé and Niamey mesosites, respectively. Brief inspection of both figures reveals there are considerable year-to-year variations at both mesosites.

At the Ouémé mesosite, a distinct peak of rainfall in the evening occurs in most of the years (see Figure D.3). An exception is 2004, when the morning peak of rainfall is much more pronounced than is usually the case. The strongest evening peaks are visible in 2005, 2009, and 2010. During 2000–02 the CMORPH and PERSIANN products most strongly overestimate the evening peak. In general, the satellite products are able to capture the year-to-year variations of the diurnal cycles of rainfall. However, a diurnal cycle averaged over only five months has a larger variability and a less smooth diurnal cycle since the number of rainfall events used for averaging is relatively small. In turn, single events might heavily impact this comparison. In PR, TMI, and TRMM-COMB the deviations are larger, and the peaks are often overestimated. This behavior can most likely be attributed to a limited temporal sampling of the TRMM-only products.

The diurnal cycles during the individual years show larger deviations at the Niamey mesosite compared to the Ouémé mesosite. A prevailing early morning peak of rainfall is observed. Exceptions are the years 2000, 2005, and 2007, when the early morning peak of rainfall hardly exits (see Figure D.4). The most pronounced early mooring peaks occurred during 2004 and 2006. Again, the CMORPH-hq data take advantage of the high temporal resolution and can capture much of the observed variability. Overall, PERSIANN tends toward overestimating the results and the TRMM-only products partly show overestimating peaks (e.g., during 2004, 2005, and 2007).

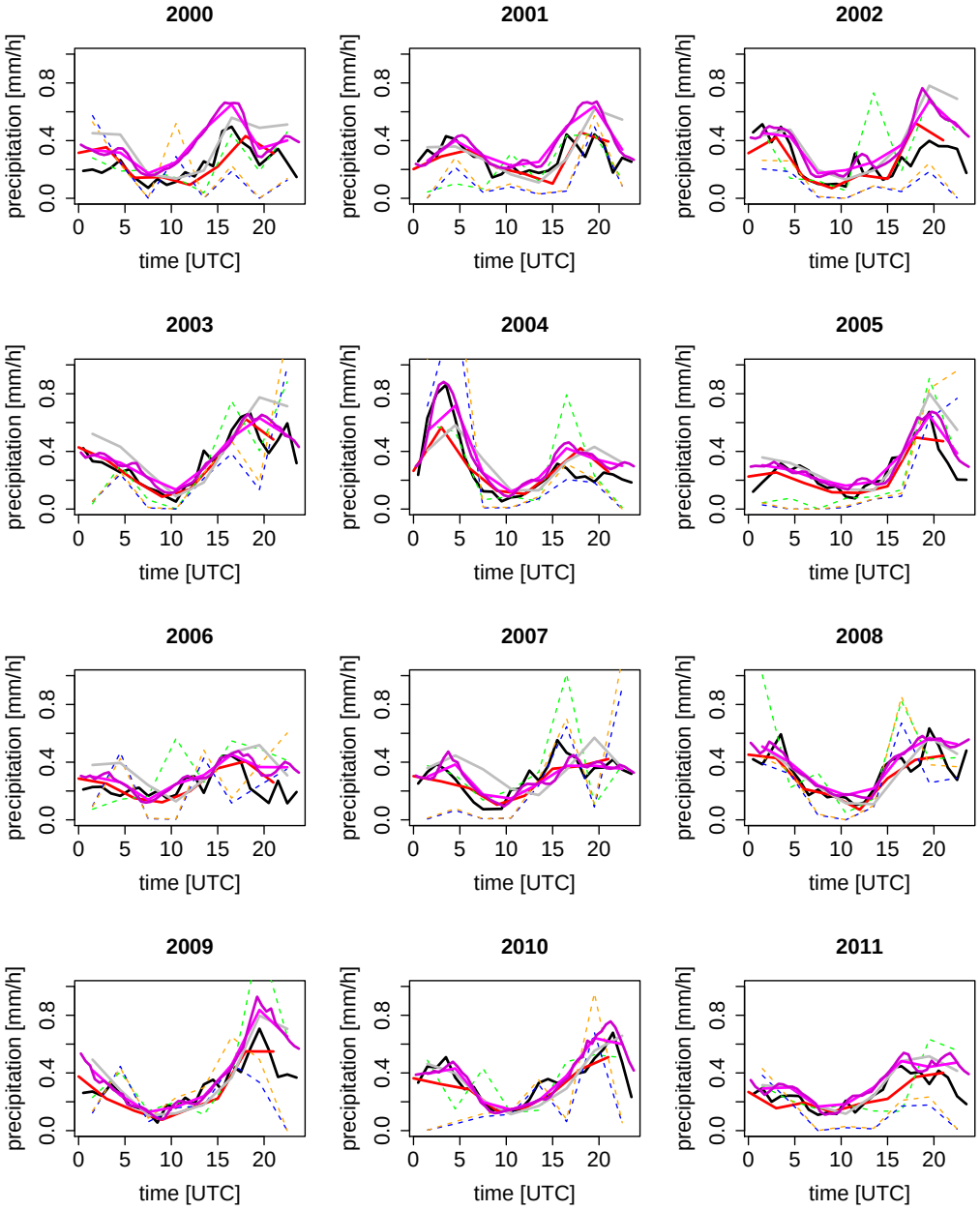

Figure D.3: Annual mean diurnal cycles of the satellite-based datasets and the AMMA-CATCH data at the Ouémé mesosite during the monsoon season (MJJAS) for 2000–11. The key for the lines is provided in Fig. D.2

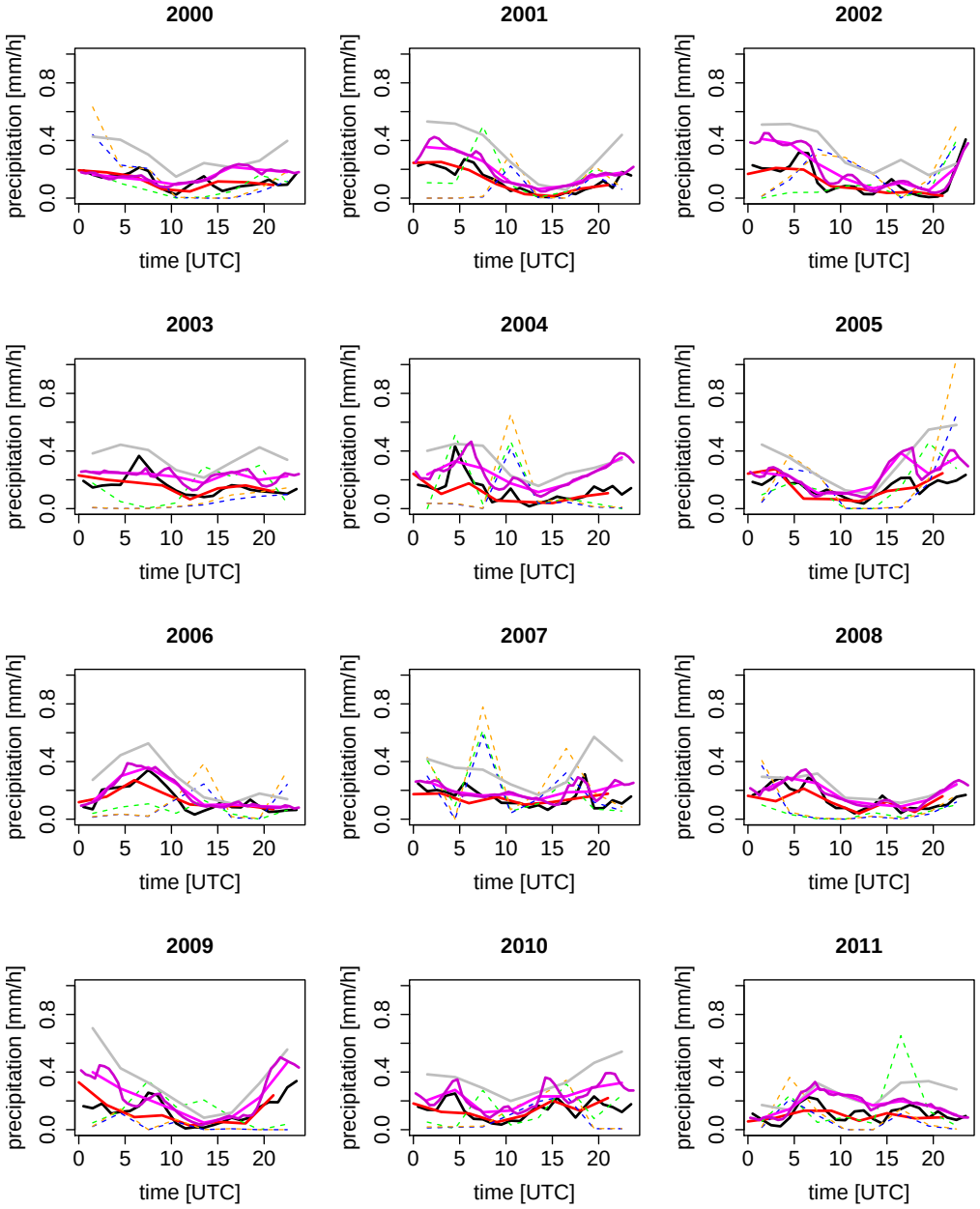

Figure D.4: Annual mean diurnal cycles of the satellite-based datasets and the AMMA-CATCH data at the Niamey mesosite during the monsoon season (MJJAS) for 2000–11. The key for the lines is provided in Fig. D.2.

D.4.4 Multi-year monthly diurnal cycles

Instead of averaging the diurnal cycles of the five monsoon months [May–September (MJJAS)], as in the previous subsection, we also analyzed the multiyear mean diurnal cycles from month to month. These diurnal cycles of rainfall are presented in Figures D.5 and D.6 for the Ouémé and Niamey mesosites, respectively. Additionally, the diurnal cycles of the CLAAS cloud-top temperatures were analyzed during the monsoon months of June–August to give a qualitative measure of the diurnal cloud development alongside to the diurnal rainfall occurrence.

At the Ouémé meso-site we can see that the diurnal cycle substantially varies throughout the monsoon season (cf. Figure D.5). In May there is a distinct peak in the early morning around 0400 UTC, while the evening peak is less pronounced. The satellite products show large differences concerning both peaks in terms of rainfall amounts. The early morning peak is underestimated by each of the satellite products, and the evening peak is partly overestimated. The TRMM 3G68 product disagrees with the reference in the evening. In June the diurnal cycle is changing: the early morning peak is weakening and the evening maximum is strengthening relative to the situation in May. In June the satellite datasets agree better with the AMMA-CATCH reference, while the morning and evening peaks are of approximately the same size. As in May the evening peak is overestimated, especially by PERSIANN and CMORPH. The deviations are smaller during the morning peak. In July the diurnal cycle of rainfall has changed further. There is no more morning peak of rainfall while the evening maximum has strengthened and moved to an earlier time of around 1800 UTC. At this stage of the monsoon we observe the typical characteristic of tropical convection over land that leads to local convective rainfall in the evening as a result of surface heating in an unstable troposphere. Here, we see a slight delay in the time of the peak rainfall among almost all of the satellite products (see Figure D.5 and also Figure D.7). This delay corresponds to the minimum in the cloud-top temperature diurnal cycle in July (see black dotted line for CTT in Figure D.5), with the coldest clouds corresponding to the maximum rainfall derived by the satellite products. In August, the diurnal cycles are strongest. Overall, the diurnal cycle is relatively similar to that in July with the exception of a double maximum in the evening. This feature is difficult to interpret and might be attributable to the spatial averaging. Again, most of the satellite datasets are on average slightly late in terms of peak rainfall while the PR and TRMM-COMB peaks coincide with the observations. In September, at the end of the monsoon, the diurnal cycle characteristics are similar to that in May, early in the monsoon, but with a slightly earlier peak.

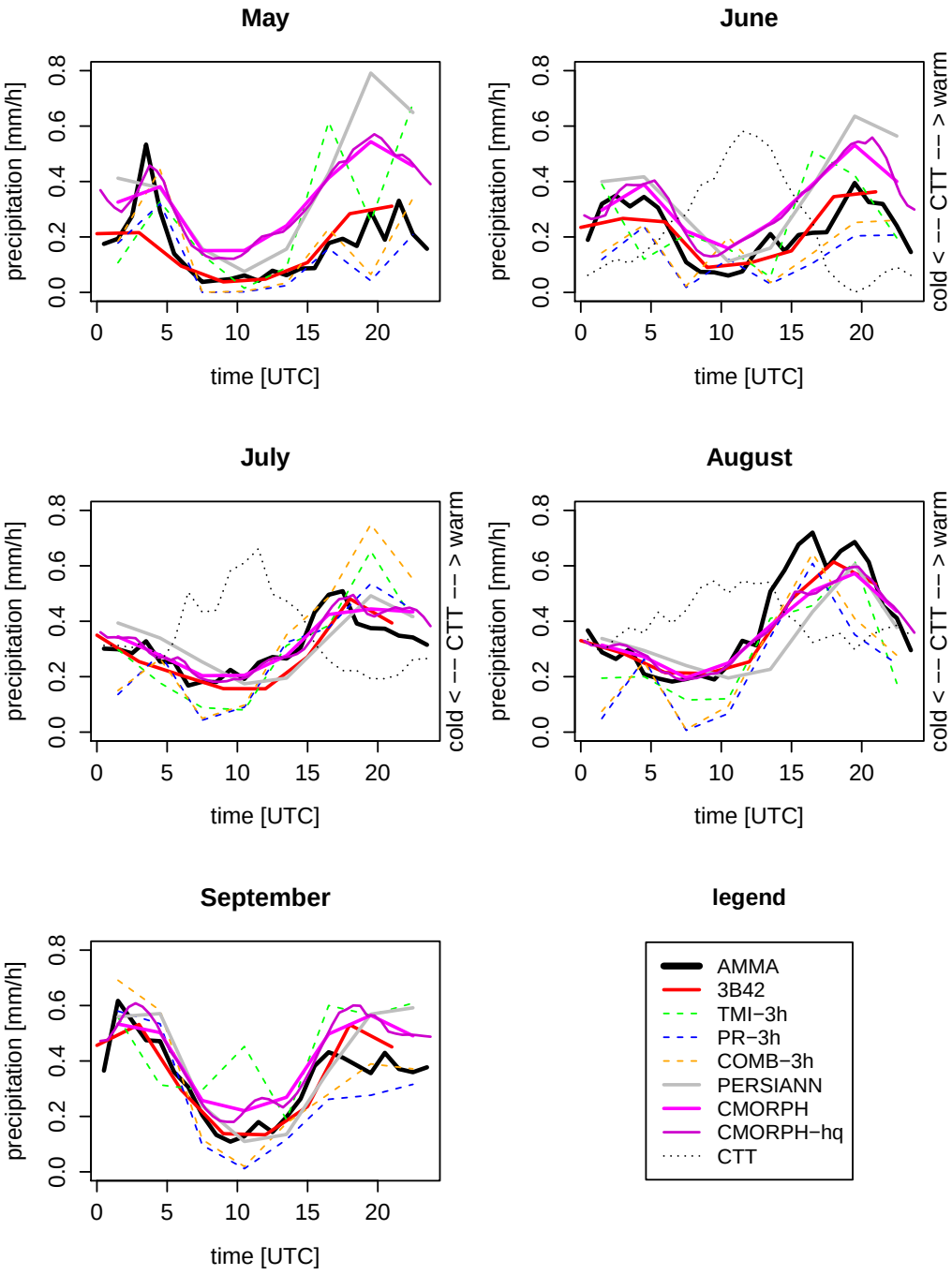

Figure D.5: Multiyear monthly mean diurnal cycles for MJJAS at the Ouémé mesosite, including CTT information for JJA. See legend at the bottom right.

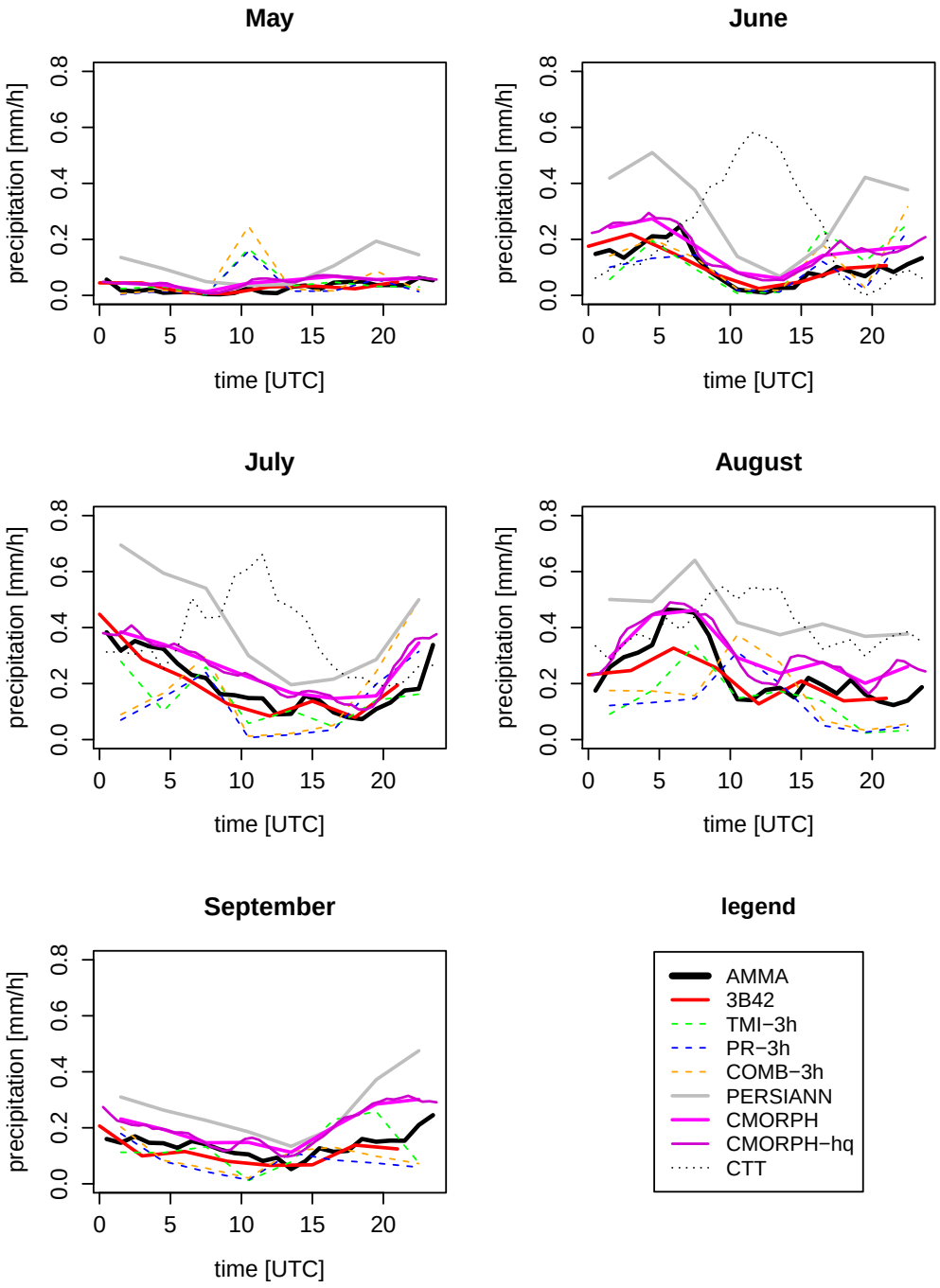

Figure D.6: Multiyear monthly mean diurnal cycles for MJJAS at the Niamey mesosite, including CTT information for JJA. See legend at the bottom right.

At the Niamey mesosite the diurnal cycle is also subject to month-to-month

variabilities throughout the monsoon (cf. Figure D.6), but the diurnal cycle characteristics are less clear than at the Ouémé mesosite. In May, the monsoonal rain is still almost absent at the Niamey site, which is changing in June. Then, the rainfall diurnal cycle characteristics are similar to those seen in Figure D.2 for the overall monsoonal mean diurnal cycle. The maximum rainfall occurs in the morning at around 0700 UTC. PERSIANN strongly overestimates rainfall, while its timing is reasonable. The early morning peak is captured too early by most of the satellite products, but overall the peak is not very pronounced. The early morning peak is absent in July. There is instead a peak around midnight that the satellite products capture reasonably well. The morning peak appears again in August and is more pronounced than in June. There the PR and TRMM-COMB data deviate most while the TMI data are closer to the reference. At the end of the monsoon, in September rainfall amounts decrease and the diurnal cycle also gets weaker.

The distinct month-to-month variability at the Ouémé mesosite (cf. Figure D.5) is further analyzed in more detail concerning the timing and intensity of the observed morning and evening peaks. Therefore, the AMMA-CATCH data are used at 3-hourly resolution, which is in line with the satellite products (beside CMORPH-hq), to avoid any artificial timing differences. Figure D.7 shows the results of the mean morning peaks of rainfall; here, the focus is on the months of May and September, when the morning peak is most distinct (marked by the black boxes in the top part of Figure D.7). While the TRMM 3G68 products capture the morning peaks too late by up to 2 h, the other satellite datasets show only small deviations in the timing of the peak rainfall. Time differences for the evening peak are more systematic during the central monsoon months of June–August, when the evening peak of rainfall dominates on average (see black box in Figure D.7, bottom). June presents a transition month when morning and evening peaks are of similar size. In July and August, when the evening peak is most distinct, a mean delay in the time of maximum rainfall in all the satellite datasets is revealed. This delay is about 1 h on average, with smaller delays by the PR, TMI, TRMM-COMB, and CMORPH/CMOPRH-hq datasets. Larger mean delays of up to 2 h are found in the TRMM 3B42 and PERSIANN datasets. Overall, the diurnal timing is captured reasonably by the satellite datasets while the CMORPH and TRMM-COMB products perform best in identifying the evening peak as observed by the AMMA-CATCH stations.

The differences of the morning and evening peak sizes of rainfall at the Ouémé mesosite are shown in Figure D.8. The morning peaks in May and September are overestimated on average by most of the satellite products. TRMM 3B42 peak sizes are closest to the AMMA reference. Overall, the overestimations on the mean peak size are on the order of 0.25 mm/h. The peak size differences in the evening (see

Figure D.8, bottom) are larger than those in the morning. Especially in May, June, and September, most of the datasets overestimate the evening rainfall peaks by 0.25–0.5 mm/h. This results in dominating evening peaks in the satellite datasets, in opposite to the ground-based measurements. In August, when the evening peak is most pronounced, the peak sizes between the satellite and the station data agree well. Owing to its higher temporal resolution, CMORPH-hq shows stronger peaks than does CMORPH.

D.5 Discussion and Conclusions

Rainfall in West Africa is characterized by convective events that are subject to high spatial and temporal variability. It has been shown by Roca et al. (2010) and Gosset et al. (2013) that multisatellite-based precipitation datasets provide valuable information on the daily and sub-daily variability of rainfall in West Africa. In this study, it is emphasized that current satellite-based datasets, especially those including geostationary infrared information that get a better temporal coverage, perform reasonably well in capturing the diurnal cycle as observed by ground stations. When averaging over longer time scales, the TRMM-only products (TRMM 3G68) provide reasonable diurnal cycles as well, while care must be taken when short time scales are considered. In this case deviations are larger (see e.g. Figure D.4), probably as a result of the reduced temporal sampling.

Concerning monsoonal mean rainfall amounts during the time period of 2000–11 the TMPA dataset preforms best at both the Niamey and Ouémé mesosites (see Figure D.2), which might be related to the fact that the TMPA product also incorporates gridded rain gauge information on a monthly scale. The overestimations found in CMORPH and PERSIANN, as well as the underestimation by PR, are in line with findings in West Africa by Pierre et al. (2011) and Gosset et al. (2013) for shorter time periods.

The diurnal cycle of rainfall is much more pronounced at the Ouémé mesosite than at the Niamey mesosite. At the latter, maximum diurnal rainfall occurs in the morning hours owing to the arrival of mesoscale convective systems (MCSs). At the Ouémé mesosite we find on average a weaker rainfall peak in the morning and a stronger peak in the evening, in line with the findings of He et al. (2015). These diurnal cycles are subject to interannual variability (see Fig. D.3). There are also pronounced variations in the multiyear monthly diurnal cycles throughout the monsoon season. A distinct morning peak in rainfall in May is followed by strong evening peaks of rainfall in July and August, when the locally initiated convective rainfall regime is dominating. In September things change again with the southward shift of the intertropical convergence zone. These results, based on a 12-yr period, agree well with findings by Fink et al. (2006) during a 1-yr period

in 2002.

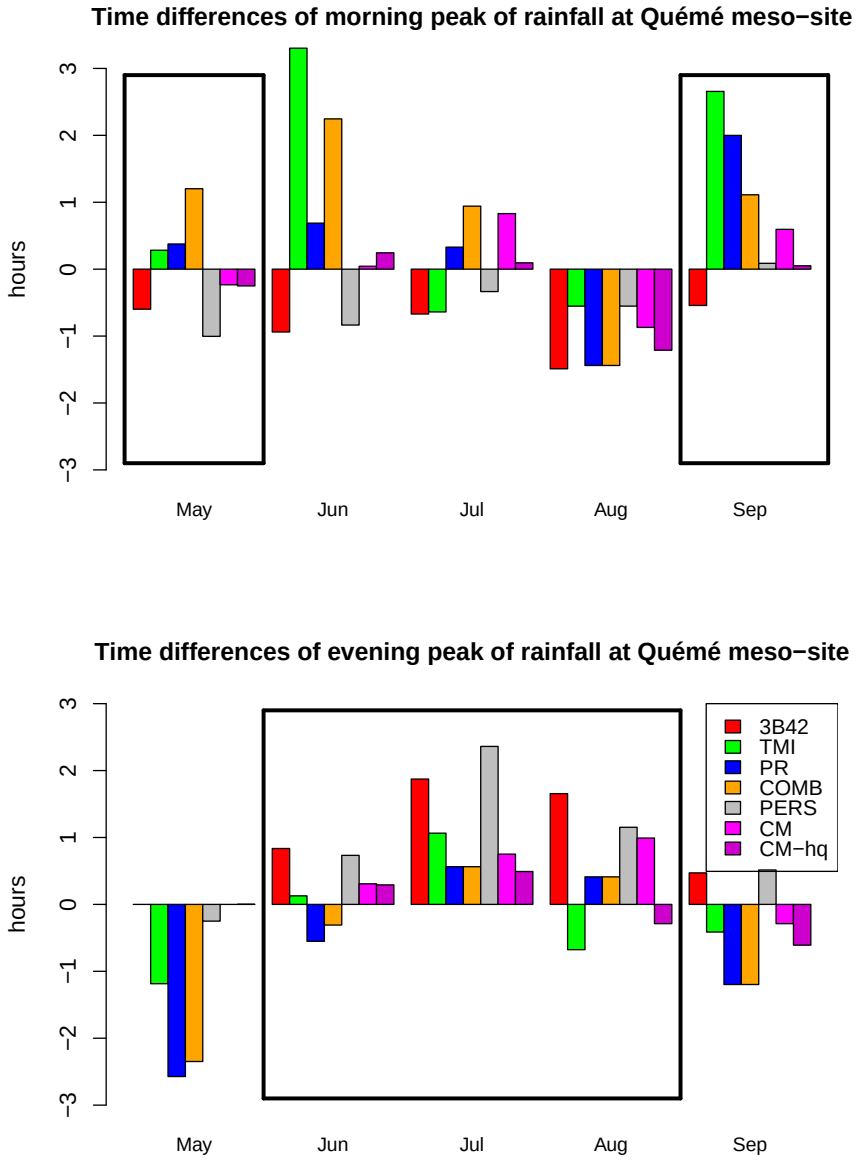

Figure D.7: Time differences (h; satellite data minus station data) in (top) morning peaks and (bottom) evening peaks of monthly mean diurnal rainfall during the monsoon months at the Ouémé mesosite. The most pronounced monthly peaks (morning peaks during MS and evening peaks during JJA) are marked by the black boxes.

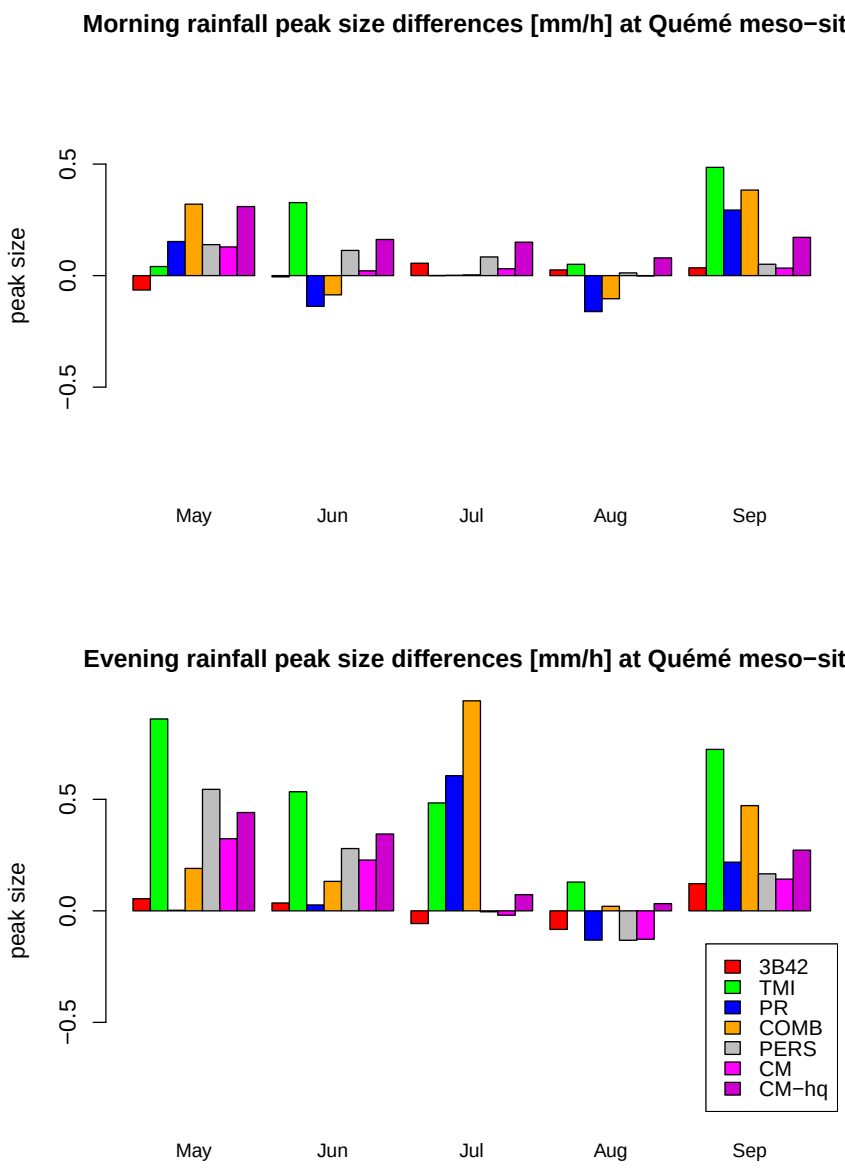

Figure D.8: Size differences (mm/h; satellite data minus station data) of monthly mean rainfall peaks in the (top) morning and (bottom) evening for the monsoon months at the Ouémé mesosite.

There also is significant year-to-year variability of the mean diurnal cycle at the Ouémé mesosite, which is expected to be defined by the prevailing precipitation regime being either more MCS dominated or dominated by local convection during

the individual years. Nevertheless, the morning and evening peaks exist in most years, with the evening peak dominating the rainfall diurnal cycle. At the Niamey mesosite interannual variability is also present. Owing to large deviations in the diurnal cycles of rainfall (cf. Figure D.6 and D.4), which might often be the result of only a few extreme events, a detailed analysis of mean diurnal cycles is not expected to be of much value even averaging over longer time time periods. For more detailed evaluations of rainfall in such an outer tropical regime, it is important to account for sampling uncertainties on spatial and temporal scales. A procedure on how to account for those sampling and algorithm uncertainties within a validation framework has been developed by Roca et al. (2010) and Kirstetter et al. (2013).

Instead, for the Ouémé mesosite the morning and evening peaks in rainfall have been analyzed in more detail as rainfall occurs more frequently. We find that there is a mean time delay of about 1 h in the diurnal rainfall maximum in the evening by most of the satellite datasets (see Figure D.7). A delay in peak rainfall has also been found by Negri et al. (2002a) in the tropics of Brazil. In the PERSIANN dataset this averaged delay is largest, at about 2 h. The TRMM-only products PR, TMI and TRMM-COMB and the CMORPH dataset show only a minor mean delay. This tendency toward a delay in the timing of the rainfall maximum in the evening can be explained by the use of infrared data in the satellite dataset generation. The infrared algorithms are only sensitive to cloud-top temperatures and convert those into a rain rate. Using cloud-top temperature observations can then lead to a systematic incorrect interpretation of the algorithm by still assuming rainfall, a problem scientists have been faced since the early days of satellite imagery interpretation (Reed and Jaffe, 1981). Tropical convective precipitation typically occurs during the early stage of convective cloud development, while little precipitation occurs at the later stages when the high and cold ice shield remains (Futyan and Del Genio, 2007). The delay of minimum cloud-top temperature with reference to the maximum rainfall peak is especially visible in July and August (see Figure D.5). This might explain why the PERSIANN dataset, which is mainly based on infrared measurements, shows the largest delay in peak precipitation (see Figure D.7). The mean sizes of the morning and evening peaks of rainfall (see Figure D.8) at the Ouémé mesosite are overestimated by most of the satellite datasets. This overestimation is stronger for the evening peak than for the morning peak. This might be related to the prevailing rainfall regimes.

However, the central Benin study region is a good example of where local knowledge of the diurnal and seasonal cycles in the types of convection can be indispensable for interpreting satellite rainfall validation studies. The peak after midnight in the Ouémé mesosite is caused by westward-propagating, organized convective systems (OCSs) that originate from the Jos plateau and reach the site toward the ends of their lifetimes (Fink et al., 2006). These OCSs develop in

high CAPE/CIN and low-level shear environments that prevail in May–June and September near the Ouémé mesosite. In July and especially August, low-shear, low CAPE/CIN, and a moist troposphere favor afternoon convection that is less organized. It can be hypothesized that the observed year-to-year variations in the two diurnal peaks are due to changes in the two convection regimes described above. Moreover, delays in the timing of the later afternoon peak might be related to the fact that this is developing convection whereas the nighttime peak might result from extensive trailing OCS-related anvils. However, this speculation is left for further studies. Since the Niamey site only has OCS-type convection (Mathon et al., 2002), the year-to-year variability in the overnight peak is likely related to random changes in the life cycles of the few OCSs that hit Niamey each year. It has been known that the overnight peak is related to OCSs that are triggered near the southern foothills of the Air Mountains in the afternoon hours and propagate at about 50 km/h toward Niamey in the evening and early night hours (Shinoda et al., 1999).

Overall the satellite products are able to reasonably capture the diurnal cycles of rainfall and its climatological variability with reference to ground-based rain gauge observations, keeping sampling issues associated with shorter temporal and smaller spatial scales in mind. In particular, the high-resolution CMORPH-hq dataset performs well and allows for more detailed analysis on rainfall diurnal cycles in the tropical regime. The timing of the precipitation diurnal cycles is of great interest for the modeling community. There is the common problem in numerical modeling with reasonably reproducing the precipitation diurnal cycles (Dirmeyer et al., 2012; Birch et al., 2014; Folkins et al., 2014). The applied parameterizations typically generate precipitation too early in the day, while explicitly resolved convection give promising results (Fosser et al., 2015). For evaluation, satellite-based precipitation datasets are often used as a reference, especially in regions sparsely covered by rain gauges like the tropics. This study shows the general suitability of selected satellite-based precipitation datasets to reasonable capture the diurnal cycle of precipitation. However, different characteristics are documented for the datasets used with respect to their ability to reproduce the diurnal cycle of precipitation on different spatial and temporal scales. These should be considered when selecting the appropriate datasets for model evaluation and other applications.

acknowledgments

We like to thank the EUMETSAT Satellite Application Facility on Climate Monitoring (CM SAF) team for their valuable support. We also thank the data providers for free data access. Thanks go to the AMMA project team for giving access to their database. Author BA acknowledges funding from the Hessian initiative for

the development of scientific and economic excellence (LOEWE) at the Biodiversity and Climate Research Centre (BiK-F), Frankfurt/Main. AHF was supported by the DACCIWA project, funded from the European Union Seventh Framework Programme (FP7/2007-2013) under Grant Agreement 603502. We thank the three anonymous reviewers whose comments helped to improve the manuscript.

Appendix E

Evaluation of the rainfall diurnal cycle in West Africa given by MERRA reanalysis and CCLM regional climate model simulations

Motivation

The diurnal cycle of precipitation as provided by various satellite-based datasets have been validated in detail in Pfeifroth et al. (2016) (see Appendix D). It has been shown that current satellite-based datasets are able to reasonable capture the diurnal cycle as observed by rain gauges. The CMORPH-hq data has shown to have a good quality in observing the diurnal cycle of precipitation. Therefore it is possible to use this satellite data to evaluate the diurnal cycle of precipitation in West Africa as simulated by models. It is known that mot Global Climate Models simulate an early peak in the diurnal cycle of rainfall over most land areas (Dai, 2006). Still it is important to check if regional models, which are higher spatially resolved in space and have more vertical layers, may perform better. Hohenegger et al. (2008) suggested that the models need to be used in cloud-resolving scales to get the the precipitation diurnal cycle better in line with observations, Here, the diurnal cycle as given by two COSMO Regional Climate Model (CCLM) simulations and by the Modern-Era Retrospective Analysis for Research and Application (MERRA) reanalysis, both making use of convection parameterizations, are validated with help of satellite data by CMORPH. The regions of interest are two sites in Benin and Niger for which the diurnal rainfall characteristics are well known due to a previous studies, e.g. by Pfeifroth et al. (2016).

Data and Methods

The MERRA and CCLM data used in this analysis are described in section 3.3.3 and 3.3.2 of this doctoral thesis. Both MERRA and CCLM precipitation data is used in 1-hourly resolution. While precipitation is a pure prognostic variable in CCLM, satellite-based rain rates by TRMM Microwave Imager (TMI) and Special Sensor Microwave Image (SSM/I) sensors are assimilated into the MERRA model system, with the intention to improve the hydrological cycle given by MERRA. The common time period of analysis is a seven year period during 2002–2008. The analysis regions are the Ouémé mesosite in Benin and the Niamey mesosite in Niger. The locations of both regions can be checked up in Figure D.1 in the Appendix D.

Results

The results clearly show that both the CCLM regional climate model and the MERRA reanalysis are not able to correctly simulate the diurnal cycles of precipitation at the Ouémé mesosite in West Africa. Both CCLM and MERRA show a diurnal cycle of precipitation that is a few hours too early with reference to the CMORPH data. The mean rainfall diurnal cycle of MERRA peaks around 12 UTC and the one of the CCLM regional climate model simulations is maximal at about 14 UTC, while CMORPH peaks at about 18 UTC (cf. Figure E.1, left). The CCLM simulation using the improved heat conductivity formulation (CCLM-CORDEX-hc) within the used soil model (called TERRA) shows a slightly later and stronger peak in precipitation compared to the standard CCLM-CORDEX simulation. This means a slight improvement in the diurnal cycle, due to an improved formulation of the heat fluxes between the soil and the troposphere. The secondary early morning peak, which occurs at about 3 to 4 UTC, is neither captured by CCLM nor by MERRA.

At the Niamey site, the CMORPH satellite data shows a mean diurnal cycle peak of precipitation in the early morning, which is in line with results from Pfeifroth et al. (2016) for a 11-year time period using rain gauge data (see Appendix D). The Niamey peak in the diurnal cycle is smaller and not as sharp than the mean diurnal peaks at the Ouémé mesosite, which is owing to the fact that rainfall is more frequent at the Ouémé mesosite. MERRA and CCLM simulations perform more differently at the Niamey site: The CCLM simulations show an early morning peak in the diurnal cycle of precipitation, which is reasonably in agreement with the CMORPH data, while the MERRA reanalysis data again shows a peak around noon. Hence, the CCLM performs better concerning the diurnal cycle at the Niamey site than the MERRA reanalysis. The early morning peak

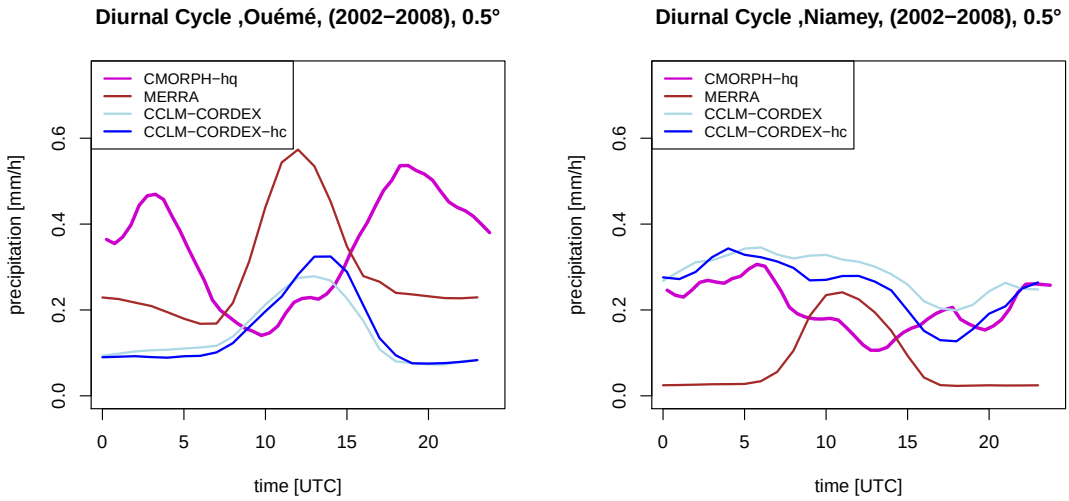

Figure E.1: Mean diurnal cycles of the CMOPRH-hq satellite data and the MERRA reanalysis and two CCLM climate simulations at the at the Ouémé (left) and Niamey (right) mesosites during the West African monsoon season (MJJAS)

of rainfall is resulting in travelling Mesoscale Convective Systems (MSCs). These MCSs seem to be somehow simulated by the CCLM regional climate model, in opposite to the MERRA reanalysis.

It is also obvious that there are biases between the CMORPH data and the model based data, which can be inferred from Figure E.1. The MERRA reanalysis data shows much larger mean precipitation values than the CCLM simulations. Consequently, MERRA is better in agreement with the CMORPH data at the Ouémé meso-site concerning mean rainfall. At the Niamey mesosite the situation is the opposite. The CCLM simulations show mean values closer to the CMORPH data, while the MERRA reanalysis underestimates rainfall amounts.

Beside the monsoonal mean diurnal cycles of rainfall, also its year-to-year variability is analyzed at the Ouémé mesosite (see Figure E.2). As presented in the study by Pfeifroth et al. (2016), there is some year-to-year variability in the precipitation diurnal cycles, which the CMORPH data is able to capture. In most of the years the double peak structure exists with the evening peak dominating. An exception is the year 2004, when the early morning peak is dominating.

The model based precipitation data by MERRA and CCLM have only little year-to-year differences in the their monsoonal mean diurnal cycles. The single peak structure with maximum rainfall around noon to early afternoon exists in year. The peak in the CCLM simlations is thereby later then the one in MERRA. There is no early morning peak neither in MERRA nor in the CCLM simulations

in any of the years. In contrast, there is some year-to-year variability in the abolute rainfall amounts. In most of the years the CCLM-CORDEX-hc simulation shows a stronger and later peak in rainfall that is somewhat closer the evening peak as observed by CMORPH.

Conclusions

The simulation of the correct diurnal cycle of precipitation is known to be a difficult task for numerical models (Dirmeyer et al., 2012). Especially when convection cannot be resolved and hence has to be parameterized, errors have to expected. In this case the diurnal cycle of rainfall usually has an early peak compared to observations (Dai, 2006). This is also observed for the diurnal cycle at the Ouémé site in this study, where locally initiated convective rainfall regularly occurs. Both the two CCLM simulations and the MERRA reanalysis have similar difficulties in case the locally initiated convection. Possible error sources in the models are a too strong moisture convergence in the boundary layer and the early initiation of convection owing to a too weak convective inhibition (CIN) (Colby, 1984) in the model. The CIN is the energy that has to be reached until the air mass can rise to the level of free convection, from where the air is lifted further. With the limited vertical resolution of the models it is challenging to get a reasonable CIN.

At the Niamey site the mean diurnal cycle as simulated by the CCLM shows an early morning maximum of rainfall, which is in fair agreement with the CMORPH satellite data. The MCS controlled climate at the Niamey site is somehow reproduced. On the other hand, the correct travelling of the MCSs that cause the early morning rainfall peak at the Ouémé site is not simulated.

Nevertheless the overall performance of the MERRA reanalyis and the CCLM regional climate model, both using convective parametrizations, to simulate the diurnal rainfall climate can be considered as quite limited. It will be important to see in if future long-term convective resolving simulations provide improved results for the West African monsoonal climate.

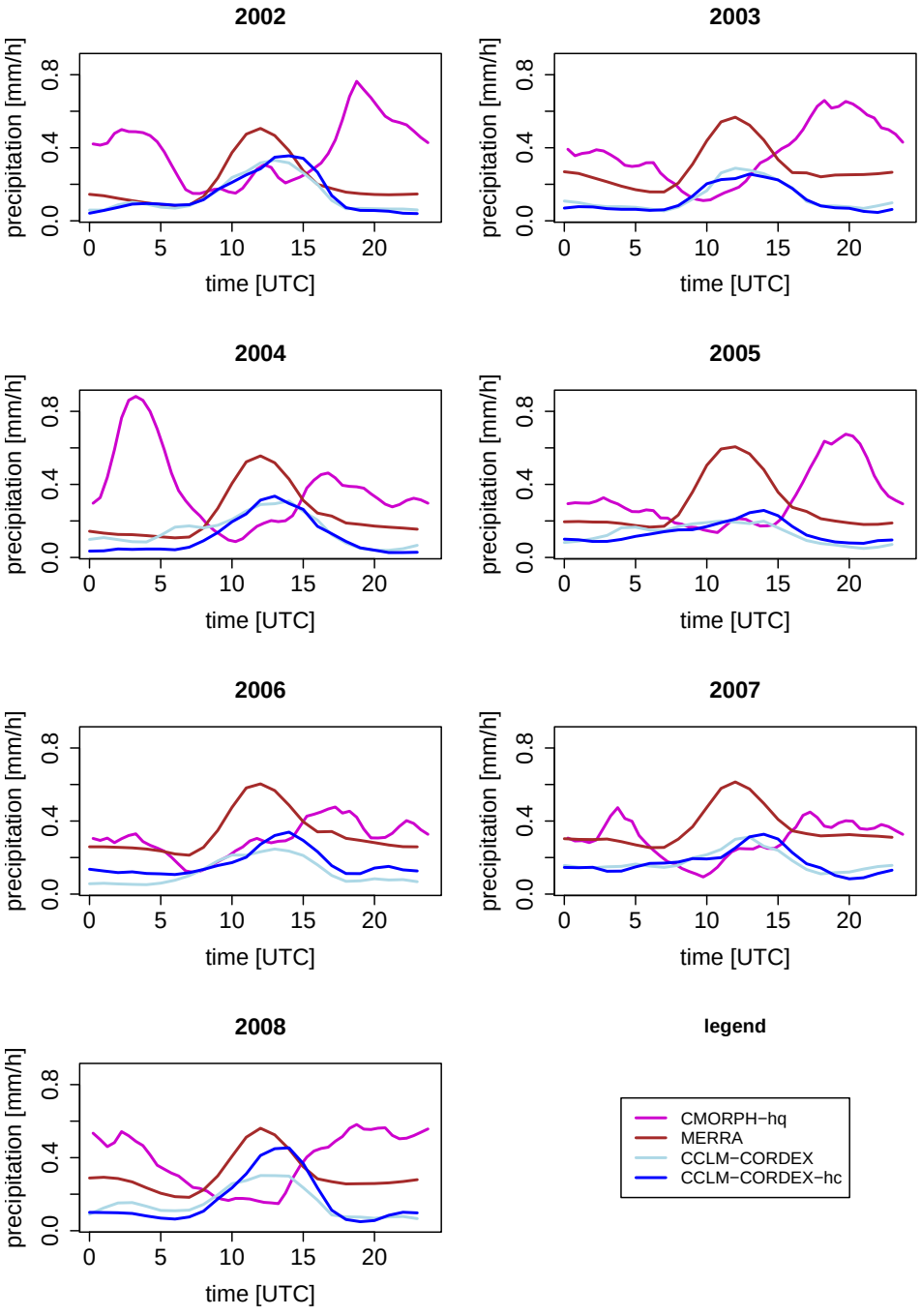

Figure E.2: Annual mean diurnal cycles of the CMOPRH-hq satellite data and the MERRA reanalysis and two CCLM climate simulations, and of the AMMA-CATCH data at the Ouémé mesosite during the monsoon season (MJJAS) for the years of 2000 to 2011

Bibliography

Adler, R. F., Gu, G., and Huffman, G. J. (2012). Estimating climatological bias errors for the global precipitation climatology project (GPCP). *Journal of Applied Meteorology and Climatology*, 51(1):84–99.

Adler, R. F., Huffman, G. J., and Al, E. (2003). The Version-2 Global Precipitation Climatology Project (GPCP) Monthly Precipitation Analysis (1979 – Present). *Journal of Hydrometeorology*, 4:1147–1167.

Adler, R. F., Kidd, C., Petty, G., Morissey, M., and Goodman, H. M. (2001). Intercomparison of global precipitation products: The third precipitation intercomparison project (PIP-3). *Bulletin of the American Meteorological Society*, 82(7):1377–1396.

Ahrens, B. and Beck, A. (2008). On upscaling of rain-gauge data for evaluating numerical weather forecasts. *Meteorology and Atmospheric Physics*, 99(2002):155–167.

Ahrens, B., Karstens, U., Rockel, B., and Stuhlmann, R. (1998). Meteorology and Atmospheric Physics On the Validation of the Atmospheric Model REMO with ISCCP Data and Precipitation Measurements Using Simple Statistics. *Meteorology and Atmospheric Physics*, 58:127–142.

Andersson, A., Fennig, K., Klepp, C., Bakan, S., Graß l, H., and Schulz, J. (2010). The Hamburg Ocean Atmosphere Parameters and Fluxes from Satellite Data – HOAPS-3. *Earth System Science Data*, 2(2):215–234.

Andersson, A., Klepp, C., Fennig, K., Bakan, S., Grassl, H., and Schulz, J. (2011). Evaluation of HOAPS-3 Ocean Surface Freshwater Flux Components. *Journal of Applied Meteorology and Climatology*, 50:379–398.

Arakawa, A. and Schubert, W. H. (1974). Interaction of a Cumulus Cloud Ensemble with the Large-Scale En1. Arakawa A, Schubert WH. Interaction of a Cumulus Cloud Ensemble with the Large-Scale Environment, Part I. J Atmos Sci.

1974;31(3):674–701. doi:10.1175/1520-0469(1974)031<0674:IOACCE>2.0.CO;. *Journal of the Atmospheric Sciences*, 31(3):674–701.

Arkin, A. (1991). The Radiative Effects of Clouds and their Impact on Climate. *Bulletin of the American Meteorological Society*, 71(6):795–813.

Asharaf, S., Dobler, A., and Ahrens, B. (2012). Soil Moisture–Precipitation Feedback Processes in the Indian Summer Monsoon Season. *Journal of Hydrometeorology*, 13:1461–1474.

Ashouri, H., Hsu, K.-L., Sorooshian, S., Braithwaite, D. K., Knapp, K. R., Cecil, L. D., R., N. B., and Prat, O. P. (2015). PERSIANN-CDR - Daily Precipitation Climate Data Record from Multisatellite Observations for Hydrological and Climate Studies. *Bulletin of the American Meteorological Society*, 96(1):69–83.

Ban, N., Schmidli, J., and Schär, C. (2014). Evaluation of the convection-resolving regional climate modeling approach in decade-long simulations. *Journal of Geophysical Research: Atmospheres*, 119:7889–7907.

Bechtold, P., Noureddine, S., Philippe, L., Chamboureau, J.-P., Beljaars, A., and Bormann, N. (2014). Representing Equilibrium and Nonequilibrium Convection in Large-Scale Models. *Journal of Atmospheric Sciences*, 71:734–753.

Béranger, K., Barnier, B., Gulev, S., and Crépon, M. (2006). Comparing 20 years of precipitation estimates from different sources over the world ocean. *Ocean Dynamics*, 56(2):104–138.

Bergman, J. W. and Salby, M. L. (1996). Diurnal Variations of Cloud Cover and Their Relationship to Climatological Conditions. *Journal of Climate*, 9:2802–2820.

Birch, C. E., Parker, D. J., Marsham, J. H., Copsey, D., and Garcia-Carreras, L. (2014). A seamless assessment of the role of convection in the water cycle of the West African Monsoon. *Journal of Geophysical Research: Atmospheres*, 119:2890–2912.

Bony, S., Stevens, B., Frierson, D. M. W., Jakob, C., Kageyama, M., Pincus, R., Shepherd, T. G., Sherwood, S. C., Siebesma, a. P., Sobel, A. H., Watanabe, M., and Webb, M. J. (2015). Clouds, circulation and climate sensitivity. *Nature Geoscience*, 8(4):261–268.

Bowman, K. P. (2005). Comparison of TRMM Precipitation Retrievals with Rain Gauge Data from Ocean Buoys. *Journal of Climate*, 18(1):178–190.

Bowman, K. P., Amy B. Phillips, and North, G. R. (2003). Comparison of TRMM rainfall retrievals with rain gauge data from the TAO/TRITON buoy array. *Geophysical Research Letters*, 30(14):1757.

Bowman, K. P., Homeyer, C. R., and Stone, D. G. (2009). A Comparison of Oceanic Precipitation Estimates in the Tropics and Subtropics. *Journal of Applied Meteorology and Climatology*, 48(7):1335–1344.

Brisson, E., Weverberg, K. V., Demuzere, M., Devis, A., Saeed, S., and Stengel, M. (2016). How well can a convection-permitting climate model reproduce decadal statistics of precipitation, temperature and cloud characteristics? *Climate Dynamics*, accepted.

Cairns, B. (1995). Diurnal variations of cloud from ISCCP data. *Atmospheric Research*, 37(1-3):133–146.

Cetrone, J. and Houze, R. A. (2009). Anvil clouds of tropical mesoscale convective systems in monsoon regions. *Quarterly Journal of the Royal Meteorological Society*, 317(February):305–317.

Chen, Y., Ebert, E. E., Walsh, K. J., and Davidson, N. E. (2013). Evaluation of TRMM 3B42 precipitation estimates of tropical cyclone rainfall using PACRAIN data. *Journal of Geophysical Research: Atmospheres*, 118(5):2184–2196.

Cleveland, W. S. (1981). LOWESS: A Program for Smoothing Scatterplots by Robust Locally Weighted Regression. *The American Statistician*, 35(1):54.

Colby, F. P. J. (1984). Convective Inhibition as a Predictor of Convection during AVE-SESAME 2. *Monthly Weather Review*, 112(11):2239–2252.

Crétat, J., Vizy, E. K., and Cook, K. H. (2014). How well are daily intense rainfall events captured by current climate models over Africa? *Climate Dynamics*, 42(9-10):2691–2711.

Dai, A. (2006). Precipitation characteristics in eighteen coupled climate models. *Journal of Climate*, 19(18):4605–4630.

Dai, A., Trenberth, K. E., and Karl, T. R. (1999). Effects of clouds, soil moisture, precipitation, and water vapor on diurnal temperature range. *Journal of Climate*, 12(8 PART 2):2451–2473.

Dee, D. P., Uppala, S. M., Simmons, A. J., Berrisford, P., Poli, P., Kobayashi, S., Andrae, U., Balmaseda, M. A., Balsamo, G., Bauer, P., Bechtold, P., Beljaars, A. C. M., van de Berg, L., Bidlot, J., Bormann, N., Delsol, C., Dragani, R.,

Fuentes, M., Geer, A. J., Haimberger, L., Healy, S. B., Hersbach, H., Hólm, E. V., Isaksen, L., Kå llberg, P., Köhler, M., Matricardi, M., Mcnally, A. P., Monge-Sanz, B. M., Morcrette, J. J., Park, B. K., Peubey, C., de Rosnay, P., Tavolato, C., Thépaut, J. N., and Vitart, F. (2011). The ERA-Interim reanalysis: Configuration and performance of the data assimilation system. *Quarterly Journal of the Royal Meteorological Society*, 137(656):553–597.

Derrien, M. and Le Gléau, H. (2005). MSG/SEVIRI cloud mask and type from SAFNWC. *International Journal of Remote Sensing*, 26(21):4707–4732.

Dirmeyer, P. A., Cash, B. A., Kinter, J. L., Jung, T., Marx, L., Satoh, M., Stan, C., Tomita, H., Towers, P., Wedi, N., Achuthavarier, D., Adams, J. M., Altshuler, E. L., Huang, B., Jin, E. K., and Manganello, J. (2012). Simulating the diurnal cycle of rainfall in global climate models : resolution versus parameterization. *Climate Dynamics*, 39:399–418.

Dobler, A. and Ahrens, B. (2008). Precipitation by a regional climate model and bias correction in Europe and South Asia. *Meteorologische Zeitschrift*, 17(4):499–509.

Dobler, A. and Ahrens, B. (2010). Analysis of the Indian summer monsoon system in the regional climate model COSMO-CLM. *Journal of Geophysical Research*, 115(D16):D16101.

Dybbroe, A., Karlsson, K.-G., and Thoss, A. (2005). NWCSAF AVHRR Cloud Detection and Analysis Using Dynamic Thresholds and Radiative Transfer Modeling. Part II: Tuning and Validation. *Journal of Applied Meteorology*, 44(1):39–54.

Eastman, R. and Warren, S. G. (2013). A 39-Yr Survey of Cloud Changes from Land Stations Worldwide 1971–2009: Long-Term Trends, Relation to Aerosols, and Expansion of the Tropical Belt. *Journal of Climate*, 26(4):1286–1303.

Ebert, E. E., Janowiak, J. E., and Kidd, C. (2007). Comparison of Near-Real-Time Precipitation Estimates from Satellite Observations and Numerical Models. *Bulletin of the American Meteorological Society*, 88(1):47–64.

Feijt, A. J. (2000). *Quantitative Cloud Analysis using Meteorological Satellites*. Wageningen University, Netherlands.

Ferraro, R. R. (1997). Special sensor microwave imager derived global rainfall estimates for climatological applications. *Journal of Geophysical Research*, 102(D14):16715–16735.

Ferraro, R. R., Weng, F., Grody, N. C., and Basist, A. (1996). An Eight-Year (1987-1994) Time Series of Rainfall, Clouds, Water Vapor, Snow Cover, and Sea Ice Derived from SSM/I Measurements.

Fink, A. H., Pohle, S., and Hoffmann, R. (2008). Spatial and Temporal Rainfall Climatologies of Benin. In *IMPETUS Atlas Benin. Research Results 2000-2007.* Departement of Geography, University of Bonn, Germany, 3 edition.

Fink, A. H., Vincent, D. G., and Ermert, V. (2006). Rainfall Types in the West African Sudanian Zone during the Summer Monsoon 2002. *Monthly Weather Review*, 134(8):2143–2164.

Folkins, I., Mitovski, T., and Pierce, J. R. (2014). A simple way to improve the diurnal cycle in convective rainfall over land in climate models. *Journal of Geophysical Research: Atmospheres*, 119:2113–2130.

Fosser, G., Khodayar, S., and Berg, P. (2015). Benefit of convection permitting climate model simulations in the representation of convective precipitation. *Climate Dynamics*, 44:45–60.

Futyan, J. M. and Del Genio, A. D. (2007). Deep Convective System Evolution over Africa and the Tropical Atlantic. *Journal of Climate*, 20(20):5041–5060.

Gosset, M., Viarre, J., Quantin, G., and Alcoba, M. (2013). Evaluation of several rainfall products used for hydrological applications over West Africa using two high-resolution gauge networks. *Quarterly Journal of the Royal Meteorological Society*, 139(673):923–940.

Gounou, A., Guichard, F., and Couvreux, F. (2012). Observations of Diurnal Cycles Over a West African Meridional Transect: Pre-Monsoon and Full-Monsoon Seasons. *Boundary-Layer Meteorology*, 144(3):329–357.

Greene, J. S., Klatt, M., Morrissey, M., and Postawko, S. (2008). The Comprehensive Pacific Rainfall Database. *Journal of Atmospheric and Oceanic Technology*, 25(1):71–82.

Haddad, Z. S., Smith, E. A., Kummerow, C. D., Iguchi, T., R., F. M., Durden, S. L., Alves, M., and Olson, W. S. (1997). The TRMM 'Day-1' Radar/Radiometer Combined Rain-Profiling Algorithm. *Journal of the Meteorological Society of Japan*, 75(4):799–809.

Harris, I., Jones, P. D., Osborn, T. J., and Lister, D. H. (2014). Updated high-resolution grids of monthly climatic observations - the CRU TS3.10 Dataset. *International Journal of Climatology*, 34(3):623–642.

Haylock, M. R., Hofstra, N., Klein Tank, a. M. G., Klok, E. J., Jones, P. D., and New, M. (2008). A European daily high-resolution gridded data set of surface temperature and precipitation for 1950–2006. *Journal of Geophysical Research*, 113(D20):D20119.

He, X., Kim, H., Kirstetter, P.-E., Yoshimura, K., Chang, E.-C., Ferguson, C. R., Erlingis, J. M., Hong, Y., and Oki, T. (2015). The Diurnal Cycle of Precipitation in Regional Spectral Model Simulations over West Africa : Sensitivities to Resolution and Cumulus Schemes. *Weather and Forecasting*, 30:424–445.

Hohenegger, C., Brockhaus, P., Bretherton, C. S., and Schär, C. (2009). The Soil Moisture–Precipitation Feedback in Simulations with Explicit and Parameterized Convection. *Journal of Climate*, 22(19):5003–5020.

Hohenegger, C., Brockhaus, P., and Schär, C. (2008). Towards climate simulations at cloud-resolving scales. *Meteorologische Zeitschrift*, 17(4):383–394.

Houze Jr., R. A. (2004). Mesoscale Convective Systems. *Reviews of Geophysics*, 42:1–43.

Houze Jr., R. A., Rasmussen, K. L., Zuluaga, M. D., and Brodzik, S. R. (2015). The variable nature of convection in the tropics and subtropics: A legacy of 16 years of the Tropical Rainfall Measuring Mission satellite. *Reviews of Geophysics*, 53:994–1021.

Huffman, G. and Bolvin, D. T. (2007). The TRMM Multisatellite Precipitation Analysis (TMPA): Quasi-global, multiyear, combined-sensor precipitation estimates at fine scales. *Journal of Hydrometeorology*, 8(1):38–55.

Huffman, G. J., Adler, R. F., Bolvin, D. T., and Gu, G. (2009). Improving the global precipitation record: GPCP Version 2.1. *Geophysical Research Letters*, 36(17):L17808.

Jaeger, E. B., Anders, I., Lüthi, D., Rockel, B., Schär, C., and Seneviratne, S. I. (2008). Analysis of ERA40-driven CLM simulations for Europe. *Meteorologische Zeitschrift*, 17(4):349–367.

Janowiak, J. E., Kousky, V. E., and Joyce, R. J. (2005). Diurnal cycle of precipitation determined from the CMORPH high spatial and temporal resolution global precipitation analyses. *Journal of Geophysical Research*, 110(D23):D23105.

Jin, Y., Rossow, W. B., and Wylie, D. P. (1996). Comparison of the Climatologies of High-Level Clouds from HIRS and ISCCP. *Journal of Climate*, 9(11):2850 – 2879.

Jones, P. D. (1999). First- and Second-Order Conservative Remapping Schemes for Grids in Spherical Coordinates. *Monthly Weather Review*, 127(3):2204–2210.

Joyce, R., Janowiak, J., Arkin, P. A., and Xie, P. (2004). CMORPH : A Method that Produces Global Precipitation Estimates from Passive Microwave and Infrared Data at High Spatial and Temporal Resolution. *Journal of Hydrometeorology*, 5:478–503.

Karlsson, J., Svensson, G., and Rodhe, H. (2008). Cloud radiative forcing of subtropical low level clouds in global models. *Climate Dynamics*, 30:779–788.

Karlsson, K.-G., Meirink, J. F., Stengel, M., and Hollmann, R. (2011). EUMETSAT SAF on Climate Monitoring: Products User Manual CLOUDS. Technical Report 1.5, EUMETSAT CM SAF.

Kidd, C. and Huffman, G. (2011). Review: Global precipitation measurement. *Meteorological Applications*, 18(3):334–353.

Kidd, C. and Levizzani, V. (2011). Status of satellite precipitation retrievals. *Hydrology and Earth System Sciences*, 15(4):1109–1116.

Kiehl, J. T. and Trenberth, K. E. (1997). Earth's Annual Global Mean Energy Budget. *Bulletin of the American Meteorological Society*, 78(2):197–208.

Kikuchi, K. and Wang, B. (2008). Diurnal Precipitation Regimes in the Global Tropics. *Journal of Climate*, 21(11):2680–2696.

Kirstetter, P.-E., Viltard, N., and Gosset, M. (2013). An error model for instantaneous satellite rainfall estimates : evaluation of BRAIN-TMI over West Africa. *Quarterly Journal of the Royal Meteorological Society*, 139:894–911.

Klepp, C.-P., Bakan, S., and Graß l, H. (2003). Improvements of Satellite-Derived Cyclonic Rainfall over the North Atlantic. *Journal of Climate*, 16(4):657–669.

Kniffka, A., Stengel, M., Lockhoff, M., Bennartz, R., and Hollmann, R. (2014). Characteristics of cloud liquid water path from SEVIRI onboard the Meteosat Second Generation 2 satellite for several cloud types. *Atmospheric Measurement Techniques*, 7:887–905.

Knippertz, P., Coe, H., Chiu, J. C., Evans, M. J., Fink, A. H., Kalthoff, N., Liousse, C., Mari, C., Allan, R. P., Brooks, B., Danour, S., Flamant, C., Jegede, O. O., Lohou, F., and Marsham, J. H. (2015). The DACCIWA Project: Dynamics–Aerosol–Chemistry–Cloud Interactions in West Africa. *Bulletin of the American Meteorological Society*, 96(9):1451–1460.

Koster, R. D., Dirmeyer, P. a., Guo, Z., Bonan, G., Chan, E., Cox, P., Gordon, C. T., Kanae, S., Kowalczyk, E., Lawrence, D., Liu, P., Lu, C.-H., Malyshev, S., McAvaney, B., Mitchell, K., Mocko, D., Oki, T., Oleson, K., Pitman, A., Sud, Y. C., Taylor, C. M., Verseghy, D., Vasic, R., Xue, Y., and Yamada, T. (2004). Regions of Strong Coupling Between Soil Moisture and Precipitation. *Science*, 305(5687):1138–1140.

Kothe, S., Dobler, A., Beck, A., and Ahrens, B. (2010). The radiation budget in a regional climate model. *Climate Dynamics*, 36(5-6):1023–1036.

Kothe, S., Lüthi, D., and Ahrens, B. (2014). Analysis of the West African Monsoon system in the regional climate model COSMO-CLM. *International Journal of Climatology*, 34(2):481–493.

Kucera, P. A., Ebert, E. E., Turk, F., Levizzani, V., Kirschbaum, D., Tapiador, F. J., Loew, A., and Borsche, M. (2013). Precipitation from Space. *Bulletin of the American Meteorological Society*, pages 365–375.

Kummerow, C., Barnes, W., Kozu, T., Shiue, J., and Simpson, J. (1998). The Tropical Rainfall Measuring Mission (TRMM) Sensor Package. *Journal of Atmospheric and Oceanic Technology*, 15(3):809–817.

Lafore, J.-P. P., Flamant, C., Guichard, F., Parker, D. J., Bouniol, D., Fink, a. H., Giraud, V., Gosset, M., Hall, N., Höller, H., Jones, S. C., Protat, a., Roca, R., Roux, F., Saïd, F., and Thorncroft, C. (2011). Progress in understanding of weather systems in West Africa. *Atmospheric Science Letters*, 12(1):7–12.

Lau, W. K. M., Kim, K.-M., and Lee, M.-I. (2007). Characteristics of Diurnal and Seasonal Cycles in Global Monsoon Systems. *Journal of the Meteorological Society of Japan*, 85A:403–416.

Lebel, T., Parker, D. J., Flamant, C., Bourlès, B., Marticorena, B., Mougin, E., Peugeot, C., Diedhiou, A., Haywood, J. M., Ngamini, J. B., Polcher, J., Redelsperger, J.-L., and Thorncroft, C. D. (2010). The AMMA field campaigns: Multiscale and multidisciplinary observations in the West African region. *Quarterly Journal of the Royal Meteorological Society*, 136:8–33.

Loeb, N. G., Wielicki, B. a., Doelling, D. R., Smith, G. L., Keyes, D. F., Kato, S., Manalo-Smith, N., and Wong, T. (2009). Toward optimal closure of the Earth's top-of-atmosphere radiation budget. *Journal of Climate*, 22(3):748–766.

Mathon, V., Laurent, H., and Lebel, T. (2002). Mesoscale Convective System Rainfall in the Sahel. *Journal of Applied Meteorology*, 41(11):1081–1092.

Meinke, I. (2006). A Comparison of Simulated Clouds to ISCCP Data. *Monthly Weather Review*, 134(6):1669–1681.

Meskhidze, N., Remer, L. a., Platnick, S., Negrón Juárez, R., Lichtenberger, A. M., and Aiyyer, A. R. (2009). Exploring the differences in cloud properties observed by the Terra and Aqua MODIS sensors. *Atmospheric Chemistry and Physics Discussions*, 9:3461–3475.

Michaelides, S., Levizzani, V., Anagnostou, E., Bauer, P., Kasparis, T., and Lane, J. E. (2009). Precipitation: Measurement, remote sensing, climatology and modeling. *Atmospheric Research*, 94(4):512–533.

Minnis, P., Heck, P. W., Young, D. F., Fairall, C. W., and Snider, J. B. (1992). Stratocumulus cloud properties derived from simultaneous satellite and island-based instrumentation during FIRE. *Journal of Applied Meteorology*, 31:317–339.

Moorthi, S. and Suarez, M. J. (1992). Relaxed Arakawa-Schubert. A Parameterization of Moist Convection for General Circulation Models. *Monthly Weather Review*, 120(6):978–1002.

Morrissey, M. L. (1991). Using Sparse Raingages to Test Satellite-Based Rainfall Algorithms. *Journal of Geophysical Research*, 96(D10):18561–18571.

Muggeo, V. M. R. (2008). R news. *An R Package to Fit Regression Models with Broken-Line Relationships*, 8(1):20–25.

Negri, A. J., Adler, R. F., and Xu, L. (2002a). A TRMM-calibrated infrared rainfall algorithm applied over Brazil. *Journal of Geophysical Research*, 107(D20).

Negri, A. J., Bell, T. L., and Xu, L. (2002b). Sampling of the Diurnal Cycle of Precipitation Using TRMM. *Journal of Atmospheric and Oceanic Technology*, 19:1333–1344.

New, M., Todd, M., Mike, H., and Jones, P. (2001). Precipitation Measurements and trends in the twentieth century. *International Journal of Climatology*, 21:1899–1922.

Pfeifroth, U., Hollmann, R., and Ahrens, B. (2012). Cloud Cover Diurnal Cycles in Satellite Data and Regional Climate Model Simulations. *Meteorologische Zeitschrift*, 21(6):551–560.

Pfeifroth, U., Mueller, R., and Ahrens, B. (2013). Evaluation of Satellite-Based and Reanalysis Precipitation Data in the Tropical Pacific. *Journal of Applied Meteorology and Climatology*, 52(3):634–644.

Pfeifroth, U., Trentmann, J., Fink, A. H., and Ahrens, B. (2016). Evaluating satellite-based diurnal cycles of precipitation in the African tropics. *Journal of Applied Meteorology and Climatology*, 55(1):23–39.

Pierre, C., Bergametti, G., Marticorena, B., Mougin, E., Lebel, T., and Ali, A. (2011). Pluriannual comparisons of satellite-based rainfall products over the Sahelian belt for seasonal vegetation modeling. *Journal of Geophysical Research*, 116(D18).

Pohl, B., Rouault, M., and Roy, S. S. (2014). Simulation of the annual and diurnal cycles of rainfall over South Africa by a regional climate model. *Climate Dynamics*, 43:2207–2226.

Randall, D., Khairoutdinov, M., Arakawa, A., and Grabowski, W. (2003). Breaking the Cloud Parameterization Deadlock. *Bulletin of the American Meteorological Society*, 84(11):1547–1564.

Raschke, E., Ohmura, A., Rossow, W. B., Carlson, B. E., Zhang, Y.-C. C., Stubenrauch, C., Kottek, M., and Wild, M. (2005). Cloud effects on the radiation budget based on ISCCP data (1991 to 1995). *International Journal of Climatology*, 25(8):1103–1125.

Rasmussen, K. L., Choi, S. L., Zuluaga, M. D., and Houze Jr., R. A. (2013). TRMM precipitation bias in extreme storms in South America. *Geophysical Research Letters*, 40:3457–3461.

Redelsperger, J.-l., Thorncroft, C. D., Diedhiou, A., Lebel, T., Parker, D. J., and Polcher, J. (2006). African Monsoon Multidisciplinary Analysis: An International Research Project and Field Campaign. *Bulletin of the American Meteorological Society*, 87:1739–1746.

Reed, R. J. and Jaffe, K. D. (1981). Diurnal Variation of Summer Convection Over West Africa and the Tropical Eastern Atlantic During 1974 and 1978. *Monthly Weather Review*, 109:2527–2534.

Reuter, M., Thomas, W., Albert, P., Lockhoff, M., Weber, R., Karlsson, K.-G., and Fischer, J. (2009). The CM-SAF and FUB Cloud Detection Schemes for SEVIRI: Validation with Synoptic Data and Initial Comparison with MODIS and CALIPSO. *Journal of Applied Meteorology and Climatology*, 48(2):301–316.

Rienecker, M. M., Suarez, M. J., Gelaro, R., Todling, R., Bacmeister, J., Liu, E., Bosilovich, M. G., Schubert, S. D., Takacs, L., Kim, G.-K., Bloom, S., Chen, J., Collins, D., Conaty, A., da Silva, A., Gu, W., Joiner, J., Koster, R. D., Lucchesi, R., Molod, A., Owens, T., Pawson, S., Pegion, P., Redder, C. R.,

Reichle, R., Robertson, F. R., Ruddick, A. G., Sienkiewicz, M., and Woollen, J. (2011). MERRA: NASA's Modern-Era Retrospective Analysis for Research and Applications. *Journal of Climate*, 24(14):3624–3648.

Roca, R., Chambon, P., Jobard, I., Kirstetter, P.-E., Gosset, M., and Bergès, J. C. (2010). Comparing Satellite and Surface Rainfall Products over West Africa at Meteorologically Relevant Scales during the AMMA Campaign Using Error Estimates. *Journal of Applied Meteorology and Climatology*, 49(4):715–731.

Rockel, B., Will, A., and Hense, A. (2008). The Regional Climate Model COSMO-CLM (CCLM). *Meteorologische Zeitschrift*, 17(4):347–348.

Roebeling, R., Baum, B., Bennartz, R., Hamann, U., Heidinger, A., Fokke, J., Stengel, M., Thoss, A., Walther, A., and Watts, P. (2014). Outcome of the fourth Cloud Retrieval Evaluation Workshop. *Bulletin of the American Meteorological Society*, 16(April).

Roebeling, R. a. and van Meijgaard, E. (2009). Evaluation of the Daylight Cycle of Model-Predicted Cloud Amount and Condensed Water Path over Europe with Observations from MSG SEVIRI. *Journal of Climate*, 22(7):1749–1766.

Rossow, W. B. and Garder, L. C. (1993). Cloud Detection Using Satellite Measurements of Infrared and Visible Radiances for ISCCP. *Journal of Climate*, 6:2341–2369.

Rossow, W. B. and Schiffer, R. a. (1999). Advances in Understanding Clouds from ISCCP. *Bulletin of the American Meteorological Society*, 80(11):2261–2287.

Rozendaal, M. A., Leovy, C. B., and Klein, S. a. (1995). An Observational Study of Diurnal Variations of Marine Stratiform Cloud. *Journal of Climate*, 8:1795–1809.

Rückel, S. (2014). Tagesgang tropischer Niederschläge, Master Thesis, Goethe-University Frankfurt.

Sane, Y., Bonazzola, M., Rio, C., Chambon, P., Fiolleau, T., Musat, I., Hourdin, F., Roca, R., Grandpeix, J., and Diedhiou, A. (2012). An analysis of the diurnal cycle of precipitation over Dakar using local rain-gauge data and a general circulation model. *Quarterly Journal of the Royal Meteorological Society*, 138:2182–2195.

Sapiano, M. R. P. and Arkin, P. A. (2009). An Intercomparison and Validation of High-Resolution Satellite Precipitation Estimates with 3-Hourly Gauge Data. *Journal of Hydrometeorology*, 10(1):149–166.

Sato, T., Miura, H., Satoh, M., Takayabu, Y. N., and Wang, Y. (2009). Diurnal Cycle of Precipitation in the Tropics Simulated in a Global Cloud-Resolving Model. *Journal of Climate*, 22(18):4809–4826.

Schneider, U., Becker, A., Finger, P., Meyer-Christoffer, A., Ziese, M., and Rudolf, B. (2013). GPCC's new land surface precipitation climatology based on quality-controlled in situ data and its role in quantifying the global water cycle. *Theoretical and Applied Climatology*.

Schönwiese, C.-D. (2003). *Klimatologie*. UTB, Stuttgart.

Schulz, J., Albert, P., Behr, H.-D., Caprion, D., Deneke, H., Dewitte, S., Dürr, B., Fuchs, P., Gratzki, A., Hechler, P., Hollmann, R., Johnston, S., Karlsson, K.-G., Manninen, T., Müller, R., Reuter, M., Riihelä, A., Roebeling, R., Selbach, N., Tetzlaff, A., Thomas, W., Werscheck, M., Wolters, E., and Zelenka, A. (2009). Operational climate monitoring from space: the EUMETSAT Satellite Application Facility on Climate Monitoring (CM-SAF). *Atmospheric Chemistry and Physics*, 9(5):1687–1709.

Schulz, J.-P., Vogel, G., Becker, C., and Ahrens, B. (2016). On the ground heat flux simulated by the land surface scheme TERRA of the COSMO atmospheric model. *Meteorologische Zeitschrift*, accepted.

Shin, D. B., Kim, J. H., and Park, H. J. (2011). Agreement between monthly precipitation estimates from TRMM satellite, NCEP reanalysis, and merged gauge-satellite analysis. *Journal of Geophysical Research: Atmospheres*, 116(May):1–8.

Shin, D. W., Cocke, S., and LaRow, T. E. (2007). Diurnal cycle of precipitation in a climate model. *Journal of Geophysical Research: Atmospheres*, 112(D13):n/a–n/a.

Shinoda, M., Okatani, T., and Saloum, M. (1999). Diurnal Variations of Rainfall over Niger in the West African Sahel: A Comparison between Wet and Drought Years. *International Journal of Climatology*, 19:81–94.

Sobel, A. H., Burleyson, C. D., and Yuter, S. E. (2011). Rain on small tropical islands. *Journal of Geophysical Research*, 116.

Sohn, B. J. and Robertson, F. R. (1993). Intercomparison of Observed Cloud Radiative Forcing: A Zonal and Global Perspective. *Bulletin of the American Meteorological Society*, 74(6):997–1006.

Sorooshian, S., Hsu, K.-l., Gao, X., Gupta, H. V., Imam, B., and Braithwaite, D. (2000). Evaluation of PERSIANN System Satellite-Based Estimates of Tropical Rainfall. *Bulletin of the American Meteorological Society*, 81(9):2035–2046.

Stengel, M. S., Kniffka, A. K., Meirink, J. F. M., Lockhoff, M. L., Tan, J. T., and Hollmann, R. H. (2014). CLAAS: The CM SAF cloud property data set using SEVIRI. *Atmospheric Chemistry and Physics*, 14:4297–4311.

Stephens, G. L., Li, J., Wild, M., Clayson, C. A., Loeb, N., Kato, S., L'Ecuyer, T., Stackhouse, P. W., Lebsock, M., and Andrews, T. (2012). An update on Earth's energy balance in light of the latest global observations. *Nature Geoscience*, 5(10):691–696.

Stubenrauch, C., Rossow, W. B., Chéruy, F., Chédin, A., and Scott, N. A. (1999). Clouds as Seen by Satellite Sounders (3I) and Imagers (ISCCP). Part I : Evaluation of Cloud Parameters. *Journal of Climate*, 12:2189–2213.

Stubenrauch, C. J., Cros, S., Guignard, A., and Lamquin, N. (2010). A 6-year global cloud climatology from the Atmospheric InfraRed Sounder AIRS and a statistical analysis in synergy with CALIPSO and CloudSat. *Atmospheric Chemistry and Physics*, 10(15):7197–7214.

Stuhlmann, R. (1995). The impact of clouds on the radiative heating of the earth surface-atmosphere system determined from satellite data. *Advances in Space Research*, 16(10):37–49.

Tapiador, F. J., Turk, F., Petersen, W., Hou, A. Y., García-Ortega, E., Machado, L. A., Angelis, C. F., Salio, P., Kidd, C., Huffman, G. J., and de Castro, M. (2012). Global precipitation measurement: Methods, datasets and applications. *Atmospheric Research*, 104-105:70–97.

Tian, Y. and Peters-Lidard, C. D. (2010). A global map of uncertainties in satellite-based precipitation measurements. *Geophysical Research Letters*, 37(24).

Tiedke, M. (1989). A Comprehensive Mass Flux Scheme for Cumulus Parameterization in Large-Scale Models. *Monthly Weather Review*.

Trenberth, K. E., Fasullo, J. T., and Kiehl, J. (2009). Earth's Global Energy Budget. *Bulletin of the American Meteorological Society*, 90(3):311–323.

Wai, M. M.-K. (1991). The Breakup of marine boundary-layer Clouds over an inhomogeneous Sea Surface Temperature Field. *Boundary-Layer Meteorology*, 57:139–165.

Wild, M., Folini, D., Hakuba, M. Z., Schär, C., Seneviratne, S. I., Kato, S., Rutan, D., Ammann, C., Wood, E. F., and König-Langlo, G. (2015). The energy balance over land and oceans: an assessment based on direct observations and CMIP5 climate models. *Climate Dynamics*, 44(11-12):3393–3429.

Wilheit, T. T., Chang, A. T. C., Rao, M. S. V., Rodgers, E. B., and Theon, J. S. (1977). A Satellite Technique for Quantitatively Mapping Rainfall Rates over Oceans. *Journal of Applied Meteorology*, 16:551–560.

Xie, P. and Arkin, P. A. (1997). Global Precipitation: A 17-Year Monthly Analysis Based on Gauge Observations, Satellite Estimates, and Numerical Model Outputs. *Bulletin of the American Meteorological Society*, 78(11):2539–2558.

Yang, G.-Y. and Slingo, J. (2001). The Diurnal Cycle in the Tropics. *Monthly Weather Review*, 129:784–801.

Zipser, E. J., Cecil, D. J., Liu, C., Nesbitt, S. W., and Yorty, D. P. (2006). Where are the most intense Thunderstorms on Earth? *Bulletin of the American Meteorological Society*, 87(8):1057–1071.

Danksagung

Ich möchte allen danken die dazu beigetragen haben, und mich dabei unterstützt haben, diese Doktorarbeit zu verfassen. Mein Dank gilt zuerst meinem Doktorvater Prof. Dr. Bodo Ahrens, der mir mit Rat und Tat zur Seite stand und mir den nötigen Freiraum zustand, eigene Ideen umzusetzen. Zudem gilt mein Dank auch der Arbeitsgruppe Mesoskalige Meteorologie und Klima des Instituts für Atmosphäre und Umwelt der Goethe Universität Frankfurt, für viele gute und motivierende wissenschaftliche und private Diskussionen.

Prof. Dr. Andreas Fink möchte ich herzlich für die Unterstützung in der entscheidenden Phase dieser Arbeit danken.

Ein großes Dankeschön geht an Dr. Jörg Trentmann, Dr. Richard Müller und Dr. Rainer Hollmann, deren Kompetenz und Erfahrung mich stets weitergebracht haben. Mein Dank gilt auch allen Mitarbeitern des CM SAF, und der gesamten Abteilung für Satellitengestütztes Klimamonitoring des Deutschen Wetterdienstes, auf deren Kompetenz und Rat ich mich verlassen kann.

Zuletzt möchte ich meiner Familie für die große Unterstützung danken. Ein ganz großes Dankeschön gilt meiner lieben Frau Sonja: Du warst und bist immer für mich da – Du stärkst und motivierst mich! Zuletzt, ein großes Dankeschön an meine Eltern, die mich stets unterstützen, und ohne die ich sicher nicht bis hierhin gekommen wäre.